CENTRAL RESEARCH LIBRARY
DOCUMENT COLLECTION

2

OAK RIDGE NATIONAL LABORATORY
operated by
UNION CARBIDE CORPORATION
NUCLEAR DIVISION
for the
U.S. ATOMIC ENERGY COMMISSION

LOCKHEED MARTIN ENERGY RESEARCH LIBRARIES
3 4456 0513756 2

ORNL-TM-2613

ELECTRON ATTACHMENT TO POLYATOMIC MOLECULES

(Thesis)

E. L. Chaney and L. G. Christophorou

OAK RIDGE NATIONAL LABORATORY
CENTRAL RESEARCH LIBRARY
DOCUMENT COLLECTION
LIBRARY LOAN COPY
DO NOT TRANSFER TO ANOTHER PERSON
If you wish someone else to see this document, send in name with document and the library will arrange a loan.
UCN-7969
13 3-67

Submitted by E. L. Chaney as a dissertation to the Graduate School of The University of Tennessee in partial fulfillment of the requirements for the degree of Doctor of Philosophy.

LEGAL NOTICE

This report was prepared as an account of Government sponsored work. Neither the United States, nor the Commission, nor any person acting on behalf of the Commission:

A. Makes any warranty or representation, expressed or implied, with respect to the accuracy, completeness, or usefulness of the information contained in this report, or that the use of any information, apparatus, method, or process disclosed in this report may not infringe privately owned rights; or

B. Assumes any liabilities with respect to the use of, or for damages resulting from the use of any information, apparatus, method, or process disclosed in this report.

As used in the above, "person acting on behalf of the Commission" includes any employee or contractor of the Commission, or employee of such contractor, to the extent that such employee or contractor of the Commission, or employee of such contractor prepares, disseminates, or provides access to, any information pursuant to his employment or contract with the Commission, or his employment with such contractor.

ORNL-TM-2613

Contract No. W-7405-eng-26

HEALTH PHYSICS DIVISION

ELECTRON ATTACHMENT TO POLYATOMIC MOLECULES

E. L. Chaney and L. G. Christophorou

Submitted by E. L. Chaney as a dissertation to the
Graduate School of The University of Tennessee
in partial fulfillment of the requirements
for the degree of
Doctor of Philosophy

JANUARY 1970

OAK RIDGE NATIONAL LABORATORY
Oak Ridge, Tennessee
operated by
UNION CARBIDE CORPORATION
for the
U. S. ATOMIC ENERGY COMMISSION

LOCKHEED MARTIN ENERGY RESEARCH LIBRARIES

3 4456 0513756 2

ACKNOWLEDGEMENTS

The authors greatefully acknowledge the invaluable help of and stimulating discussions with R. P. Blaunstein, J. G. Carter, A. A. Christodoulides, and P. M. Collins. We are also thankful to J. T. Cox, J. A. Harter, and A. G. Kenerly for technical assistance and to M. P. Feezell and B. L. McGill for computational help.

One of us (ELC) acknowledges the financial assistance from Oak Ridge Associated Universities while this research was being conducted.

ABSTRACT

Low-energy ($\lesssim$ 10 eV) electron attachment to a number of polyatomic molecules has been investigated using a high-temperature electron swarm apparatus. Results are reported for nitrous oxide (N_2O), azulene ($C_{10}H_8$), biphenyl $(C_6H_5)_2$, aniline ($C_6H_5NH_3$), acenaphthene ($C_{12}H_8$), and 1,4-naphthoquinone ($C_{10}H_6O_2$). A simple model of electron attachment to polyatomic molecules is discussed and electron affinity calculations based on this model are presented for a number of molecules. Also, experimental data are presented and discussed which strongly support certain forms for the energy distribution functions for electron swarms in the carrier gases C_2H_4, N_2, and Ar.

TABLE OF CONTENTS

CHAPTER PAGE

I. INTRODUCTION 1

General Comments 1

Electron Attachment to Molecules 3

Mechanisms of electron attachment 3

Experimental methods 6

Theory 8

II. EXPERIMENTAL AND ANALYTICAL TECHNIQUES FOR ELECTRON ATTACHMENT STUDIES 11

Experimental Technique 11

High temperature apparatus 15

Procedure 20

Sources of error 21

Analytical Technique 23

III. ELECTRON SWARM ENERGY DISTRIBUTION FUNCTIONS 26

Introduction. 26

Motions of Slow Electrons in Gases 28

General Comments 28

Electron swarm energy distribution functions for the carrier gas argon 29

CHAPTER PAGE

Electron swarm energy distribution functions for the carrier gas nitrogen 31

Electron swarm energy distribution functions for the carrier gas ethylene 33

Consideration of Experimental Data 35

Discussion 35

Argon 37

Nitrogen 37

Ethylene 44

Summary 45

IV. ELECTRON ATTACHMENT TO N_2O 47

Introduction 47

Review of Previous Work on Electron Attachment to N_2O . . . 48

Multiple-collision experiments 48

Single-collision beam experiments 50

Comments on available data on electron attachment to N_2O 52

Experimental Considerations 53

Experimental Results 54

N_2O-Ar mixtures 54

N_2O-N_2 mixtures 65

CHAPTER PAGE

Discussion and Conclusions 69

Summary 76

V. ELECTRON ATTACHMENT TO AROMATIC HYDROCARBONS . . . 79

Introduction 79

Dissociative attachment 80

Nuclear-excited Feshbach resonant capture 81

Electron-excited Feshbach resonant capture 82

Electron Attachment to Biphenyl, Aniline, and

Acenaphthene 83

Biphenyl 83

Aniline 84

Acenaphthene 87

Electron Attachment to Azulene 87

Introduction 87

Experimental results 88

Discussion and conclusions 98

Electron Attachment to p-Benzoquinone and

1, 4-Naphthoquinone 101

Introduction 101

p-Benzoquinone 101

1, 4-Naphthoquinone 103

CHAPTER PAGE

Discussion 106

Summary 106

VI. THEORETICAL CONSIDERATIONS OF ELECTRON ATTACHMENT TO POLYATOMIC MOLECULES AND THE MOLECULAR ELECTRON AFFINITY 108

A Simple Model of Electron Attachment 108

Electron Affinity Calculations 114

Summary 115

VII. SUMMARY 118

BIBLIOGRAPHY 121

LIST OF TABLES

TABLE PAGE

II-I. Electron Swarm Drift Velocities versus E/P in C_2H_4, N_2, and Ar 22

III-I. Mean Electron Energy $\langle \epsilon_e \rangle$ versus E/P at 300° K for Electron Swarms in Ar, N_2, and C_2H_4 46

IV-I. Swarm-Beam Data on O^-/N_2O 64

VI-I. Some Calculated Electron Affinities 116

LIST OF FIGURES

FIGURE PAGE

II-1. Schematic of Electron Attachment in a Uniform Electric Field 13

II-2. Dependence of Pulse Height on τ_0/t_1 for Various Values of f 16

II-3. Swarm Apparatus for Measurement of Electron Attachment Rate and the Drift Velocity 17

II-4. Schematic of High Temperature Swarm Apparatus 19

III-1. Two Different Calculations of $f(\epsilon, E/P)$ for N_2 at the Same E/P Value 32

III-2. Maxwell and Druyvestyn Representations of $f(\epsilon, E/P)$ for the Same $\langle \epsilon_e \rangle$ 34

III-3. Calculated and Experimental αw for N_2O in Ar 38

III-4. Overlap Between $\sigma_a(\epsilon)$ for O^-/N_2O and $f(\epsilon, E/P)$ for Ar 39

III-5. Comparison of $f(\epsilon, E/P)$ for N_2 and Ar for Nearly Equal $\langle \epsilon_e \rangle$ 40

III-6. Comparison of Calculated αw for N_2O in N_2 and Ar 42

III-7. αw for p-Benzoquinone in C_2H_4, N_2, and Ar; Comparison of Carrier Gases 43

FIGURE PAGE

IV-1. Experimental αw for N_2O in Ar as a Function of P_{N_2O} for Various E/P Values 55

IV-2. Experimental αw for N_2O in Ar as a Function of E/P for Various Values of P_{N_2O} 56

IV-3. Experimental αw for N_2O in Ar versus P_{N_2O}/P_{Ar} for Various E/P Values 58

IV-4. Experimental αw for N_2O in Ar versus E/P for $P_{N_2O} \rightarrow 0$ at Several Temperatures 59

IV-5. Comparison of Experimental and Calculated αw for N_2O in Ar 60

IV-6. $\sigma_a(\epsilon)$ for O^-/N_2O at 323°K Using Swarm-Beam Combination . . 62

IV-7. $\sigma_a(\epsilon)$ for O^-/N_2O at 373°K Using Swarm-Beam Combination . . 63

IV-8. Experimental αw for N_2O in N_2 versus P_{N_2} for Various E/P Values 67

IV-9. Summary of Results on N_2O; αw for O^-/N_2O versus $\langle \epsilon_e \rangle$ in Ar and N_2 68

IV-10. k versus $\langle \epsilon_e \rangle$ in N_2 72

IV-11. αw for $E/P \rightarrow 0$ in N_2 versus P_{N_2} 73

IV-12. Comparison of the Curves $|d\alpha w/dP_{N_2O}|$ versus E/P and αw versus E/P in Ar 75

IV-13. Experimental αw versus E/P in Ar for Various P_{Ar} 77

FIGURE PAGE

V-1. Experimental αw for Aniline in N_2 at 473° K versus E/P 85

V-2. αw for Aniline in N_2 for $E/P \rightarrow 0$ 86

V-3. Experimental αw for Azulene in Ar versus P_{Ar} for Various E/P Values 90

V-4. Experimental αw for Azulene versus $\langle \epsilon_e \rangle$ in C_2H_4, N_2, CO_2, and Ar 91

V-5. Comparison of Thermal Electron Attachment Resonances for SF_6 and $C_{10}H_8$ 93

V-6. Comparison of Experimental and Calculated αw for $C_{10}H_8$ . . 95

V-7. αw versus $\langle \epsilon_e \rangle$ for BQ in C_2H_4, N_2, and Ar 102

V-8. $\sigma_a(\epsilon)$ for BQ^-/BQ Peaking at 2.1 eV 104

V-9. αw versus $\langle \epsilon_e \rangle$ for NQ in C_2H_4, N_2, and Ar 105

VI-1. Correction Factor ω' versus ϵ' 111

CHAPTER I

INTRODUCTION

I. GENERAL COMMENTS

The existence of negative ions has been recognized since the early days of physics. Their intrinsically interesting properties and physical, chemical and biological importance, however, were not fully appreciated until the middle of the century. The wide range of importance of negative ions spans phenomena occurring at the geophysical and astrophysical levels to life-supporting, as well as toxic, biological functions. Of immediate interest to the radiation physicist is the role that negative ions play in the intermediate reactions leading to the final results observed when radiation interacts with matter. The radiation chemist can gain valuable information concerning bond dissociation energies and heats of vaporization by studying negative-ion processes. The molecular physicist is finding that negative ions of complex molecules are revealing new phenomena which allow a deeper understanding of molecular structure and interaction. For example, he has found that electron-scattering interactions which proceed via formation of a temporary negative ion provide new information concerning the location of energy levels of molecules. The study of negative ions is basic to the understanding of the physics of the upper atmosphere of the earth as well as to

the understanding of the physics of the atmospheres of other celestial bodies, such as stars and gaseous nebulae [Seaton (1968), Boyd (1968), and Dalgarno (1968)]. In the field of molecular biology it is known that electron transport and charge transfer phenomena are important in vital cellular reactions. Thus toxic properties of certain substances may be related to their electron-donating or electron-accepting capabilities. Blaunstein and Christophorou (1968a), for example, observed a broad correlation between the so-called toxicity indices and the thermal values of the mean electron attachment cross sections for several halogenated aliphatic hydrocarbons. Also, some of the present theories of chemical carcinogenesis imply a relationship between carcinogenic action and electron attachment [see Blaunstein and Christophorou (1968b) for a review of present theories].

Much of the more reliable work on negative ions has been done in the last two decades and has been confined mainly to atomic systems. It has only been within the last decade that interest has been turning to the more complicated molecular systems. Some of the more comprehensive reviews on negative ions are given by Massey (1950), Loeb (1955), Branscomb (1957), McDaniel (1964), Christophorou and Compton (1967), Christophorou (1969), and Compton and Huebner (1969).

The present study is confined to the investigation of the interactions of low-energy ($\lesssim 10$ eV) electrons with polyatomic molecules in the gas phase. The interaction of particular interest, which may proceed via one of several mechanisms, is negative ion formation. The experimentally

determined quantity is the absolute electron attachment rate. In this chapter the general importance of negative ions is indicated and introductory remarks are made concerning electron attachment mechanisms. Experimental and theoretical techniques are also briefly mentioned. In Chapter II the experimental and analytical techniques used in the present study are described. In Chapter III we consider electron energy distribution functions for several carrier gases. In Chapter IV we present experimental data on nitrous oxide (N_2O) and in Chapter V we are concerned with electron attachment to a number of aromatic hydrocarbons. In Chapter VI a simple model is discussed which relates the electron attachment cross section to the number of degrees of freedom of a polyatomic molecule, the electron affinity of the molecule, and the parent negative-ion lifetime. In Chapter VII the present research is summarized.

II. ELECTRON ATTACHMENT TO MOLECULES

Mechanisms of Electron Attachment

The most important modes of electron attachment to molecules are discussed below.

Dissociative attachment. Dissociative electron attachment may be represented by the reaction [Christophorou (1969)]

$$e + AB \xrightarrow{\sigma_a\,(cm^2)} AB^{-*} \begin{cases} \xrightarrow{P_e} AB + e & \text{elastic scattering} \quad (a) \\ \xrightarrow{P_{in}} AB^* + e' & \text{inelastic scattering} \quad (b) \\ \xrightarrow{P_{da}} A(^*) + B^- & \text{dissociative attachment} \quad (c) \end{cases} \qquad \text{(I-1)}$$

where A and B are molecular fragments; σ_a is the cross section for formation of AB^{-*}; and P_e, P_{in}, and P_{da} are probabilities for elastic scattering, inelastic scattering, and dissociative attachment, respectively. The asterisk indicates excitation energy and the prime notation (e′) indicates that the scattered electron does not have the same energy as the incident electron. The parentheses indicate that A may or may not be left in an excited state. If the autoionization lifetime, i.e., the lifetime against autodetachment of the extra electron, of AB^{-*} is long compared with the time between molecular collisions, and if the electron affinity (Chapter VI) of AB is positive, then the parent negative ion AB^- may be formed by collisional stabilization, i.e., the removal of excess energy by a third body (stabilization by radiation is not important). In general, channels (a), (b), and (c) of reaction (I-1) are in competition although one particular mode may dominate.

Parent-negative-ion formation. For molecules which attach molecules strictly via a nondissociative mode, parent-negative-ion formation may be represented by the reaction

$$e + AB \xrightarrow[\tau(\mathrm{sec})]{\sigma_a(\mathrm{cm}^2)} AB^{-(*)} \rightarrow e(') + AB^{(*)}. \qquad \text{(I-2)}$$

The parentheses indicate that there may or may not be an inelastic exchange of energy. The quantity τ is the autoionization lifetime of the parent ion AB^-. Excited electronic states of the ion may be involved.

It is convenient to classify τ according to the experimental method which is used for observation of AB^- [Chaney et al. (1969)]:

1. Short ($10^{-15} \lesssim \tau \lesssim 10^{-13}$ sec). The complex AB^- is manifested through resonances in electron scattering experiments. The complex in general does not live long enough for collisional stabilization to occur in cases where the electron affinity of AB is positive.
2. Moderate or intermediate ($10^{-12} \lesssim \tau \lesssim 10^{-6}$ sec). Such ions can be observed either directly or indirectly in high pressure (multiple-collision) experiments where collisional stabilization is possible.
3. Long ($\tau > 10^{-6}$ sec). Such ions can be detected in negative-ion mass spectrometers and their mean autoionization lifetime can be measured.

The parent negative ion AB^- may be thought of as a quasi-stable system in that the extra electron is in a temporary bound state characterized by a finite autoionization lifetime [Bardsley and Mandl (1968)].

Experimental Methods

There are two basic types of experiments which may be used to study negative ions by electron impact. These are discussed below.

Electron beam experiments. In this type of experiment a quasi-monoenergetic beam of electrons interacts with the target molecules at low pressure. Either scattered electrons or resulting negative ions may be observed under either single-collision or multiple-collision conditions. If the energy width of the electron beam is narrow compared to the negative-ion resonance being observed, then the shape of the electron attachment cross section can be obtained by measuring the negative-ion yield as a function of electron energy. Temporary-negative-ion resonances due to ions of intermediate and short lifetimes can be detected by examining scattered electrons in a suitable interaction chamber. Also, a variety of ion-molecule reactions can be studied under multiple-collision conditions.

A time-of-flight mass spectrometer (TOFMS) has been used in conjunction with some of the work reported in the present study. In this type of electron beam apparatus [see, for example, Compton *et al.* (1966)] negative ions are formed in an interaction chamber and are pulsed down a flight tube, of known length, where they are collected. The time of flight of the negative ion is simply related to its mass; hence mass analysis is possible. Also, the mean autoionization lifetime, τ, of a particular negative ion can be determined from the relation

$$\tau = \frac{t}{\ln[(N^- + N^o)/N^-]} \tag{I-3}$$

where t is the flight time, N^- is the number of negative ions collected at time t, and N^o is the number of ions which have decayed into neutral molecules during time t. Lifetimes less than ~ 1 μsec could not be measured in the TOFMS used in conjunction with the present study.

A disadvantage of electron beam experiments is that at near-thermal energies the percent energy spread of the electron beam becomes significant and a monoenergetic beam can no longer be obtained; however, quite useful data can still be taken. Also, attachment cross sections are usually measured in relative units. Other problems may include difficulties in calibrating the energy scale of the electron beam and variation of the negative-ion collection efficiency with electron energy.

Swarm experiments. In electron swarm experiments a pulse or swarm of electrons with a broad distribution of energies interacts with a gas at high pressure. Thus, average values of quantities such as the absolute electron attachment rate are obtained. Swarm experiments are simple in principle but suffer from difficulties associated with interpretation of data. In Chapter II a technique is described for combining electron beam and electron swarm data to obtain the absolute electron attachment cross section.

Different experimental methods within the two types of experiments mentioned above are discussed by McDaniel (1964), Prasad and Craggs (1962), Loeb (1960), and Christophorou (1969).

Theory

The first significant attempt to explain unimolecular electron attachment was made by Bloch and Bradbury (1935) who assumed that weak coupling occurred between the nuclear motions within the molecule and the free electron, the result being electron capture. The Bloch-Bradbury mechanism and capture into a resonance state, i.e., a temporary bound state, represent the two basic types of theoretical explanation for electron capture. One formula of particular interest [O'Malley (1966)] derived from resonance scattering theory is

$$\sigma_a(\epsilon)_{v=0} = \frac{4\pi^{3/2}}{k^2}\,\bar{g}\,\frac{\Gamma_{\bar{i}}}{\Gamma_d}\exp\left[\frac{\frac{1}{2}\Gamma_i^2 - (\bar{E}-\epsilon)^2}{\frac{1}{2}\Gamma_d^2}\right]\exp-\rho(\epsilon) \qquad \text{(I-4)}$$

where $\sigma_a(\epsilon)_{v=0}$ is the dissociative attachment cross section from the $v=0$ vibrational level of the ground electronic state for an electron of energy ϵ, $k^2 = (2m/\hbar^2)\epsilon$, m is the electron mass, $\bar{g}$ is a statistical factor, $\Gamma_{\bar{i}}$ is the partial autoionization or autodetachment width, Γ_i is the total autoionization width, Γ_d is the experimental dissociation width, $\epsilon^{-\rho(\epsilon)}$ is the probability that the ion will not dissociate, and $\bar{E} = E + 1/2\,\hbar\omega$ where E is the electron energy at the peak of the cross section and $1/2\,\hbar\omega$ is the zero-point energy

associated with the bond that is severed when the ion dissociates. Dissociative electron attachment to 30 molecular systems was discussed by Christophorou and Stockdale (1968) within the framework of the O'Malley formulation, i.e., Equation (I-4), and it was found that the peak cross section was a strong function of the resonance energy of the cross section and that a break in the dependence occurred when electronic excitation of the neutral molecule became energetically possible, thus showing the effect of increased autoionization on the dissociative attachment cross section.

The various theoretical treatments are quite complicated and will not be discussed here. Chen and Mittleman (1968) discuss problems concerned with previous theoretical work, and Chen (1969) gives a comprehensive review of theoretical studies. Bardsley and Mandl (1968) and Burke (1968) review resonance electron attachment. As yet there has been limited consideration of electron attachment to large molecules. In general, the theory that is available is difficult to check experimentally due to the many unknown molecular properties that enter into the theory.

Bardsley and Mandl (1968) classify electron-capture resonances according to three different categories based on the mechanism by which the electron is trapped in the molecule, as discussed below.

Shape resonances. If the electron is bound by an attractive potential which is surrounded by a repulsive potential, the resonance is said to be a shape resonance. A nuclear analog is a nucleus unstable toward

α-particle emission; the α particle is bound by a short-range nuclear force but is surrounded by a repulsive Coulomb barrier through which the α particle must tunnel in order to escape.

Electron-excited Feshbach resonances. Electron-excited Feshbach resonances occur when the incident electron excites one or more electrons of the target molecule and is left with insufficient energy to escape. In order to escape, the trapped electron must reabsorb energy from the target. It has recently been found [Christophorou, Carter, and Christodoulides (1969) and Chapter V] that the electron-excited Feshbach resonances are important for certain large molecules.

Nuclear-excited Feshbach resonances. A nuclear-excited Feshbach resonance occurs when the energy of the incident electron is distributed among the nuclear motions of the target molecule. This type of capture involves coupling of nuclear and electronic motion and thus results from a breakdown of the Born-Oppenheimer approximation concerning the separability of nuclear and electronic motions. Nuclear-excited Feshbach resonances are particularly important for large molecules; the energy of the incident electron becomes distributed among the many degrees of freedom and hence the resulting ions may live for relatively long periods of time (~ 1 to 10^3 μsec). The cross section for this type of resonance can be expressed in terms of the negative-ion lifetime, the electron affinity, and the number of degrees of freedom of the target molecule (Chapter VI).

CHAPTER II

EXPERIMENTAL AND ANALYTICAL TECHNIQUES FOR ELECTRON ATTACHMENT STUDIES

I. EXPERIMENTAL TECHNIQUE

In a typical electron swarm experiment a swarm of electrons drifts through a gas at high pressure under the influence of an electric field. For a uniform field the energy distribution of the electrons is characteristic of the gas and the ratio E/P, the pressure-reduced electric field expressed in $V^{-1}\,cm^{-1}\,torr^{-1}$ at room temperature. For electron attachment studies three common gases, so-called "carrier gases," which do not remove electrons from the swarm over the specific energy range of interest are ethylene (C_2H_4), molecular nitrogen (N_2), and argon (Ar). These gases were used in the present study and are discussed further in Chapter III.

In the present study small amounts of the attaching gas under study were mixed with the carrier gas at high total pressure. The assumption was made that the electron energy distribution of the swarm was characteristic of the carrier gas and was undisturbed by the presence of the attaching gas. This assumption was checked when possible by measuring the electron attachment rate αw ($sec^{-1}\,torr^{-1}$) as a function of the attaching gas pressure. However, for strongly attaching gases only very small amounts are needed

(often at fractions of the total pressure $< 10^{-5}$) and the above assumption is valid.

The basic method used in the present study was first described by Bortner and Hurst (1958). Electrons drift through a gas at high total pressure under the influence of a uniform electric field between the plates of a parallel-plate ionization chamber, and electrons are removed from the swarm by the attaching gas (Figure II-1). The number dN of electrons attached in a distance dx is given by

$$dN = -\alpha N(x) f_1 P dx \qquad \text{(II-1)}$$

where α, the attachment coefficient, is the attachment probability per torr of attaching gas (normalized to room temperature) per unit distance traveled in the drift direction, N(x) is the total number of electrons in the swarm at x, and $f_1 P$ is the pressure in torr of attaching gas. Integrating Equation (II-1), we have

$$N(x) = N(0) \exp - \alpha f_1 P x \qquad \text{(II-2)}$$

where N(0) is the total number of electrons in the swarm at x = 0. The change in potential dV at the positive electrode due to the electron swarm moving the distance dx is given by

$$dV = N(x) \frac{V_o}{d} dx \qquad \text{(II-3)}$$

where V_o is the change in potential at the positive plate due to the drift of

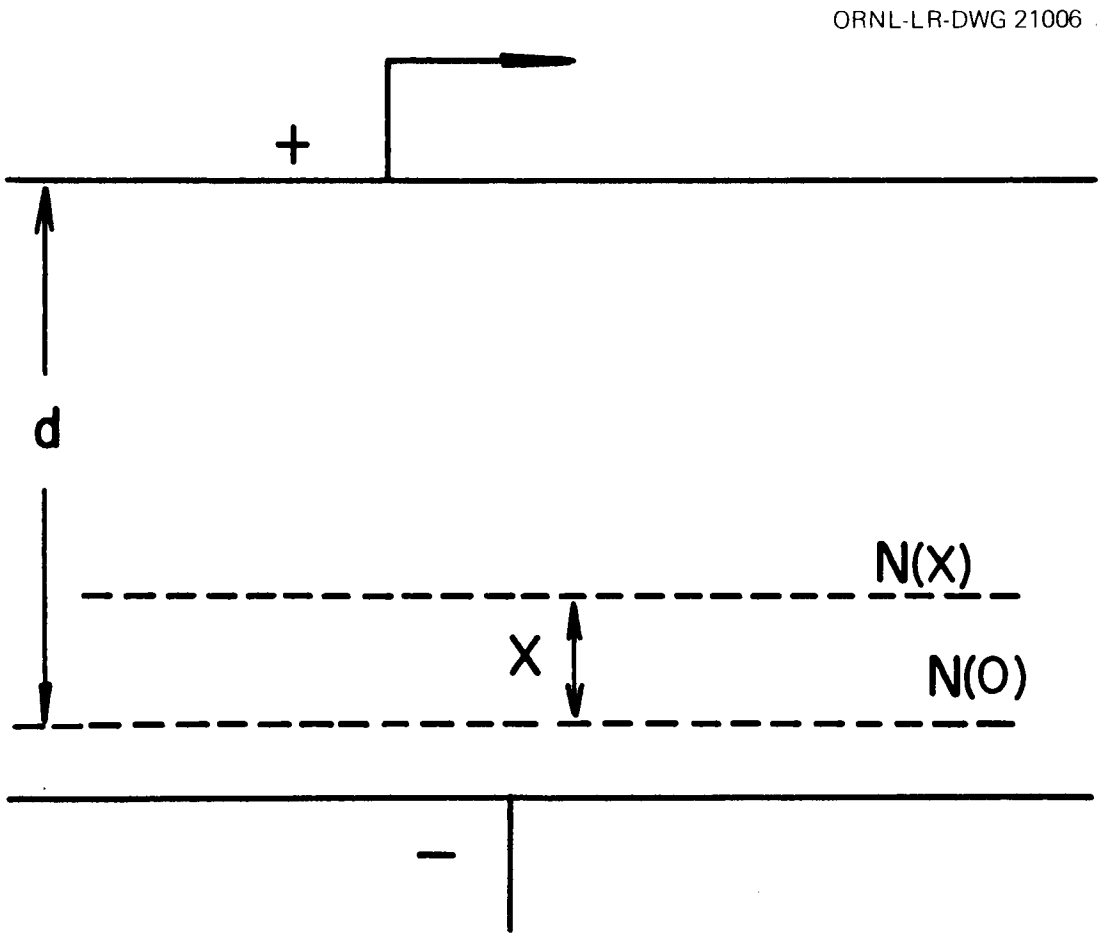

Figure II-1. Schematic of electron attachment in a uniform electric field.

one electron through the entire drift distance d. Using Equation (II-2) for N(x) and integrating Equation (II-3), one obtains for the change in potential after the swarm has moved a distance x'

$$V(x') = \frac{N(0)V_o}{\alpha f_1 Pd}\left[1 - \exp(-\alpha f_1 Px')\right]. \tag{II-4}$$

To find the time variation of the potential at the positive electrode, one replaces x' by td/τ_o, where τ_o is the collection time and is given by $\tau_o = d/w$, where w is the drift velocity of the electron swarm. Thus one obtains

$$V(t) = \frac{A}{f}\left[1 - \exp(-ft/\tau_o)\right], \tag{II-5}$$

where $A = N(0)V_o$ and $f = \alpha f_1 Pd$.

If the voltage pulse given by Equation (II-5) is observed with a linear pulse amplifier having a response to a step function given by

$$V'(t) = \frac{t}{t_1}\exp(-t/t_1), \tag{II-6}$$

where t_1 is both the amplifier differentiating and the integrating time constant, then the output pulse will be given by

$$V(\tau) = \int_o^{\tau_o} \frac{dV(t)}{dt} V'(\tau - t)\,dt \tag{II-7}$$

for $\tau > \tau_o$. Integrating Equation (II-7), one obtains

$$V(\tau) = \frac{A}{(\tau_o - t_1 f)} \left[\left(\exp\left\{ (\tau_o - t_1 f)/t_1 \right\} - 1 \right) \tau \right.$$

$$\left. - \exp\left\{ (\tau_o - t_1 f)/t_1 \right\} \left(\tau_o - \frac{t_1 \tau_o}{\tau_o - t_1 f} \right) - \frac{t_1 \tau_o}{\tau_o - t_1 f} \right] \times \exp(-\tau/t_1). \quad \text{(II-8)}$$

The maximum of $V(\tau)$, occurring at τ', is plotted in Figure II-2 as a function of τ_o/t_1 for various values of f.

Implicit in the above derivation is the assumption that voltage variations due to the drift of negative ions can be neglected, an assumption which in general is valid.

High Temperature Apparatus

Figure II-3 is a schematic drawing of the main chamber. An α-particle source is situated at a known distance between the positive and negative electrodes. The source is collimated so that the α particles are emitted in a plane parallel to the two electrodes. The α particles ionize the gas present in the chamber and create a pulse or swarm of electrons which then begins to drift toward the positive electrode (collector). The electron detector situated at the collector plate and the light entrance window are for drift velocity measurements and were not used in the present study [see, however, Hendrick, Christophorou, and Hurst (1968)].

The chamber was milled from one piece of non-magnetic stainless steel in order to obtain minimum outgassing and to reduce background noise

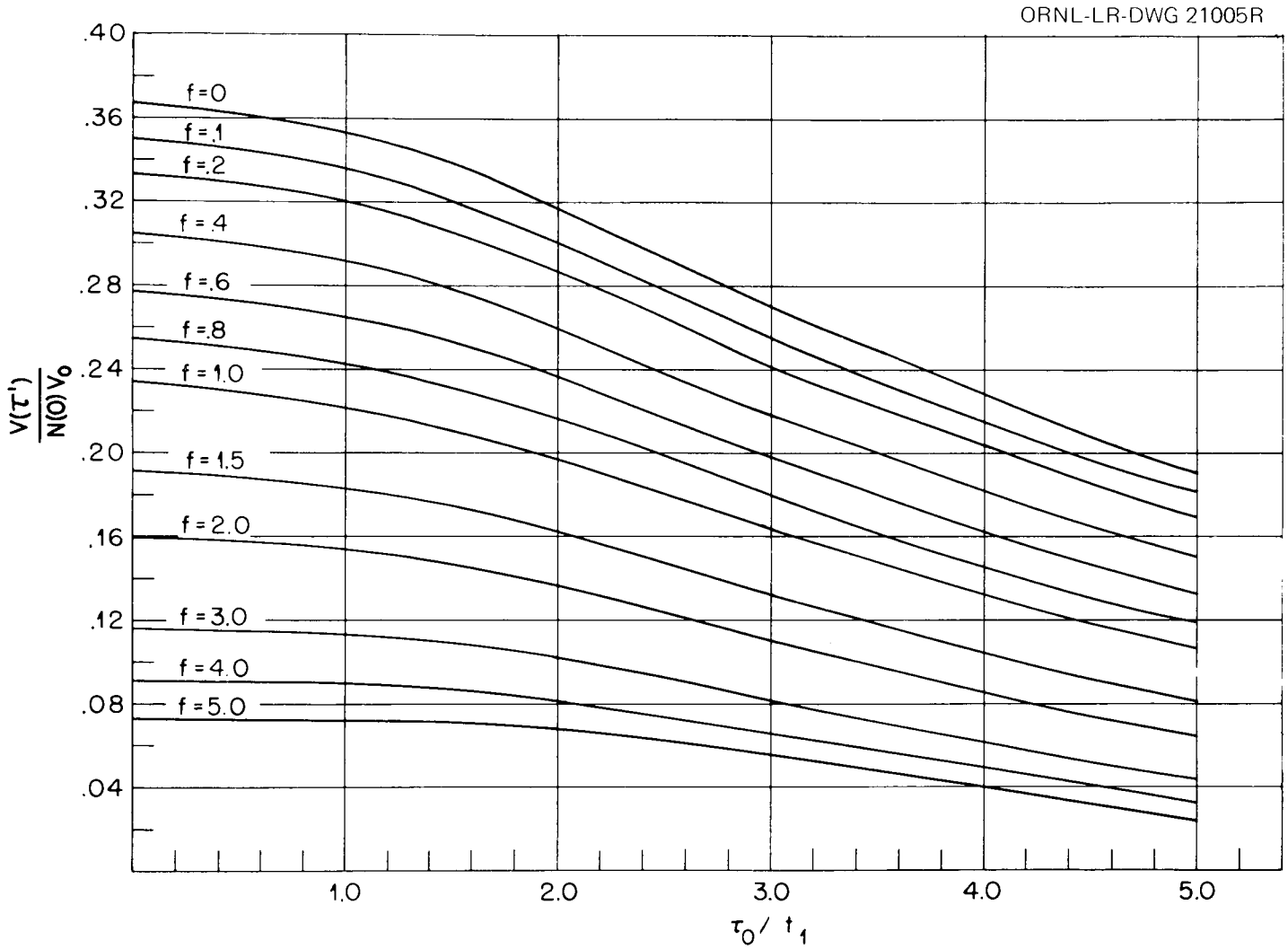

Figure II-2. Dependence of pulse height on τ_0/t_1 for various values of f.

ORNL-DWG. 65-2326A

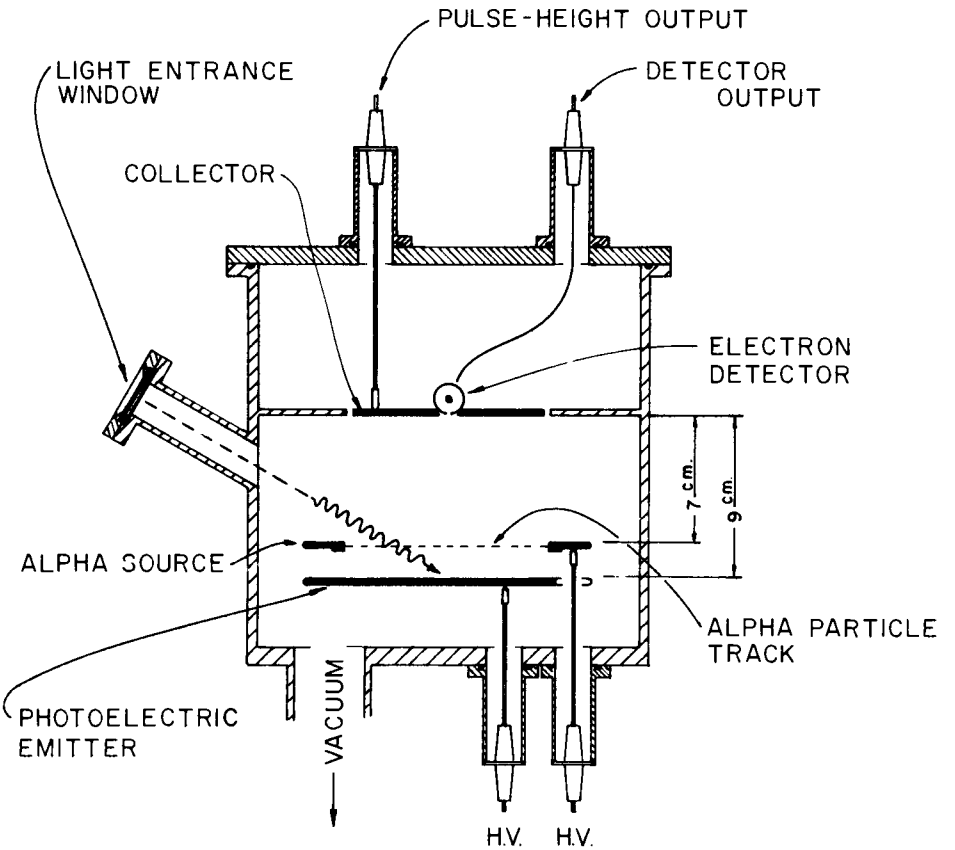

Figure II-3. Swarm apparatus for measurement of electron attachment rate and the drift velocity.

pickup within the chamber. All seals are either metal to metal, including "O" rings, or welded joints.

The temperature of the chamber and all auxiliary tubing leading to the chamber was controlled by wrapping the system with 200-watt heater tapes and by mounting small 200-watt iron heaters on the top and bottom of the chamber. Temperature was regulated to within $\pm$ 1% by a Honeywell-Brown pyrovane temperature regulator, which monitored an iron-constantan thermocouple situated in the chamber, and by several General Radio Company variac autotransformers which were controlled manually. The temperature was monitored by several chromel-constantan thermocouples placed throughout the chamber, which were read with a Honeywell-Brown multipoint recorder. The system is capable of a maximum temperature of about 210°C.

Figure II-4 is a schematic of the complete apparatus except for the auxiliary electronic equipment. Ethylene was vacuum distilled through a set of liquid nitrogen cold traps. Nitrogen and argon were passed through these same cold traps before entry into the chamber. Total pressures were measured with a pressure-sensitive transducer calibrated against a Wallace and Tiernan gauge. The attaching gas pressure was measured with an MKS Baratron pressure meter. A type 90M-XR indicator and 90H-1E 1-torr pressure head capable of pressure readings as low as 1×10^{-5} torr were used. The sensitivity of this type instrument (capacitance manometer) is discussed by Utterback and Griffith (1966).

ORNL DWG. 68-3566

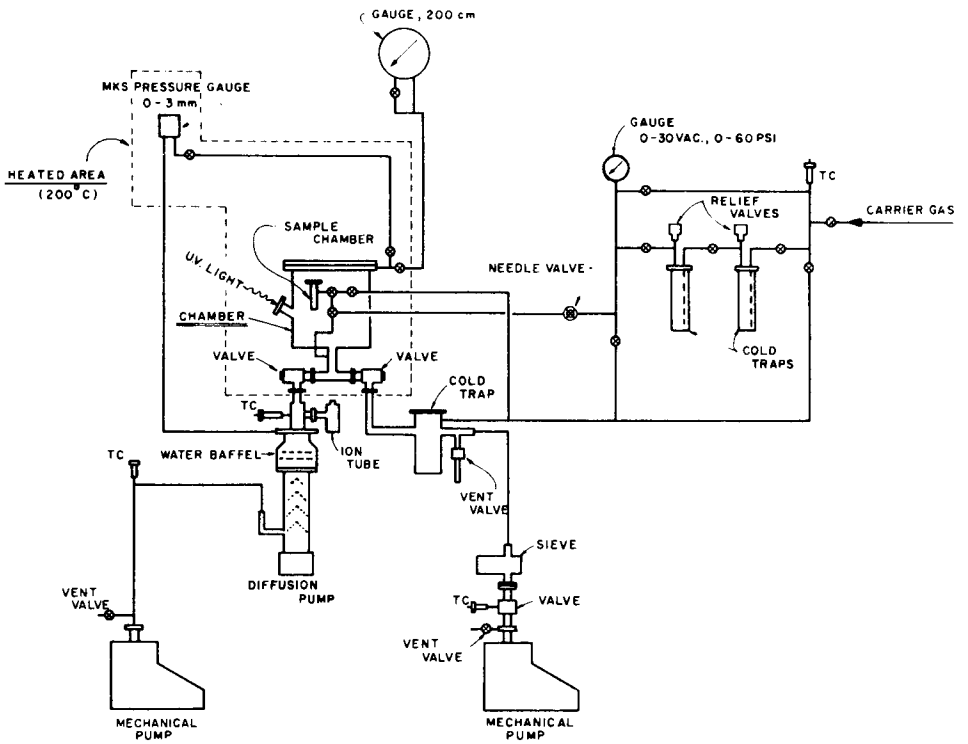

Figure II-4. Schematic of high temperature swarm apparatus.

All other features of the complete apparatus, including auxiliary electronic equipment, are described in detail by Hendrick, Christophorou, and Hurst (1968), and modifications are described by Blaunstein and Christophorou (1968b).

Procedure

Initially the carrier gas was distilled through the liquid nitrogen cold traps on the carrier gas manifold (Figure II-4), and the purified gas was passed into the chamber. Reference pulse heights (maximum voltage variations at the collector) were then collected as a function of E/P. The system was evacuated and a background outgassing rate was obtained prior to entry of the attaching gas sample. The attaching gas was then passed into the chamber and a pressure reading was taken and corrected for outgassing. The carrier gas was passed into the chamber until the same pressure was attained at which the reference pulse heights were taken, and pulse heights were again taken at the same E/P values as the reference pulse heights. From the ratio of the two pulse heights taken at the same E/P value we determined, with the aid of tables given by Eldridge (1962), the quantity $\alpha f_1 Pd$. Knowing the values of $f_1 P$ (sample pressure) and d (drift distance), we then calculated α, the attachment probability per torr of attaching gas per unit distance in the drift direction. The attachment rate was then obtained by multiplying α by the known values of the drift velocity w for the particular carrier gas used. Measurements show [Blaunstein and

Christophorou (1968b)] that the drift velocities in the pure carrier gas are virtually unaffected by the presence of small amounts of attaching gas.

The drift velocities used in the present study were taken from curves given by Christophorou (1969) and represent averages of the best data available. Table II-I gives w versus E/P for C_2H_4, N_2, and Ar at room temperature [Christophorou (1969)]. For higher temperatures the drift velocities of Hendrick, Christophorou, and Hurst (1968) for C_2H_4 and N_2 were used after normalizing their room temperature data to the values given in Table II-I. The drift velocities in Ar do not vary significantly over the temperature range of interest [Pack, Voshall, and Phelps (1962)].

Sources of Error

The main source of error in the present study relates to the pressure measurement of the attaching gas. For extremely low sample pressures, e.g., $\lesssim 1\mu$ ($1\mu = 10^{-3}$ torr), the attachment rate could be reproduced within $\pm$ 20%. For higher sample pressures, αw could usually be reproduced within $\pm$ 10% or better. Negligible error resulted from pulse height measurements. It was found that reference pulse heights were highly reproducible over long periods of time; hence it can be assumed that the pulse height measurements with the attaching gas present were accurate. There was virtually no error in total pressure measurements.

TABLE II-I

ELECTRON SWARM DRIFT VELOCITIES VERSUS E/P IN C_2H_4, N_2, AND Ar

E/P ($V\ cm^{-1}\ torr^{-1}$)	w^a (cm/μsec)		
	C_2H_4	N_2	Ar
0.01	0.098	0.107	0.128
0.02	0.194	0.187	0.155
0.04	0.390	0.255	0.191
0.06	0.580	0.282	0.210
0.08	0.760	0.298	0.224
0.10	0.940	0.314	0.236
0.20	1.750	0.378	0.275
0.30	2.350	0.429	0.300
0.40	2.850	0.475	0.318
0.50	3.310	0.520	0.336
0.60	3.690	0.575	0.353
0.70	4.010	0.630	
0.80	4.260	0.685	
0.90	4.460	0.738	
1.00	4.510	0.792	
1.10	4.740	0.839	
1.20	4.840	0.885	
1.40	4.980	0.977	
2.00	5.100	1.257	

[a]Taken from curves given by L. G. Christophorou, Atomic and Molecular Radiation Physics (John Wiley and Sons, Inc., New York, 1969) (in press).

II. ANALYTICAL TECHNIQUE

The two-body electron attachment rate αw (sec^{-1} $torr^{-1}$) for a particular process is given by

$$\alpha w = N_o (2/m)^{\frac{1}{2}} \int_0^\infty \epsilon^{\frac{1}{2}} \sigma_a(\epsilon) f(\epsilon, E/P) d\epsilon , \qquad \text{(II-9)}$$

where N_o is the number density of attaching molecules per torr at room temperature, m is the mass of the electron, ϵ is the electron energy, $\sigma_a(\epsilon)$ is the attachment cross section, and $f(\epsilon, E/P)$ is the electron energy distribution function. Usually $\sigma_a(\epsilon)$ is not known in absolute units. However, negative-ion yields due to electron impact measured in electron beam studies reflect the shape of the attachment cross section. This is true only when the energy spread of the electron beam is narrow compared to the width of the cross section; otherwise an unfolding procedure is necessary [Christophorou, Compton, and Dickson (1968)]. Thus, if $f(\epsilon, E/P)$ is known (see Chapter III), then one can utilize Equation (II-9) to determine $\sigma_a(\epsilon)$ as described below.

The swarm-beam combination has been described by Christophorou et al. (1965). The attachment cross section can be expressed in terms of the negative-ion current $I(\epsilon)$ through the relation

$$\sigma_{aj} = K_j T_j I(\epsilon), \qquad \text{(II-10)}$$

where K_j is a multiplier that transfers the negative-ion current from

relative to absolute cross section units, and T_j is an operator that translates the energy scale of the negative-ion current so that an independent energy scale calibration can be obtained. The subscript j refers to a particular choice for T (which defines one value for K). Using Equation (II-10) in Equation (II-9), one defines the quantity M_j through the relation

$$M_j \equiv \sum_i \left[(\alpha w)_{ij} - \alpha_i w_i \right]^2$$

$$= \sum_i \left[N_o (2/m)^{\frac{1}{2}} K_j \int_0^\infty \epsilon^{\frac{1}{2}} T_j I(\epsilon) f_i(\epsilon) d\epsilon - \alpha_i w_i \right]^2 , \qquad \text{(II-11)}$$

where $\alpha_i w_i$ is the experimental attachment rate for a particular value of E/P (denoted by the subscript i). A best fit to the experimental data is found by solving the equation

$$dM_j / dT_j = 0 \qquad \text{(II-12)}$$

and Equation (II-11) for M_j and K_j for a particular choice of T_j, using various choices of T_j until a minimum for M_j is obtained.

Several comments should be made concerning the swarm-beam technique:

1. As stated previously, the energy width of the electron beam should be narrow compared to the negative-ion resonance.
2. Corrections must be made for any differences in the negative-ion collection efficiency which may occur with incident electron energy.

3. The measured electron attachment rates must be representative of the beam-measured relative cross section, i.e., the attachment rates must reflect only primary processes. Hence, secondary effects due to collisions with third bodies must be somehow subtracted from the experimental attachment rates. This is usually done by extrapolating the attachment rates to zero carrier gas and/or zero attaching gas pressure.
4. In applying the swarm-beam technique one should use experimental attachment rates measured in a carrier gas for which the electron energy distribution functions have a maximum energy overlap with the attachment cross section; if possible, the distribution functions should overlap the cross section completely. This procedure minimizes effects due to errors in measuring either the shape of the attachment cross section or the attachment rates.

In connection with the last comment above, it should be mentioned that the maximum error in the presently accepted distribution functions (Chapter III) occurs on the high-energy side of the distributions, where the functions decrease rapidly with energy. Thus one should use caution in applying the swarm-beam combination if the attachment cross section is weighted heavily on the high-energy side of the distribution functions.

CHAPTER III

ELECTRON SWARM ENERGY DISTRIBUTION FUNCTIONS

I. INTRODUCTION

In the present swarm experiment electrons drift through a mixture of an inert carrier gas and a small sample of attaching gas under the influence of a uniform electric field. The parameters that characterize the electron swarm, w (drift velocity) and D/μ (ratio of diffusion coefficient to mobility), are functions of the carrer gas and E/P, the pressure-reduced electric field. As the electrons drift they gain energy from the electric field and lose energy through elastic and inelastic collisions with molecules of the carrier gas. In attachment studies E/P is usually such that electronic excitation and ionization processes can be ignored, although rotational and vibrational excitations are important for polyatomic carrier gases. Within several mean free paths for electron-molecule collisions the energy-loss and energy-gain mechanisms attain equilibrium. The time required to reach equilibrium is called the relaxation time and at high pressures is usually much shorter than the time required for the swarm to drift several centimeters. Thus, in this case the electron swarm is characterized by an energy distribution function $f(\epsilon, E/P)$ which depends on E/P and the carrier gas.

The distribution function $f(\epsilon, E/P)$ is defined such that $f(\epsilon, E/P)d\epsilon$ is the fraction of electrons with energies between ϵ and $\epsilon + d\epsilon$ at a particular value of E/P. Thus,

$$\int_0^\infty f(\epsilon, E/P)d\epsilon = 1. \qquad \text{(III-1)}$$

The need for accurate knowledge of the various energy distribution functions is made manifest when one attempts to analyze swarm data on electron attachment in terms of the absolute attachment cross section $\sigma_a(\epsilon)$. The swarm-determined attachment rate αw (sec^{-1} $torr^{-1}$) is given by Equation (II-9), which involves $\sigma_a(\epsilon)$ and $f(\epsilon, E/P)$. Through application of the swarm-beam combination (Chapter II), $\sigma_a(\epsilon)$ can be determined. Thus, in order to render the swarm-beam combination meaningful, it is essential to have accurate knowledge of the electron energy distribution functions. In the absence of electron beam data, valuable qualitative knowledge about the attachment cross section can still be gained if the distribution functions are known.

The purpose of the present study is to examine certain experimental data which strongly support choices between the most reliable distribution functions reported for the carrier gas molecular nitrogen (N_2) and between a Maxwell and a Druyvesteyn distribution for ethylene (C_2H_4).

II. MOTIONS OF SLOW ELECTRONS IN GASES

General Comments

Discussions, general theoretical treatments, and reviews concerning the motions of low-energy electrons in gases can be found in Massey and Burhop (1952), Chapman and Cowling (1952), Allis (1956), Loeb (1960), Huxley and Crompton (1962), McDaniel (1964), and Christophorou (1969). In particular, Loeb gives a comprehensive historical account of the work done on determining various energy distribution functions before 1955 and Christophorou discusses work after 1955; Allis presents a thorough theoretical treatment of the motions of slow electrons in gases.

In general the velocity distribution function $f_v(\vec{v}, t, E/P)$ of an electron swarm obeys the Boltzman equation

$$\frac{\delta f_v}{\delta t} = \frac{\partial f_v}{\partial t} + \vec{v} \cdot \vec{\nabla} f_v + \frac{\vec{F}}{m} \cdot \vec{\nabla}_v f_v , \qquad \text{(III-2)}$$

where $\vec{v}$ is the electron velocity, m is the electron mass, $\vec{F}$ is the external force acting on the electrons, $\vec{\nabla}$ is the gradient operator in configuration space, $\vec{\nabla}_v$ is the gradient operator in velocity space, $\delta f_v/\delta t$ is the rate of change of f_v due to collisions with gas molecules, and $\partial f_v/\partial t$ is the rate of change of f_v due to variation of $\vec{F}$. In Equation (III-2) electron-electron interactions have been neglected. Under steady state conditions $\partial f_v/\partial t$ is zero, and, since $\delta f_v/\delta t$ is statistical in nature and does not involve time

explicitly, the Boltzmann equation becomes time-independent. In addition, in the presence of a homogeneous gas, $\vec{\nabla} f_v$ is also zero and Equation (III-2) becomes space-independent. It is the time- and space-independent solution of Equation (III-2) that is of interest in the present study.

Solving the Boltzmann equation is difficult in general and several methods of solution are discussed by Chapman and Cowling (1952) and by Allis (1956). Solutions are known for the space- and time-independent equation. Thus, the main problem lies in the lack of accurate cross sections for the various collision processes involved for the various gases of interest.

Electron Swarm Energy Distribution Functions for the Carrier Gas Argon

Ritchie and Whitesides (1961) used a computer program to evaluate equilibrium distribution functions for electrons undergoing only elastic collisions in a gas in the presence of a uniform electric field. The form of the solution to Equation (III-2) used was taken from Chapman and Cowling and is given by

$$f(\epsilon, E/P) = B\,\epsilon^{\frac{1}{2}} \exp\left\{ -\frac{6m}{M} \int_0^{\epsilon} \frac{\sigma_m^2(\epsilon)\,\epsilon d\epsilon}{\left[(eE/P)^2 + \frac{6m}{M}\,\epsilon\sigma_m^2(\epsilon)\,kT\right]} \right\}, \quad \text{(III-3)}$$

where e and m are the mass and charge of the electron, respectively, M is the mass of the gas molecule, E is the electric field strength, T is the gas temperature, k is Boltzmann's constant, and B is a normalization factor

such that

$$\int_0^\infty f(\epsilon, E/P)\, d\epsilon = 1 \,. \tag{III-1}$$

The quantity $\sigma_m(\epsilon)$ is related to the momentum transfer cross section and is given by

$$\sigma_m(\epsilon) = 2\pi N_o \int_0^\pi I(\theta, \epsilon)(1 - \cos\theta)\sin\theta d\theta \,, \tag{III-4}$$

where N_o is the number of gas molecules per cm^3 per torr at room temperature and $I(\theta, \epsilon)$ is the differential cross section for scatter of an electron of energy ϵ through an angle θ by a gas molecule. Ritchie and Whitesides (1961) used the values of $\sigma_m(\epsilon)$ for argon given by Barbiere (1951) to calculate distribution functions over the energy range where inelastic scattering is unimportant.

Nelson and Davis (1968) used the total scattering cross section of Golden and Bandel (1966) for argon and the computer program of Ritchie and Whitesides to calculate $f(\epsilon, E/P)$. Their results are not significantly different from those reported by Ritchie and Whitesides at energies above ~ 0.2 eV. The main difference in the two calculations is that Ritchie and Whitesides used a linear approximation to the Barbiere data which ignored the Ramsauer minimum in the scattering cross section at ~ 0.2 eV, whereas the scattering cross section used by Nelson and Davis included the Ramsauer minimum. At E/P values $\gtrsim 0.05\,V\,cm^{-1}\,torr^{-1}$ the influence of the Ramsauer minimum is negligible.

Frost and Phelps (1964) used Equation (III-3) to calculate electron energy distribution functions in helium, argon, krypton, and xenon. The authors assumed a momentum transfer cross section and adjusted the cross section to obtain consistency between experimental values of w and D/μ and calculated values using formulas given by Allis (1956). In the energy range above the Ramsauer minimum, the momentum transfer cross section determined by Frost and Phelps agrees to within 10% with the cross section of Barbiere (1951). Thus, there is reasonable agreement between the distribution functions of Ritchie and Whitesides (1961) [see also Nelson and Davis (1968)] and those of Frost and Phelps over the energy range of interest.

Electron Swarm Energy Distribution Functions for the Carrier Gas Nitrogen

Carleton and Megill (1962) analyzed the Boltzmann equation and obtained numerically computed solutions for the electron energy distribution functions in nitrogen.

Engelhardt, Phelps, and Risk (1964) obtained a self-consistent set of energy distribution functions, momentum transfer cross sections, and inelastic collision cross sections for electrons in nitrogen from an analysis of transport data (w and D/μ). The distributions of Engelhardt, Phelps, and Risk differ significantly in shape from those obtained by Carleton and Megill as seen in Figure III-1 (see Section III for experimental test).

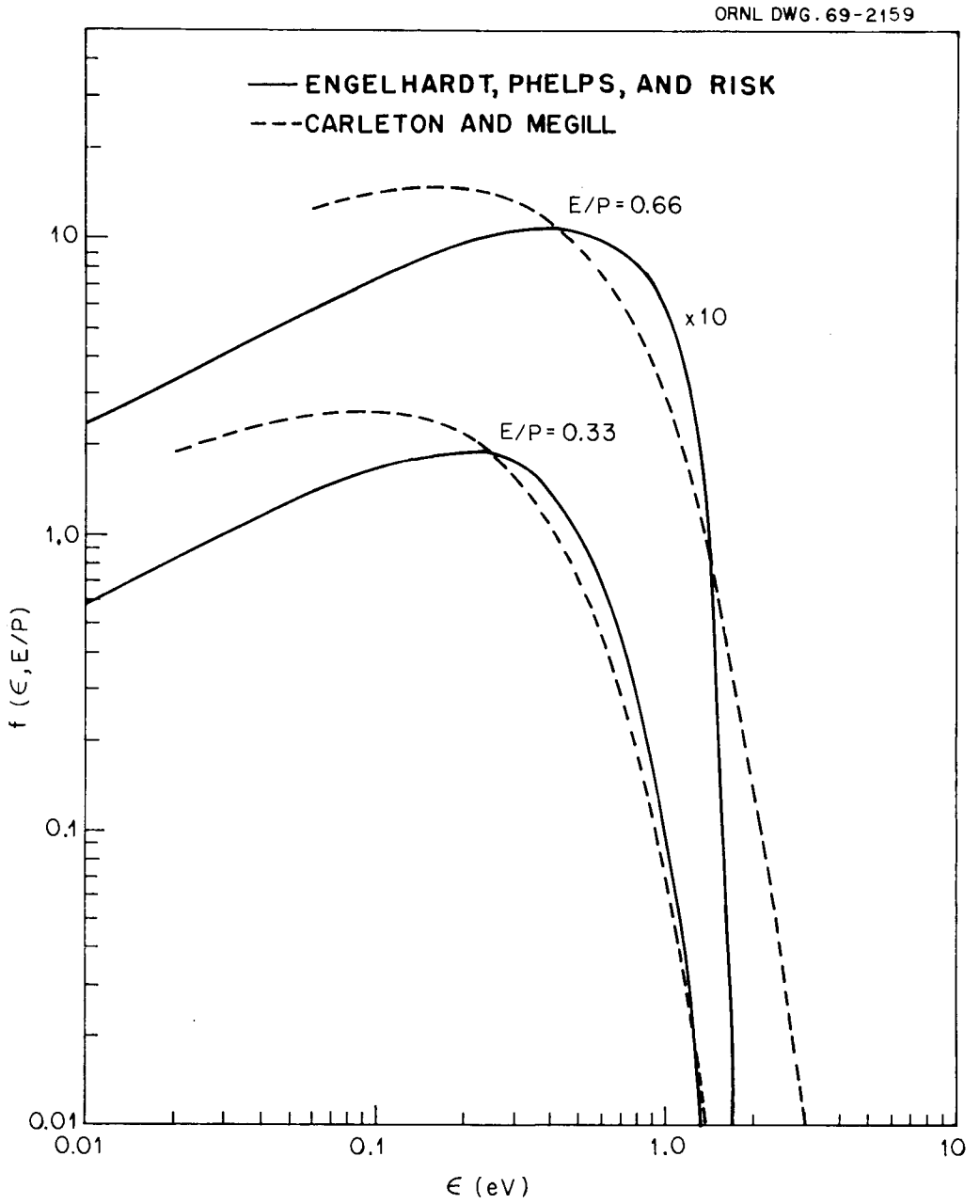

Figure III-1. Two different calculations of $f(\epsilon, E/P)$ for N_2 at the same E/P value.

Electron Swarm Energy Distribution Functions for the Carrier Gas Ethylene

Either a Maxwell or a Druyvesteyn distribution function is usually assumed for electrons in ethylene at low E/P ($\lesssim 2\,\mathrm{V\,cm^{-1}\,torr^{-1}}$). The familiar Maxwell formula is given by

$$f_M(\epsilon, E/P) = \frac{2\epsilon^{\frac{1}{2}}}{\pi^{\frac{1}{2}}(kT)^{3/2}} \exp - \epsilon/kT \,. \qquad \text{(III-5)}$$

Assuming the electronic mean free path for collisions with molecules to be constant and considering only elastic collisions, Druyvesteyn (1930) derived the following distribution function

$$f_D(\epsilon, E/P) = C\,\epsilon^{\frac{1}{2}} \exp - \frac{3m\epsilon^2}{M\lambda^2 e^2 E^2} \,, \qquad \text{(III-6)}$$

where e and m are the electron charge and mass, respectively, M is the molecular mass, λ is the electronic mean free path for collisions with molecules, and C is a normalization constant. Figure III-2 [McDaniel (1964)] compares f_M and f_D for the same mean energy. There is a significant different in the shapes of these two functions.

In order to determine the mean electron energy of a Maxwell or a Druyvesteyn distribution at a particular E/P value, one uses experimental values of D/μ as a function of E/P and the relation [see, for example, Christophorou (1969)]

$$D/\mu = \frac{2A'\,k_T\,\langle\epsilon_M\rangle}{3e} \,, \qquad \text{(III-7)}$$

ORNL DWG 69-8965R

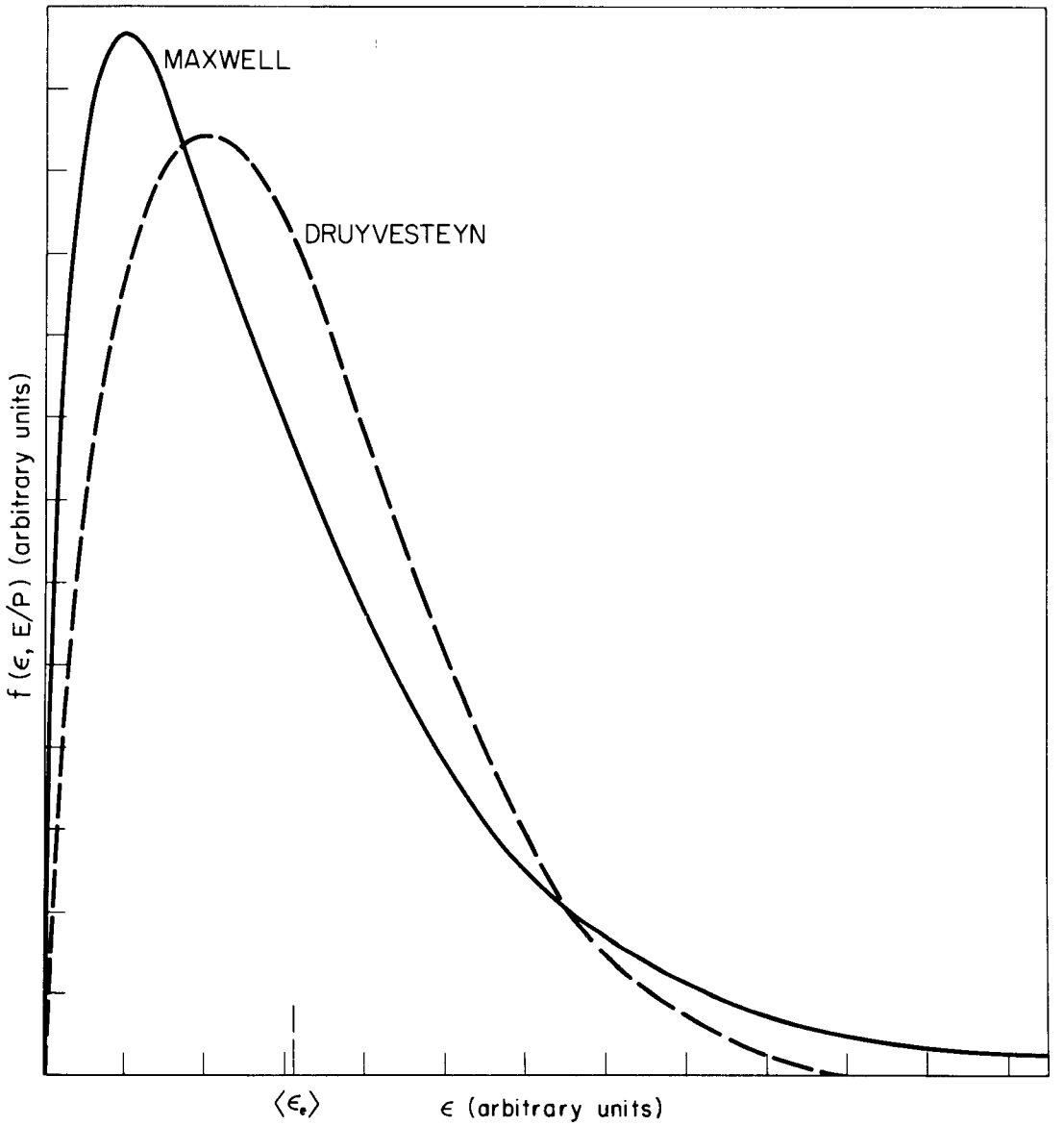

Figure III-2. Maxwell and Druyvestyn representations of $f(\epsilon, E/P)$ for the same $\langle \epsilon_e \rangle$.

where $\langle \epsilon_M \rangle$ is the mean thermal molecular energy (3/2 kT), k_T is the Townsend energy factor, and A′ is a constant depending on the energy distribution function. For a Maxwell distribution, A′ is 1.00 and for a Druyvesteyn distribution, A′ is 1.14. The Townsend energy factor is defined by the relation

$$k_T \equiv \frac{\langle \epsilon_e \rangle}{\langle \epsilon_M \rangle} , \tag{III-8}$$

where $\langle \epsilon_e \rangle$ is the average electronic energy. Thus, Equation (III-7) can be written

$$D/\mu = \frac{2A' \langle \epsilon_e \rangle}{3e} . \tag{III-9}$$

III. CONSIDERATION OF EXPERIMENTAL DATA

Discussion

There have been no direct experimental verifications of the electron energy distribution functions reported in the literature. Aside from direct observation, another way to uniquely specify a distribution function is to state all of its moments (see texts on statistics). The moment of a distribution is defined such that if $g(\eta)$ is a distribution in some quantity η, then the nth moment is given by

$$M_n \equiv \int_{\eta_{min}}^{\eta_{max}} \eta^n \, g(\eta) \, d\eta , \tag{III-10}$$

where $n = 0, 1, 2 \ldots \infty$. Unfortunately, there is no experimental method to verify even the first few moments of an electron energy distribution function.

On a purely physical basis it can be stated that the distribution function for a given gas at a particular E/P value is unique. Thus, if one has several sets of apparently reliable distribution functions, a reasonable experimental test of the distributions would be to collect a set of experimental observables related to the true distributions through a known weighting function and determine which form of the distribution function reproduces the experimental values through calculation. Thus, a test of the electron energy distribution functions would be to compare the experimentally measured attachment rates for a given process with the attachment rates calculated from Equation (II-9) using an independently determined cross section. The problem in this case is to find an accurate cross section for a process for which good swarm data are available. Usually cross sections are given in relative units, e.g., negative-ion-current values. However, if a relative cross section with accurate energy calibration is available, then one can perform the swarm-beam combination (Chapter II) and judge the reliability of the distribution functions by the magnitude of T_j, the energy shift of the negative-ion current necessary to give best fit between the experimental and calculated attachment rates. T_j should be close to zero if the distribution functions are indeed correct and if the energy calibration of the relative cross section is accurate.

Argon

Rapp and Briglia (1965) measured the cross section for O^- production from N_2O (O^-/N_2O). The cross section for this process has been found to be temperature dependent and it has been shown (Chapter IV) that the cross section of Rapp and Briglia is characteristic of a temperature close to 373° K. Figure III-3 compares the experimental attachment rates at 373° K (see Chapter IV) for N_2O in argon with the attachment rates calculated from Equation (II-9), using the Rapp and Briglia cross section and the distribution functions of Ritchie and Whitesides (1961). It is seen that the agreement is very good. Figure III-4 shows the large energy overlap between the attachment cross section and the distribution function for $E/P = 0.2\ V\,cm^{-1}\,torr^{-1}$. Due to the large overlap, the results shown in Figure III-3 are strong support for the distributions of Ritchie and Whitesides.

Chantry (1969c) has given the relative cross section for O^-/N_2O at 370° K. Using this cross section the swarm-beam combination has been performed using attachment rates to N_2O measured in argon at 373° K. The small value of T_j obtained ($T_j = 0.04$ eV) again lends credence to the distributions in argon.

Nitrogen

Figure III-5 compares the distributions of Engelhardt, Phelps, and Risk (1964) for nitrogen to those of Ritchie and Whitesides (1961) for argon. The E/P values are different but the mean energies are approximately the

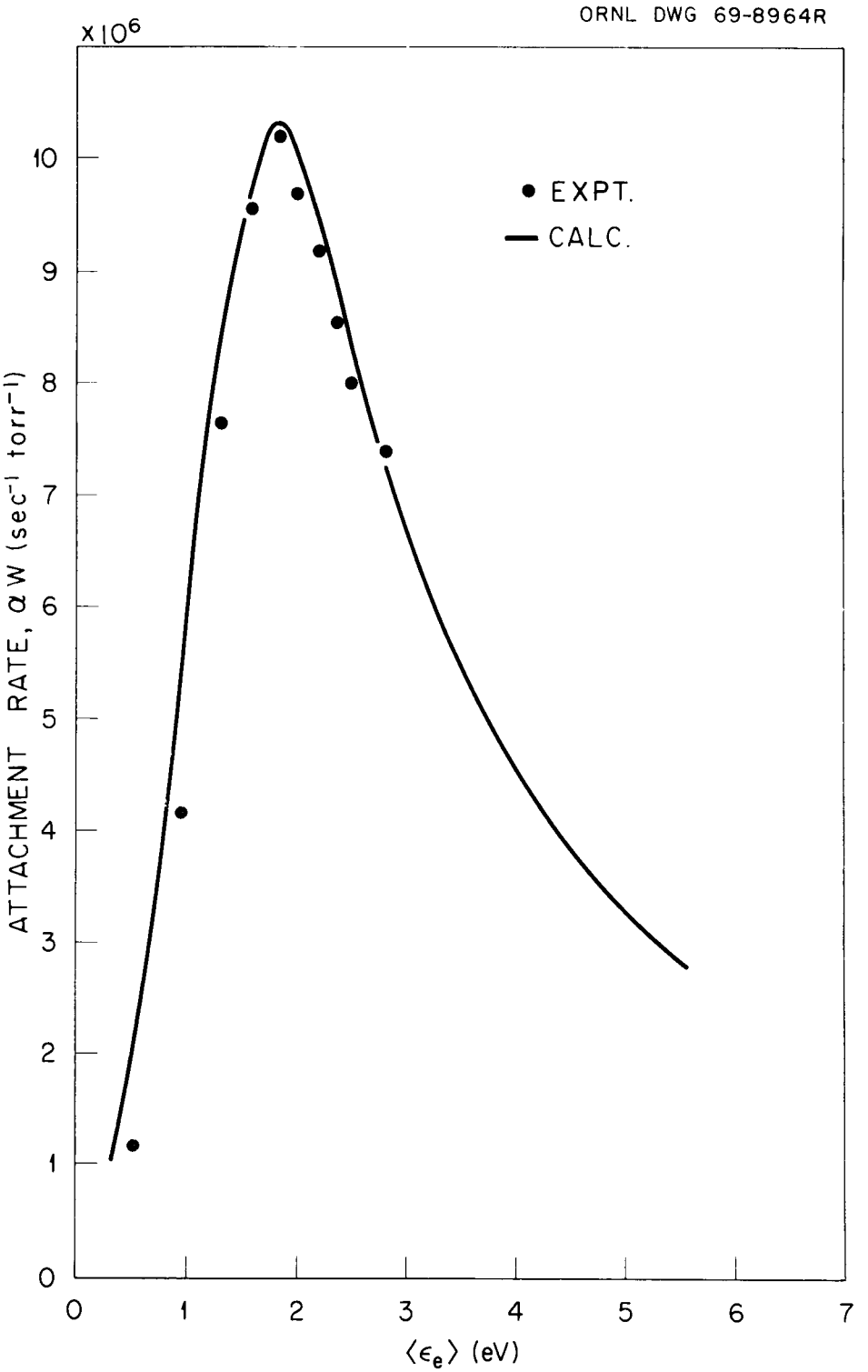

Figure III-3. Calculated and experimental αw for N_2O in Ar.

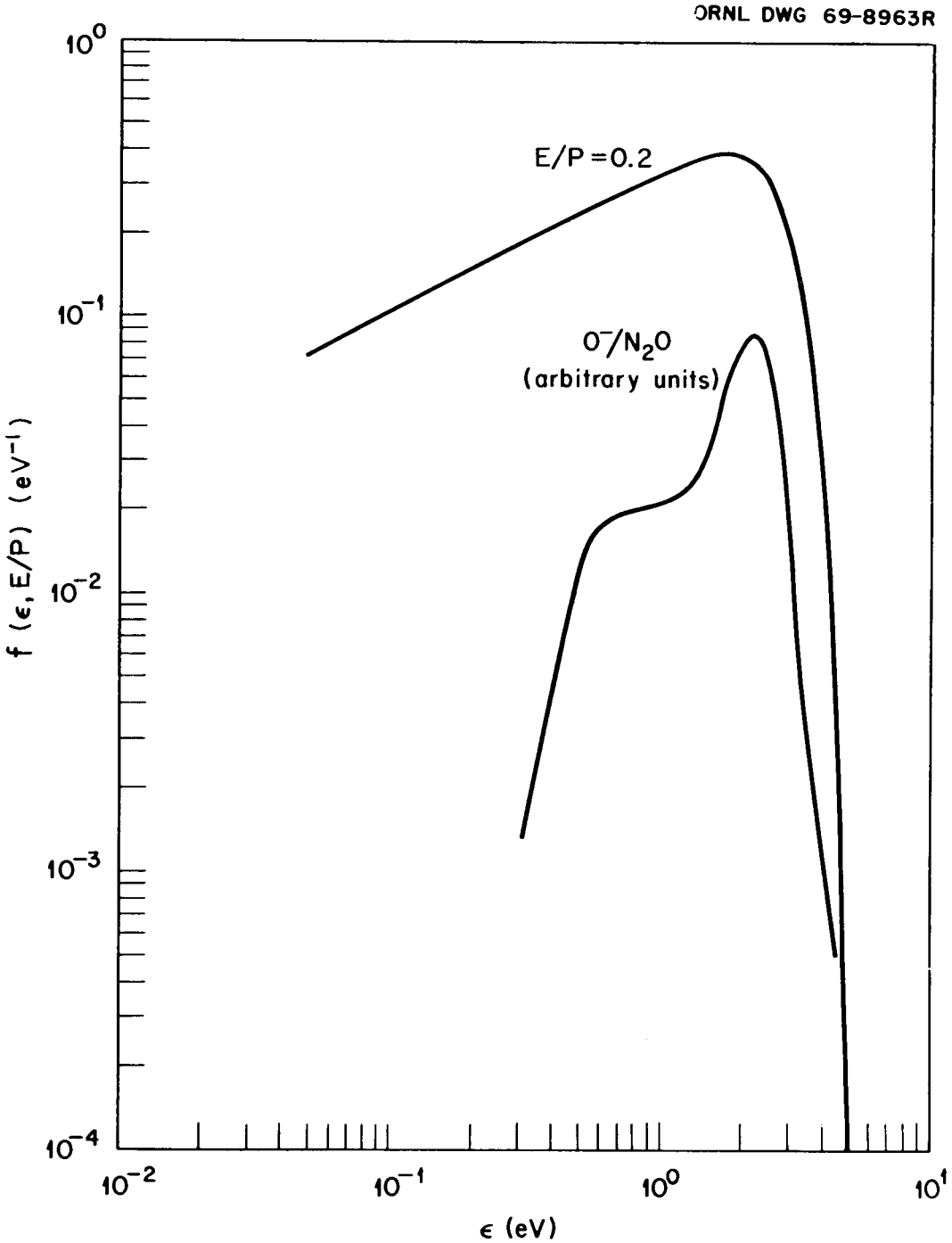

Figure III-4. Overlap between $\sigma_a(\epsilon)$ for O^-/N_2O and $f(\epsilon, E/P)$ for Ar.

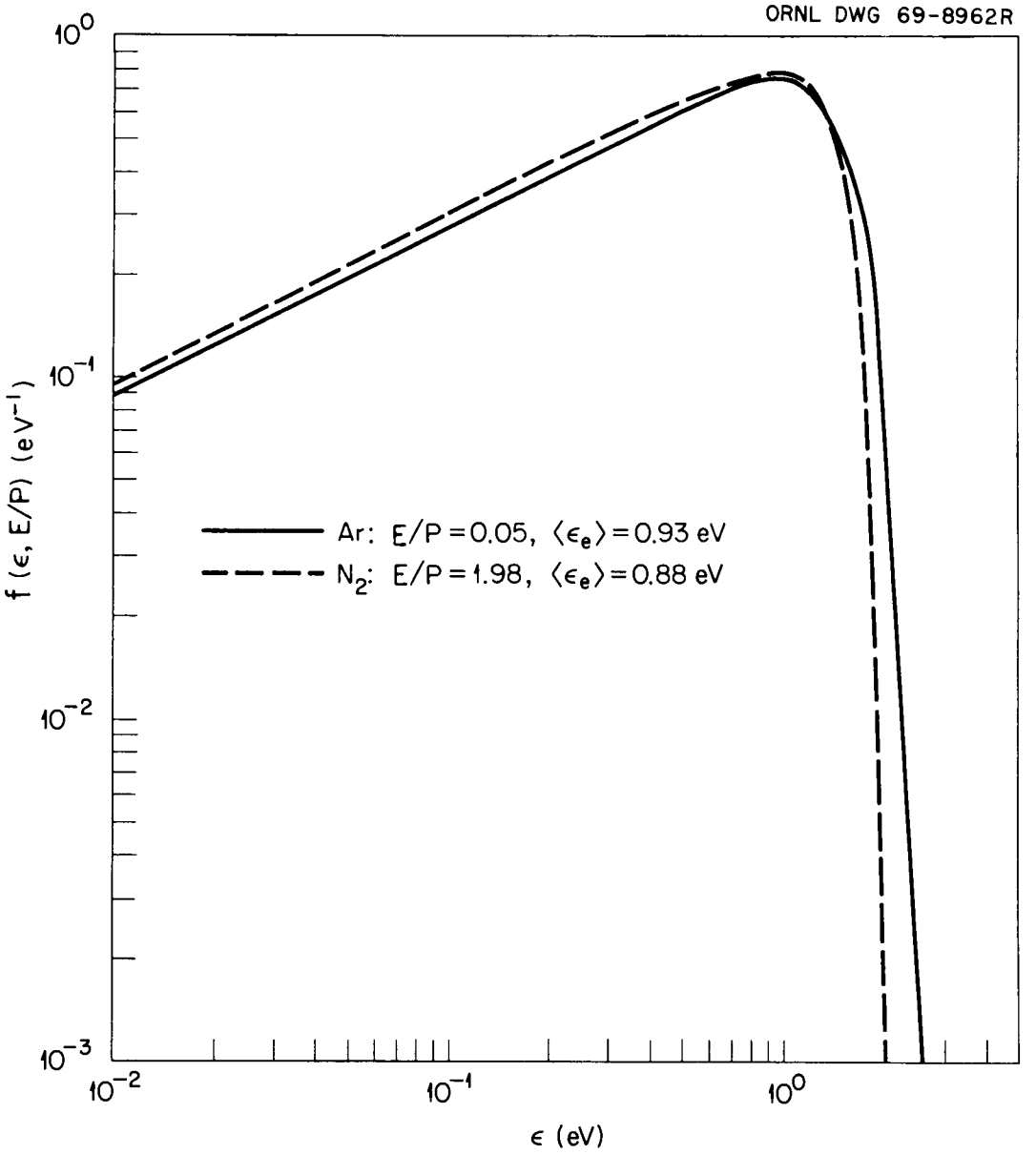

Figure III-5. Comparison of $f(\epsilon, E/P)$ for N_2 and Ar for nearly equal $\langle\epsilon_e\rangle$.

same. The shapes of the argon and nitrogen [Engelhardt, Phelps, and Risk (1964)] distributions having the same $\langle \epsilon_e \rangle$ for $\langle \epsilon_e \rangle \sim 1$ eV bear a close resemblance. As a consequence, Figure III-6 shows that the calculated attachment rates for O^-/N_2O [Christophorou, Chaney, and Christodoulides (1969)], using the argon distributions of Ritchie and Whitesides (1961) and the nitrogen distributions of Engelhardt, Phelps, and Risk, mesh and form a continuous curve when the attachment rates are plotted as a function of $\langle \epsilon_e \rangle$, the mean electron energy. The same calculations performed with the Carleton and Megill (1962) nitrogen distributions do not mesh with the argon calculations.

Christophorou, Carter, and Christodoulides (1969) have studied electron attachment to p-benzoquinone and have determined an attachment cross section peaking at 2.1 eV using the swarm-beam combination with the argon distributions of Ritchie and Whitesides. From the discussion above and Figure III-5 one would expect that if the distributions of Engelhardt, Phelps, and Risk are correct, then the experimental attachment rates measured in nitrogen should mesh with the rates measured in argon when plotted against mean electron energy. Figure III-7 [Christophorou, Chaney, and Christodoulides (1969)] shows that this indeed the case. The attachment rates in nitrogen plotted against mean electron energy as determined from the Carleton and Megill distributions are displaced toward lower energies. Similar results have been observed for azulene and 1,4-naphthoquinone

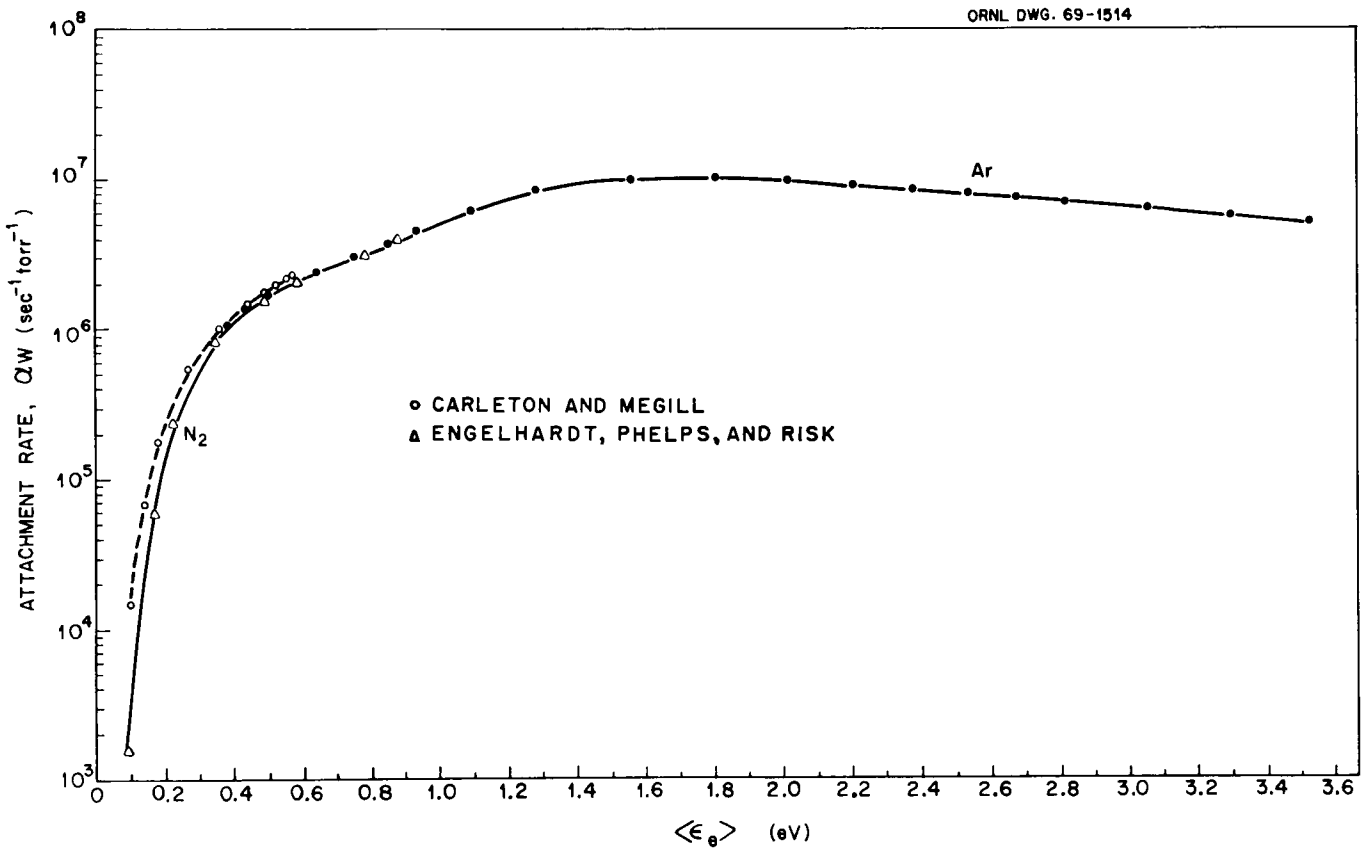

Figure III-6. Comparison of calculated αw for N_2O in N_2 and Ar.

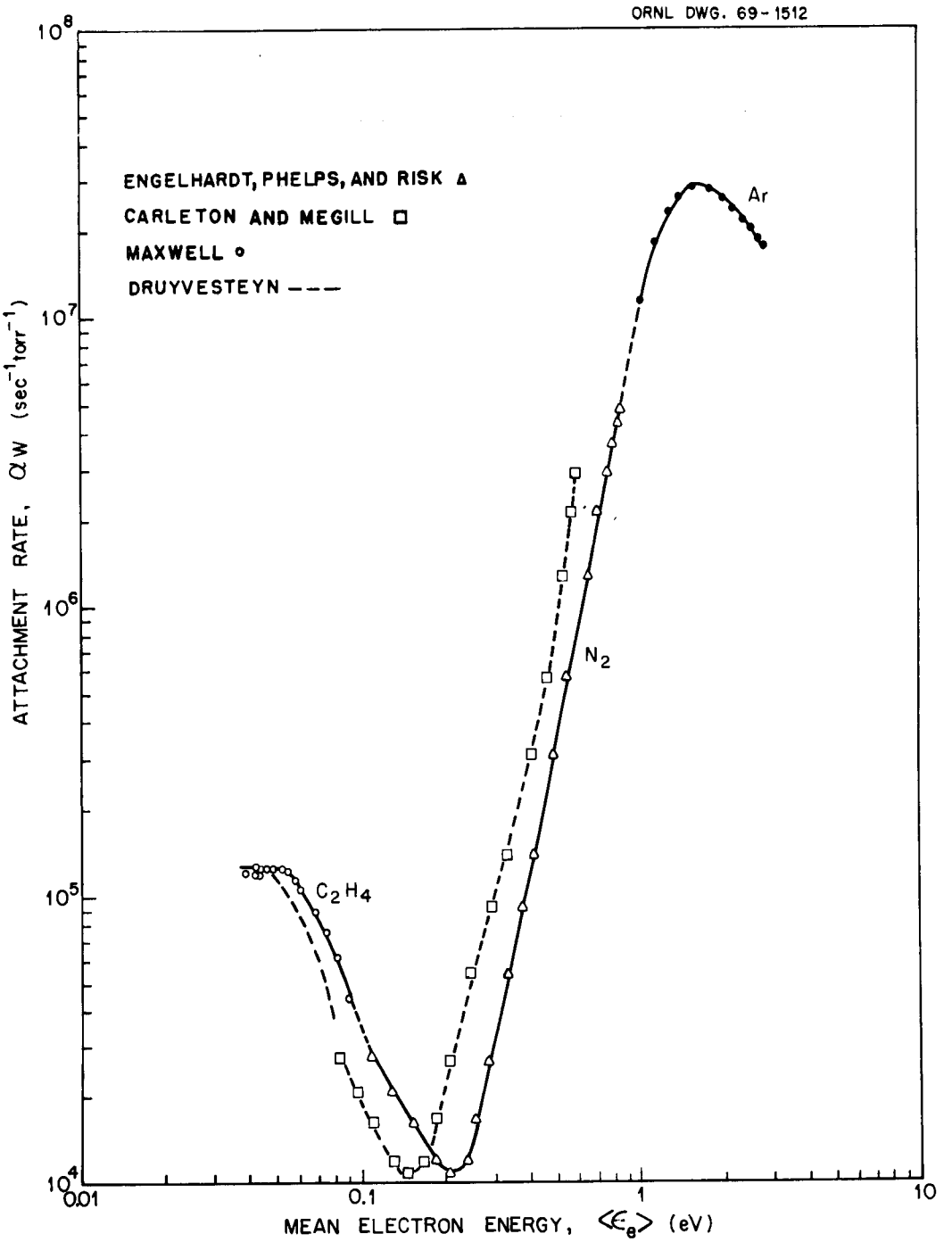

Figure III-7. αw for p-benzoquinone in C_2H_4, N_2, and Ar; comparison of carrier gases.

(Chapter V). Recent data by Christophorou and Christodoulides (1969) also consistently support the above observations.

Figure III-7 and the subsequent observations mentioned above are taken as strong support for the nitrogen distribution of Engelhardt, Phelps, and Risk (1964).

Ethylene

If it is assumed that the distribution function for nitrogen at near-thermal energies ($E/P \lesssim 0.1\ V\ cm^{-1}\ torr^{-1}$) converge to the shape of those in ethylene for the same energy region ($E/P \lesssim 2\ V\ cm^{-1}\ torr^{-1}$), then there should be agreement between data taken in ethylene and nitrogen when the data are plotted against mean electron energy. Figure III-7 shows attachment rates for p-benzoquinone measured in ethylene plotted against mean energy assuming (1) a Maxwell and (2) a Druyvesteyn form for the electron energy distribution functions. The mean energies were calculated using Equation (III-9) and the D/μ data of Wagner, Davis, and Hurst (1967). These authors measured longitudinal-diffusion coefficients, i.e., the coefficients for diffusion in a direction parallel to the electric field. Their values are in reasonable agreement with the data of Bannon and Brose (1928) for lateral diffusion, i.e., diffusion in a direction perpendicular to the electric field, but differ appreciably from the lateral-diffusion data of Cochran and Forester (1962). The latter data disagree substantially with well accepted values of diffusion coefficients for other systems. There is agreement

between attachment rates measured in nitrogen and ethylene when one assumes a Maxwell distribution for the electrons in ethylene. This result is again supported by data given in Chapter V and by the recent data of Christophorou and Christodoulides (1969). Thus, it is concluded that the distribution functions in ethylene are best represented by a Maxwell form.

As mentioned in Chapter II, the maximum error in the accepted distribution functions occurs on the high-energy side where $f(\epsilon, E/P)$ decreases rapidly with electron energy. Thus, calculations weighted heavily in this region should be used with caution.

IV. SUMMARY

Experimental data have been considered which lead one to the conclusion that the electron energy distributions of Ritchie and Whitesides (1961) for Ar and the distributions in N_2 of Engelhardt, Phelps, and Risk (1964) are correct and that the distributions in C_2H_4 are best represented by a Maxwell distribution. These distributions were used in the present study. Table III-I lists $\langle \epsilon_e \rangle$ for a number of E/P values for the three gases.

TABLE III-I

MEAN ELECTRON ENERGY VERSUS E/P AT 300° K FOR ELECTRON SWARMS IN Ar, N_2, AND C_2H_4

Ar		N_2		C_2H_4	
E/P ($V\,cm^{-1}torr^{-1}$)	$\langle\epsilon_e\rangle$[a] (eV)	E/P ($V\,cm^{-1}torr^{-1}$)	$\langle\epsilon_e\rangle$[b] (eV)	E/P ($V\,cm^{-1}torr^{-1}$)	$\langle\epsilon_e\rangle$[c] (eV)
0.01	0.50	0.033	0.057	0.05	0.043
0.05	0.94	0.066	0.093	0.10	0.048
0.10	1.28	0.132	0.162	0.20	0.054
0.15	1.56	0.198	0.225	0.30	0.057
0.20	1.80	0.330	0.349	0.50	0.060
0.25	2.01	0.412	0.421	0.80	0.076
0.30	2.20	0.495	0.490	1.00	0.083
0.40	2.53	0.577	0.538	1.20	0.090
0.50	2.81	0.660	0.583	1.40	0.096
0.80	3.49	0.824	0.656	1.80	0.108
1.00	3.87	0.989	0.710	2.20	0.118
1.20	4.21	1.154	0.754	2.60	0.127
1.50	4.68	1.320	0.787	3.00	0.136
1.70	5.10	1.648	0.841	3.20	0.140
2.00	5.54	1.980	0.878	3.30	0.142

[a]Using the distributions of R. H. Ritchie and G. E. Whitesides, Oak Ridge National Laboratory Report ORNL-3081 (1961).

[b]Using the distributions of A. G. Engelhardt, A. V. Phelps, and C. G. Risk, Phys. Rev. 135, A1566 (1964).

[c]Calculated from the D/μ data of E. B. Wagner, F. J. Davis, and G. S. Hurst, J. Chem. Phys. 47, 3138 (1967), and F. J. Davis and D. R. Nelson (unpublished data) assuming a Maxwell distribution (see text).

CHAPTER IV

ELECTRON ATTACHMENT TO N_2O

I. INTRODUCTION

Nitrous oxide (N_2O) is an interesting molecule to study in that most of the electron attachment phenomena discussed in Chapter I take place, e.g.,

1. Three-body nondissociative capture at high pressures.
2. Dissociative capture in excited vibrational levels.
3. Formation of a temporary negative ion which may decay either elastically or inelastically or may dissociate into $N_2^{(*)}$ plus O^-.

There have been many investigations in recent years concerning electron attachment processes in N_2O. However, the various reactions occurring in electron swarm and electron beam experiments are not yet fully understood, and the results of each method are in uncomfortable agreement. The work described in this chapter has been undertaken in an effort to resolve some of the existing experimental discrepancies and to determine via the swarm-beam combination the electron attachment cross section for O^-/N_2O (O^- formation from N_2O).

II. REVIEW OF PREVIOUS WORK ON ELECTRON ATTACHMENT TO N_2O

Multiple-Collision Experiments

Bradbury and Tatel (1934) studied electron attachment to N_2O at high N_2O pressures and determined the probability of electron attachment per collision as a function of E/P. For E/P values $< 2\,V\,cm^{-1}\,torr^{-1}$ in pure N_2O no attachment was observed for N_2O pressures from 3 to 21 torr. Over the same pressure range dissociative attachment was observed for E/P values $> 2\,V\,cm^{-1}\,torr^{-1}$. The authors were able to determine that the most probable mode of dissociation was cleavage of the N_2-O bond, i.e.,

$$e + N_2O \rightarrow O^- + N_2 \,. \qquad \text{(IV-1)}$$

In agreement with the above results at low electron energies, Ferguson et al. (1967) reported that no N_2O^- ions were observed when N_2O was added to a helium afterglow containing thermal electrons.

The apparent absence of electron attachment to N_2O at thermal energies has been interpreted as due to a near-zero electron affinity for N_2O. Loeb (1955) has pointed out that atoms with closed shells, electron pairs or octets do not have positive electron affinities in the ground state while most other atomic systems do. (Excited states, however, may possess a positive electron affinity even if the ground state does not.) It is further pointed out that equivalent molecular structures, e.g., $^1\Sigma$, would be expected to demonstrate similar behavior and, in particular, N_2O would not be expected to attach electrons nondissociatively in the ground state.

The existence of the N_2O^- ion, however, has been recently established by Paulson (1966) who observed its formation via an ion molecule reaction originally postulated to be

$$O^- + N_2O \rightarrow N_2O^- + O. \qquad \text{(IV-2)}$$

More recent results by Chantry (1969b), however, have shown the reaction to be

$$NO^- + N_2O \rightarrow N_2O^- + NO. \qquad \text{(IV-3)}$$

Presumably, the ions and molecules involved have several electron volts of energy available for the reaction.

Ferguson et al. (1967) discussed the apparent absence of electron attachment at low energies in terms of the differing geometries of the N_2O molecule and the N_2O^- ion. It was argued that the N_2O^- ion has a bent configuration as opposed to the linear configuration of the N_2O molecule. Thus, an activation energy of ~ 1 eV was quoted as necessary to attach an electron to N_2O.

In contrast to the above studies and comments, Phelps and Voshall (1968) presented evidence suggesting the three-body attachment process

$$e + N_2O + N_2O \rightarrow N_2O^- + N_2O + \text{energy} \qquad \text{(IV-4)}$$

in pure N_2O at thermal energies for pressures ranging from 30 to 300 torr at 300° K. A thermal value of the apparent three-body attachment rate

coefficient of $6 \pm 1 \times 10^{-33}$ $cm^6 sec^{-1}$ was obtained. At higher E/P values two-body attachment was observed, consistent with dissociative attachment at higher electron energies.

In support of the above results, Warman and Fessenden (1968) reported a thermal value of the three-body attachment rate coefficient of $5.6 \pm 0.2 \times 10^{-33}$ $cm^6 sec^{-1}$ determined in a microwave afterglow experiment for N_2O pressures from 10 to 200 torr at 300° K.

In addition to the above studies, Moruzzi and Dakin (1969) and Chantry (1969b) have studied ion-molecule reactions in N_2O. No N_2O^- ions were observed which could be attributed to process (IV-4); furthermore, no processes involving collisional detachment of electrons were postulated in any reaction schemes to explain experimental results. The latter point is important since an electron detachment process is the only ion-molecule type reaction that could affect the results of the present study since these results are insensitive to the subsequent fate of an electron once it has been removed from the swarm, unless, of course, it is returned to the swarm.

Single-Collision Beam Experiments

Knox and Burtt (1958) reported the first mass-spectrometric study of negative ions formed in N_2O on impact of 0 to 50 eV electrons. Only the O^- ion was found, with a resonance capture peak occurring at 2.5 ± 0.2 eV.

Schulz (1961) used the trapped-electron method as well as conventional electron beam techniques to study electron impact on N_2O. Results

from the trapped-electron method showed an inelastic scattering process at 2.2 eV which was attributed to inelastic decay of a temporary negative ion into vibrationally excited N_2O and a free electron. Christophorou and Carter (1968) have presented evidence, however, that the above temporary negative ion decays predominantly via an elastic mode.

In addition, the conventional beam data of Schulz (1961) on negative ion current due to O^- production revealed peaks at 0.7 eV and 2.2 eV, with onset occurring at ~ 0 eV. The low-energy process was attributed to dissociative attachment, apparently with enhanced probability, to vibrationally excited N_2O with the high-energy process being interpreted as due to subsequent dissociation of the temporary negative ion mentioned above into vibrationally excited N_2 plus O^-.

Using the relation

$$D(N_2 - O) - EA(O) = AP(O^-) \qquad \text{(IV-5)}$$

[where $D(N_2 - O)$ is the dissociation energy of the $N_2 - O$ bond, EA(O) is the electron affinity of O, and $AP(O^-)$ is the appearance potential of O^-/N_2O determined from electron beam data], and EA(O) taken from Branscomb et al. (1958), Schulz determined $D(N_2 - O)$ to be 1.2 ± 0.2 eV, in fair agreement with the value of 1.34 ± 0.2 eV determined by Curran and Fox (1961), but lower than the value of 1.67 eV determined by Schulz (1961) from thermochemical data.

In defense of the latter value of $D(N_2 - O)$, Kaufman (1967) has pointed out that there is essentially no reason to doubt the thermochemical data which have been consistently supported by many investigations dating back to the late nineteenth century. He suggests that the early O^- onset observed by Schulz (1961) may be due to contributions from electron attachment to vibrationally or rotationally excited N_2O. Such an hypothesis could be tested by temperature dependence studies of electron attachment near threshold.

In addition to the above beam experiments are the studies of Curran and Fox (1961), Rapp and Briglia (1965), and Rempt (1968). All three investigations agreed with the results of Schulz on the 2.2 eV process; however, there were profound discrepancies among all investigations as to the shape of the low-energy process, although O^- onset occurred at ~ 0 eV in each case. Mass analysis by Curran and Fox failed to yield N_2O^-.

Recently Chantry (1969a), in support of Kaufman's hypothesis, reported a very strong temperature dependence of dissociative attachment to N_2O below 2 eV for temperatures ranging from 160° K up to 1040° K. There was no observable temperature dependence above 2 eV.

Comments on Available Data on Electron Attachment to N_2O

Several striking features present themselves concerning the data reviewed above:

1. Beam data do not support the formation of N_2O^- via a primary process, i.e., process (IV-4), as apparently occurs in high-pressure experiments.
2. Electron attachment rates determined by Phelps and Voshall (1968) and deduced from earlier experiments by Bailey and Rudd (1932) and Bradbury and Tatel (1934) do not reflect the high attachment cross section determined by Rapp and Briglia (1965).
3. The apparent early O^- onset observed in various beam experiments is questionable.
4. In view of the temperature dependence of the shape of the attachment cross section below ~ 2 eV, the absolute cross section determined by Rapp and Briglia (1965), as well as the relative cross sections of others, should be assigned to a temperature.

III. EXPERIMENTAL CONSIDERATIONS

The apparatus and experimental procedure were discussed in Chapter II. The N_2O was supplied both by the J. T. Baker Chemical Company and the Matheson Company and was of 98% minimum purity. The main impurity was stated to be air; thus, the only contaminant of any consequence, O_2, was present in quantities $< 0.4\%$. The Ar ($> 99.995\%$ purity) and N_2 ($> 99.9\%$ purity) were supplied by the Matheson Company.

All straight lines shown in subsequent figures were obtained by a least squares fitting to the experimental points. All pressures were normalized to room temperature.

IV. EXPERIMENTAL RESULTS

N_2O-Ar Mixtures

The electron attachment rate, αw (sec^{-1} $torr^{-1}$), to N_2O was measured at various temperatures for N_2O-Ar mixtures containing small amounts of N_2O. Both Ar and N_2O pressures were varied. In Figure IV-1 αw is plotted as a function of N_2O pressure, P_{N_2O}, for several values of the pressure-reduced electric field, E/P ($V\,cm^{-1}torr^{-1}$), for total pressures of 1000 and 500 torr at 373° K. The variation over the higher N_2O pressures is attributed to the effect of N_2O on the electron energy distribution function in pure Ar. In support of this argument is the fact that the slope of the second line (high N_2O pressures) approaches zero for each E/P as the total pressure increases. The extrapolated values of αw indicated on the ordinate axis were highly reproducible for each E/P at all total pressures (400, 500, 750, and 1000 torr).

In Figure IV-2 αw is plotted as a function of E/P at 373° K for various N_2O partial pressures at a total pressure of 500 torr. For N_2O pressures below ~ 8 microns the value of E/P for which αw is a maximum is unchanged. As the N_2O pressure increases beyond 8 microns, however,

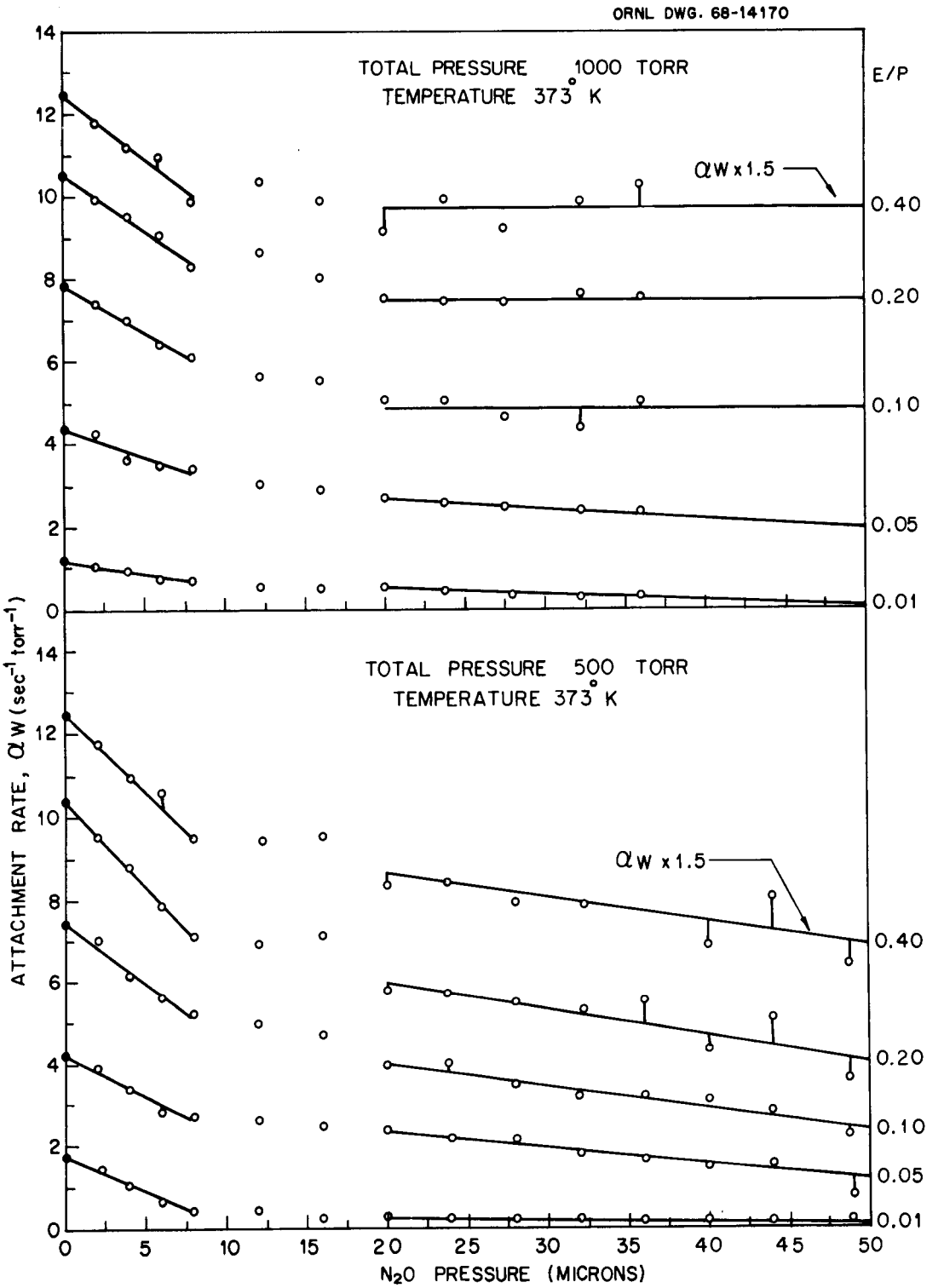

Figure IV-1. Experimental αw for N_2O in Ar as a function of P_{N_2O} for various E/P values.

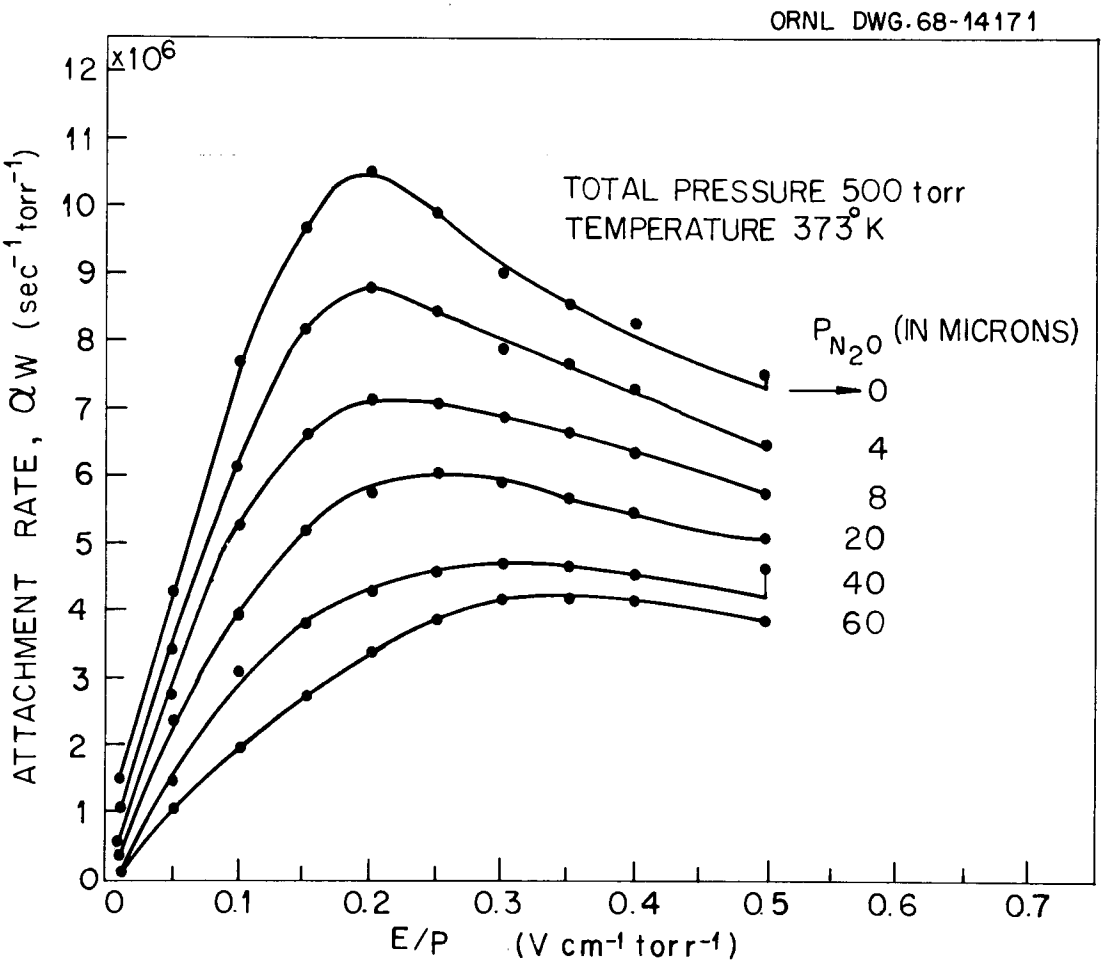

Figure IV-2. Experimental αw for N_2O in Ar as a function of E/P for various values of P_{N_2O}.

the value of E/P for which the attachment rate maximizes increases, indicating a shift of the electron energy distributions to lower energies as a result of the increasing number of elastic and inelastic collisions of electrons with N_2O molecules. From the data presented in Figures IV-1 and IV-2, one can conclude that there is no appreciable effect on the electron energy distribution functions in Ar for N_2O partial pressure $\lesssim 10^{-5}$.

Figure IV-3 shows αw versus the ratio of the N_2O to Ar pressure, P_{N_2O}/P_{Ar}. The extrapolated values of αw for $P_{N_2O}/P_{Ar} \rightarrow 0$ are in excellent agreement with the extrapolated values for $P_{N_2O} \rightarrow 0$ for each total pressure. The extrapolated values of αw are plotted in Figure IV-4 as a function of E/P for the temperatures 323°, 373°, and 473° K. For E/P value $\lesssim 0.2$ the attachment rates increase with increasing temperature, while at higher E/P values no significant change is observed.

The attachment cross section of Rapp and Briglia (1965) was used in conjunction with the electron energy distribution functions of Ritchie and Whitesides (1961) to calculate αw using the formula

$$\alpha w = N_o (2/m)^{\frac{1}{2}} \int_0^\infty \sigma_a(\epsilon)\, f(\epsilon, E/P)\, \epsilon^{\frac{1}{2}} d\epsilon \,. \qquad \text{(II-9)}$$

The results of these calculations are compared in Figure IV-5 with the present experimental results as a function of the mean electron energy, $\langle \epsilon_e \rangle$. The attachment rates calculated as described above are in excellent agreement with the present experimental results at 373° K.

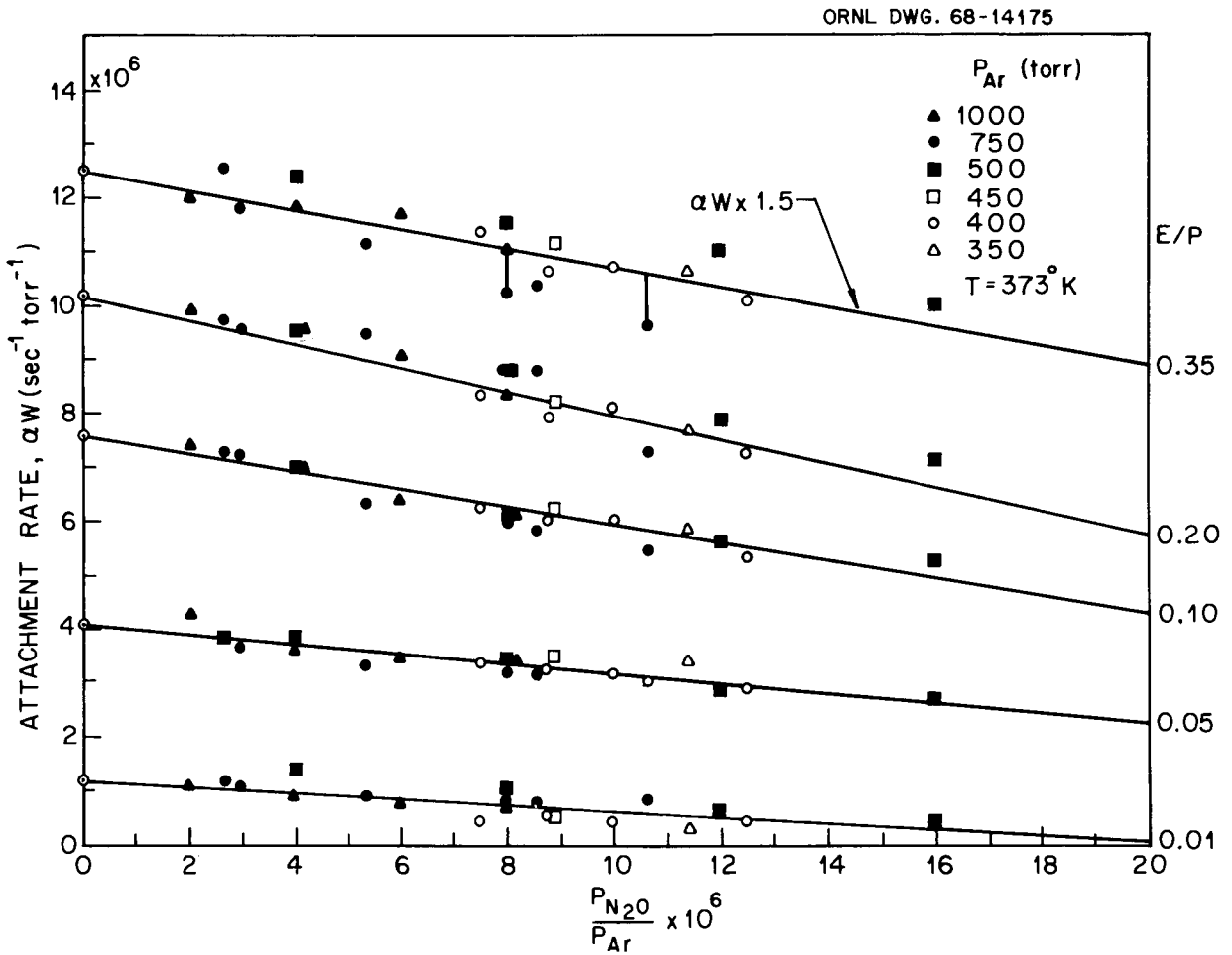

Figure IV-3. Experimental αw for N_2O in Ar versus P_{N_2O}/P_{Ar} for various E/P values.

ORNL DWG. 68-14173

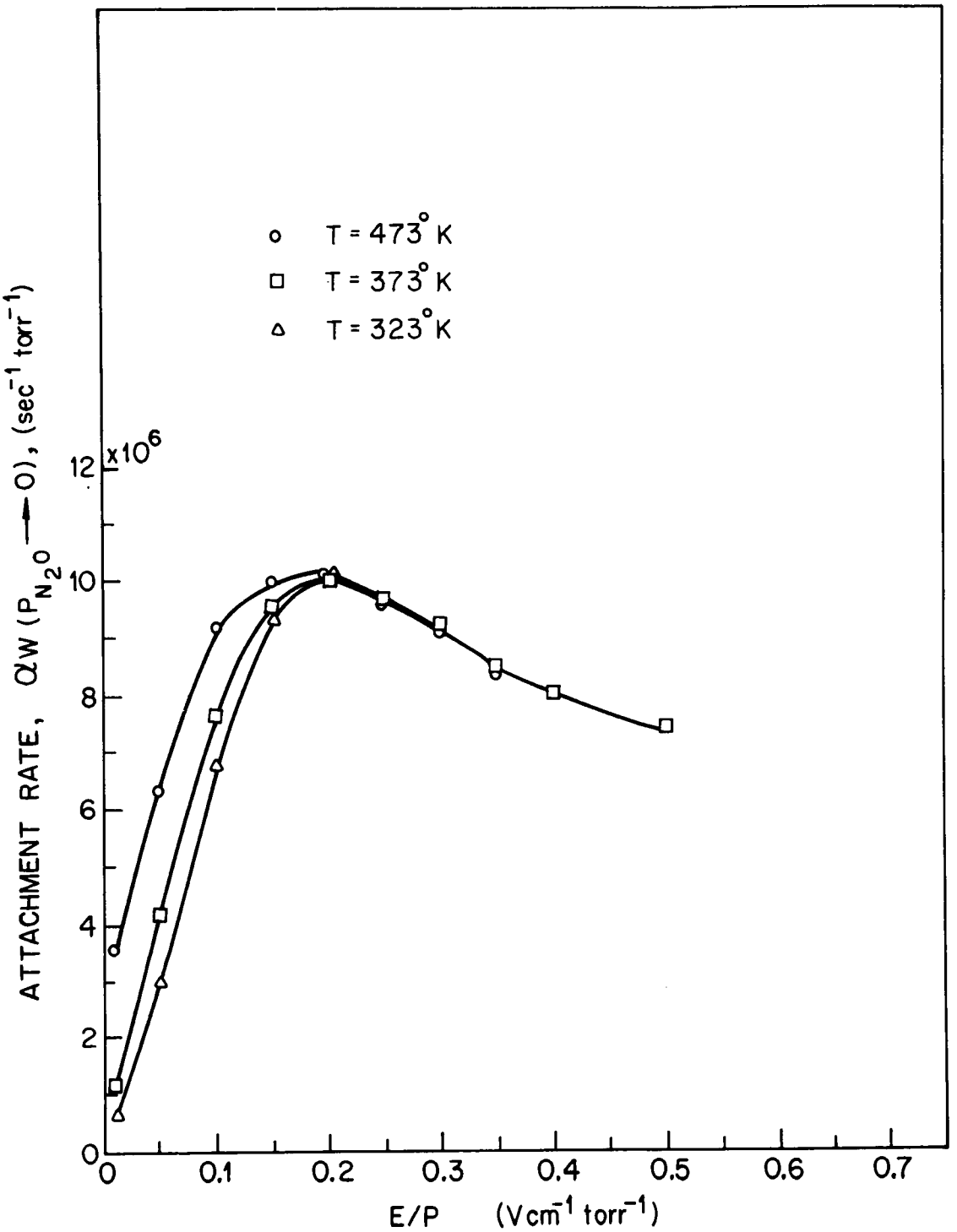

Figure IV-4. Experimental αw for N_2O in Ar versus E/P for $P_{N_2O} \rightarrow 0$ at several temperatures.

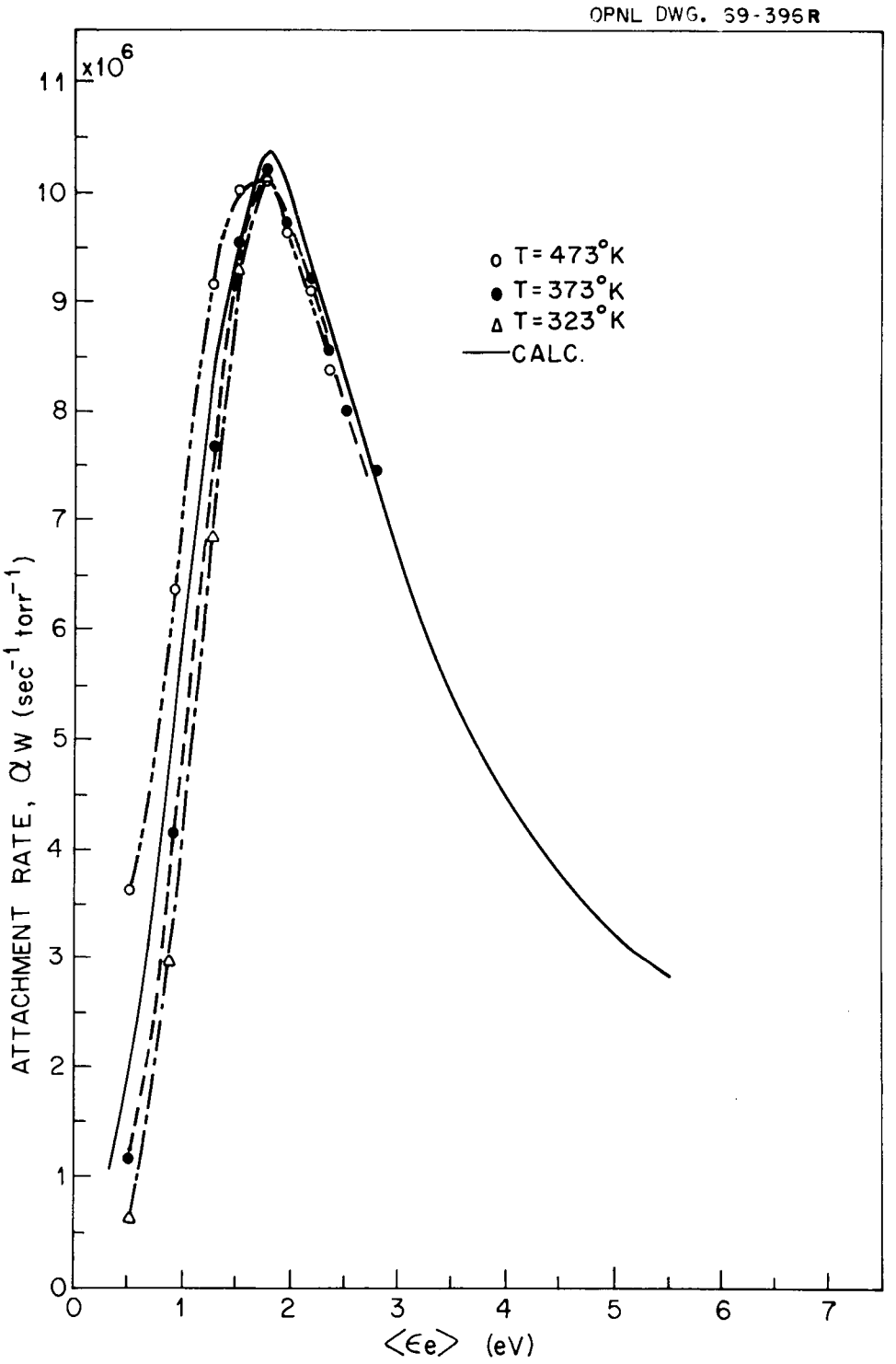

Figure IV-5. Comparison of experimental and calculated αw for N_2O in Ar.

It has been pointed out that the shapes of the negative-ion-yield curves obtained in various beam experiments differ appreciably in shape. The swarm-beam technique [Christophorou et al. (1965)], discussed in Chapter II, has been applied using the present extrapolated values of αw measured in Ar, the Ar electron energy distributions of Ritchie and Whitesides (1961), and the O^-/N_2O ion-current curves of Schulz (1961) and Rapp and Briglia (1965). The results are shown in Figures IV-6 and IV-7 for 323° and 373° K, respectively. At 323° K both the energy scales of Schulz and Rapp and Briglia had to be shifted by + 0.22 and + 0.14 eV, respectively, in order to obtain a good fit to the experimental data. If the Schulz curve is actually representative of 323° K, then the energy shift of + 0.22 eV may account for the apparent onset of O^- by $\sim$ 0.21 eV [$\approx D(N_2-O) - EA(O) = 1.67$ eV - 1.46 eV] below the energetically allowed threshold. However, it is unlikely that Schulz's curve is representative of 323° K in view of the relatively large low-energy peak, which is temperature sensitive and should be less intense at this temperature. Further, Figure IV-6 shows that the cross section obtained by Rapp and Briglia peaks at a higher value than the results of the swarm-beam combination at 323° K using the shape of their cross section. At 373° K there is excellent agreement between the cross section of Rapp and Briglia and the swarm-beam combination. Table IV-I summarizes the present results and gives a comparison in energy and magnitude of the peak cross sections, $\sigma_a(\epsilon_{max})$, determined at each temperature. ϵ_{max} is the

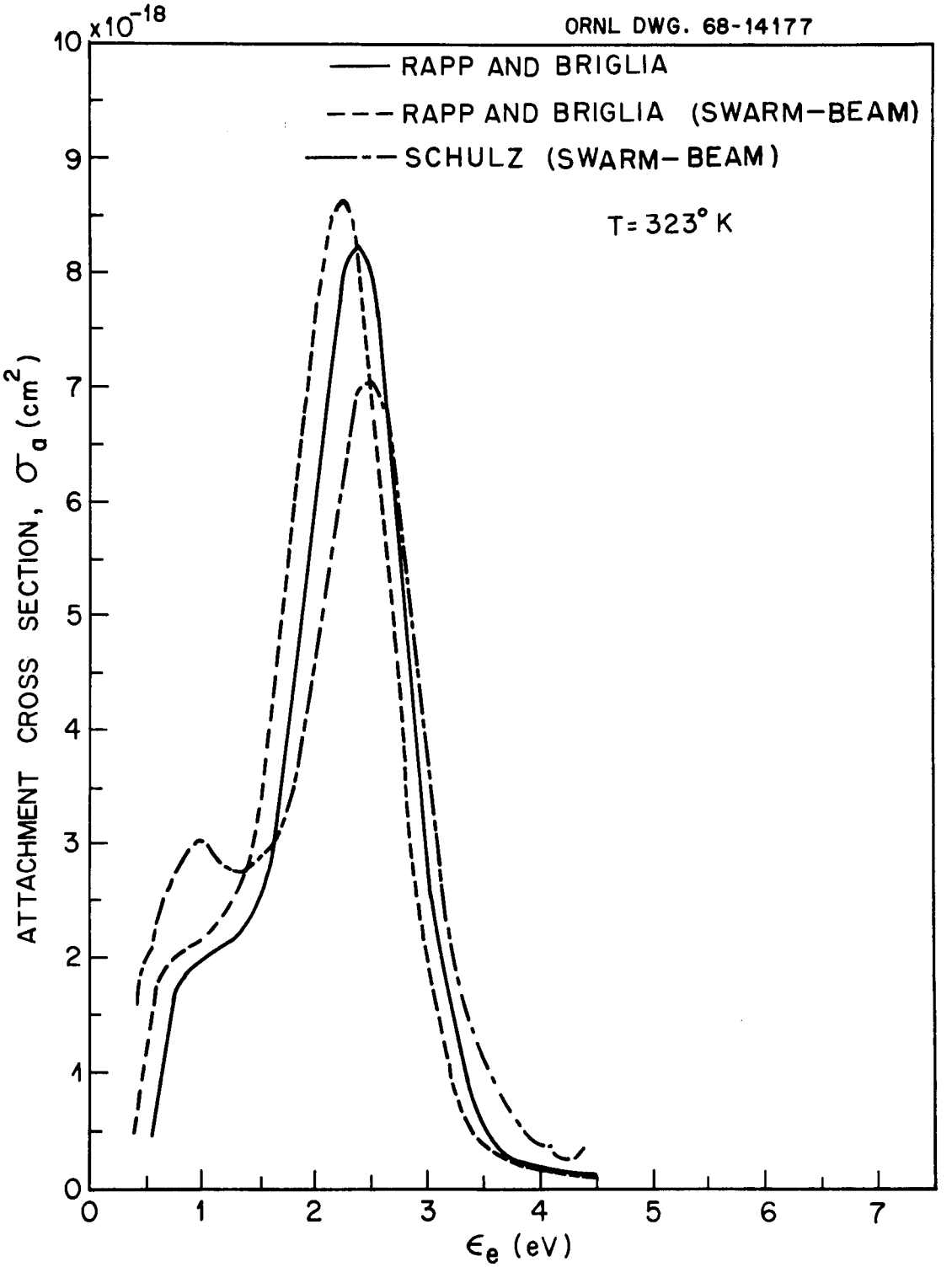

Figure IV-6. $\sigma_a(\epsilon)$ for O^-/N_2O at 323° K using swarm-beam combination.

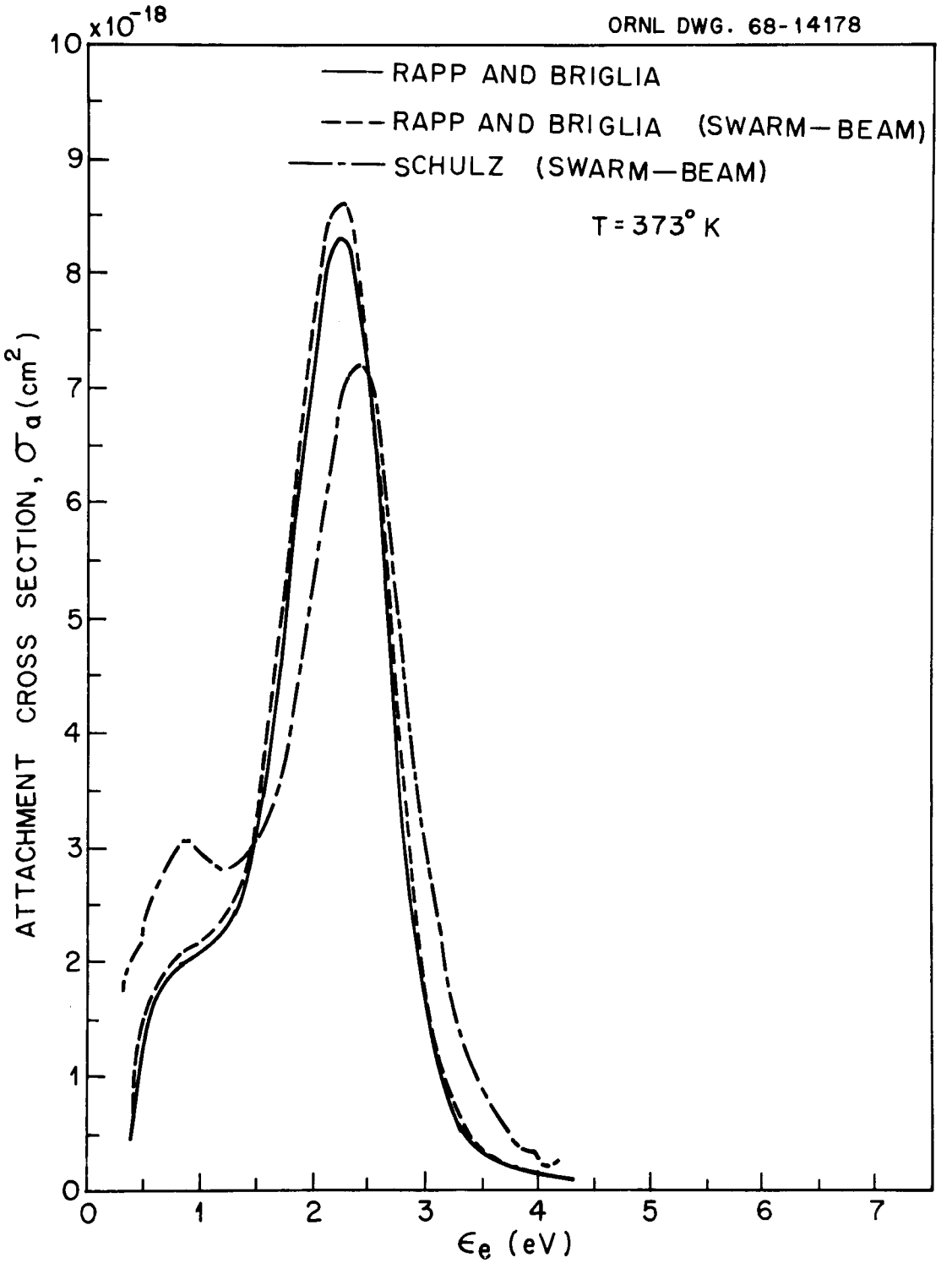

Figure IV-7. $\sigma_a(\epsilon)$ for O^-/N_2O at 373° K using swarm-beam combination.

TABLE IV-I

SWARM-BEAM DATA ON O^-/N_2O

Temperature (K°)	T_j (eV)	ϵ_{max} (eV)	$\sigma_a(\epsilon_{max})$ ($cm^2 \times 10^{18}$)
---		2.25[a]	8.6[a]
323	+ 0.22[b]	2.42[b]	7.07[b]
323	+ 0.14[c]	2.39[c]	8.18[c]
373	+ 0.12[b]	2.32[b]	7.21[b]
	+ 0.06[c]	2.31[c]	8.3[c]
473	- 0.08[b]	2.12[b]	7.58[b]
	- 0.11[c]	2.14[c]	8.6[c]

[a]D. Rapp and D. D. Briglia, J. Chem. Phys. 43, 1480 (1965).

[b]Swarm-beam method using present attachment rates and ion-current curve of G. J. Schulz, J. Chem. Phys. 34, 1778 (1961). Schulz's O^-/N_2O curve peaked at 2.2 eV.

[c]Swarm-beam method using present attachment rates and ion-current curve of Rapp and Briglia (Reference a above).

energy at which the attachment cross section, σ_a, is a maximum. The quantity T_j listed in Table IV-I represents the energy shift that has to be applied to the ion-current curves of Schulz and Rapp and Briglia in order to obtain best fit between the experimental and calculated attachment rates.

It is important to point out that the cross sections determined using the swarm-beam combination are true cross sections insofar as the shape of the ion-yield curves used reflect accurately the shapes of the cross sections. Also, the experimentally measured attachment rates must reflect the processes for which the ion-yield curves are representative. Thus, in the context of the present investigation it is probably an accurate statement that the cross section determined by Rapp and Briglia is representative of $\sim 373°$ K. Also, the ion-yield curve as reported by Schulz is representative of some temperature $> 373°$ K and, in view of the relatively small negative shift given in Table IV-I (T_j = 0 0.08) for 473° K, the representative temperature is probably $\lesssim 473°$ K.

N_2O-N_2 Mixtures

Electron attachment to N_2O has been studied in mixtures of small amounts of N_2O with N_2 at room temperature for total pressures ranging from 300 to 900 torr and N_2O pressures ranging from 0.1 to 0.9 torr. The attachment rate decreased slightly with increasing N_2O pressure, decreasing $\sim 30\%$ for example at E/P = 0.4 over an N_2O pressure range of 1 torr at a total pressure of 500 torr.

A strong dependence of αw on N_2 pressure has been observed. Figure IV-8 shows the variation of αw for $P_{N_2O} \rightarrow 0$ with N_2 pressure for several E/P values. Studies extending down to $P_{N_2O} = 25$ microns did not show indication of an initial region, i.e., change of slope, similar to that observed in Ar mixtures. This pressure dependence in N_2 is discussed later.

Figure IV-9 (curve D) is a plot of αw for $P_{N_2O} \rightarrow 0$ and $P_{N_2} \rightarrow 0$ as a function of the mean electron energy, $\langle \epsilon_e \rangle$. Curve G of Figure IV-9 shows the attachment rates deduced from the data of Phelps and Voshall (1968) using the drift velocities in N_2O of Bailey and Rudd (1932). The mean energies in this case were calculated assuming a Maxwell distribution for the electrons in N_2O and using the D/μ data of Bailey and Rudd (see Chapter III). Under these assumptions, then, it is seen that the present values of αw measured in N_2O-N_2 mixtures are higher than those reported by Phelps and Voshall measured in pure N_2O.

The decrease in αw with N_2O pressure for N_2O-N_2 mixtures may be due to a shift in the electron energy distribution functions for N_2 to lower energies, away from the region of the dissociative attachment resonance. However, this decrease could possibly be due to an electron detachment process, e.g.,

$$O^- + N_2O \rightarrow N_2O_2 + e \,. \qquad \text{(IV-6)}$$

Fehsenfeld et al. (1966) failed to observe the above reaction in a flowing afterglow experiment and established an upper limit to the rate constant for

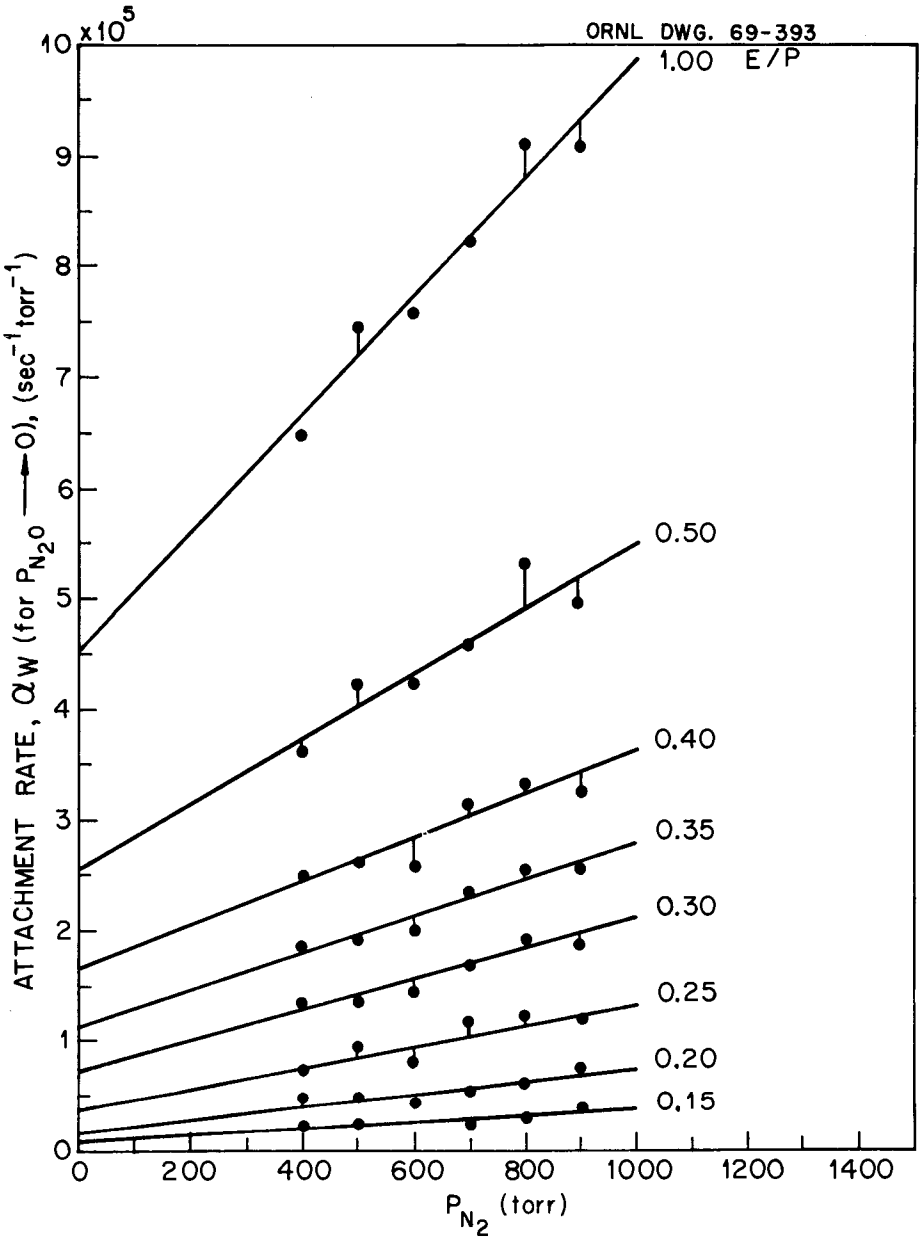

Figure IV-8. Experimental αw for N_2O in N_2 versus P_{N_2} for various E/P values.

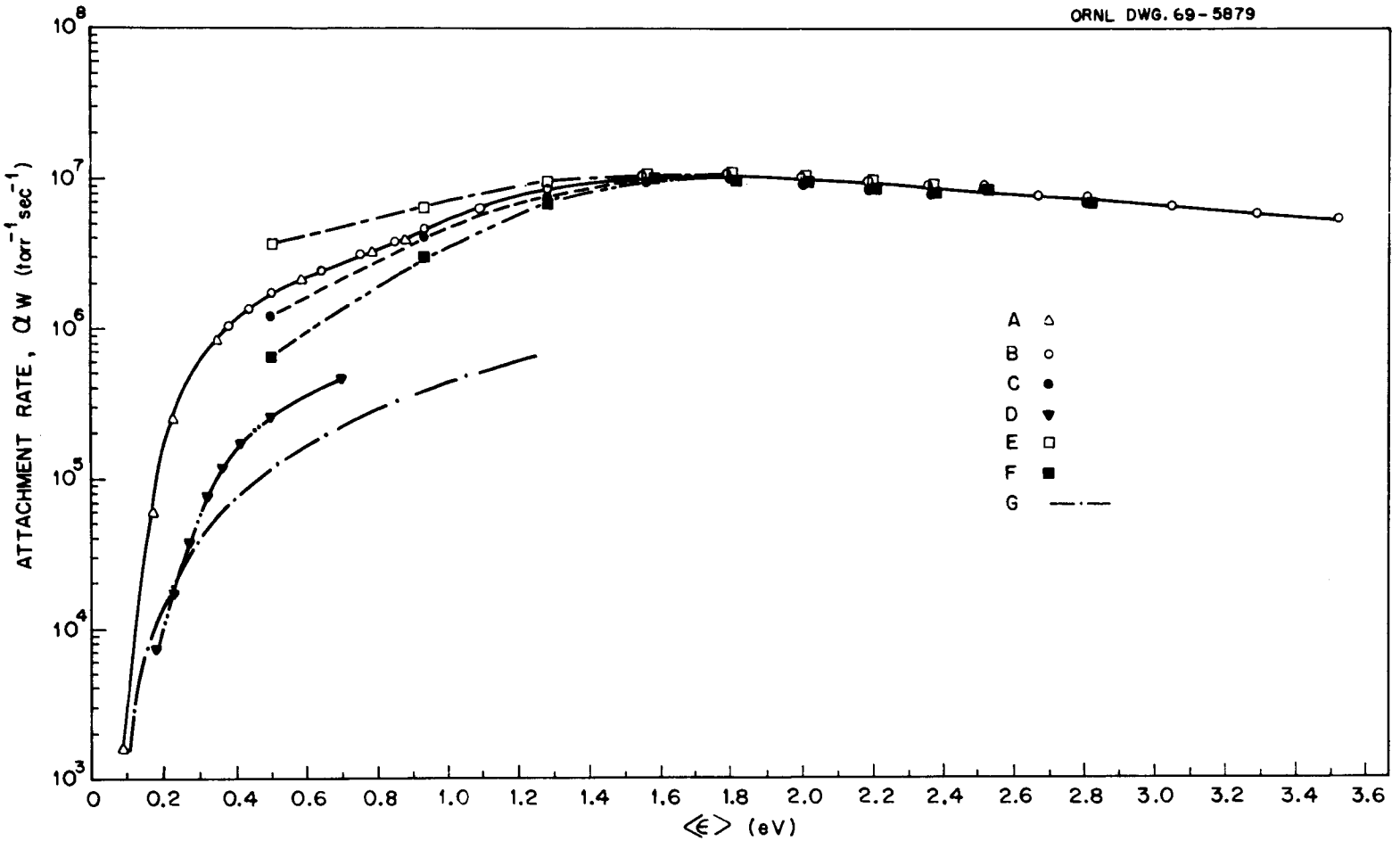

Figure IV-9. Summary of results on N_2O; αw for O^-/N_2O versus $\langle \epsilon_e \rangle$ in Ar and N_2.

(IV-6) as $1 \times 10^{-12}\,cm^3\,sec^{-1}$. Thus, process (IV-6) should not be of importance in the present study due to the small upper limit of its rate constant and the low O^- and N_2O pressures involved.

Also shown in Figure IV-9 are the attachment rates calculated using the cross section reported by Rapp and Briglia (1965) and the Ar distribution functions of Ritchie and Whitesides (1961) (curve B) and the N_2 distributions of Engelhardt et al. (1964) (curve A). Curves F, C, and E are the present experimental results for N_2O-Ar mixtures for 323°, 373°, and 473° K, respectively. From Figure IV-9 it is seen that the results for N_2O-N_2 mixtures at room temperature are in good agreement with the results in N_2O-Ar mixtures at 323° K. Results at the latter temperature should be higher due to the temperature dependence of the O^-/N_2O cross section. Thus, since the N_2O-Ar data agree well with beam data on O^- production from N_2O, one must conclude that the N_2O-N_2 results for $N_2O \rightarrow 0$ (Figure IV-9, curve D) are characteristic of the process

$$e + N_2O \xrightarrow{(\alpha w)_o} O^- + N_2 \,. \qquad \text{(IV-1)}$$

V. DISCUSSION AND CONCLUSIONS

With the present study three different sets of data are now available concerning electron attachment to N_2O:

1. Single-collision beam experiments.
2. Multiple-collision experiments with pure N_2O.
3. Multiple-collision experiments at high total pressures of mixtures of small amounts of N_2O with an inert carrier gas.

The present study provides new information on the attachment cross section from the swarm-beam technique and, in addition, gives a comparison of low pressure beam studies and high pressure swarm studies on an absolute basis. This is possible because the present swarm data reflect the primary processes occurring in beam experiments. Furthermore, the temperature dependence of αw for $\langle \epsilon_e \rangle \lesssim 1.6$ eV supports the hypothesis of enhanced dissociative attachment to higher vibrational levels of N_2O. Experimental evidence suggesting that N_2O^- is formed as a primary product of electron attachment at low energies is discussed below.

It has been pointed out that one is forced to conclude that curve D of Figure IV-9, page 68, (αw for $P_{N_2O} \rightarrow 0$ and $P_{N_2} \rightarrow 0$) is characteristic of O^- production from N_2O. The slight decrease of αw with N_2O pressure was discussed earlier. The fact that αw increases with N_2 pressure may be attributed to the process

$$e + N_2O + N_2 \xrightarrow{k} N_2O^- + N_2 + \text{energy} . \qquad \text{(IV-7)}$$

The analogous process involving N_2O as the third body, i.e.,

$$e + N_2O + N_2O \rightarrow N_2O^- + N_2O + \text{energy}, \qquad \text{(IV-4)}$$

is excluded from consideration since $P_{N_2O} << P_{N_2}$. One can write then

$$\frac{dn_e}{dt} = -\nu_a n_e = -(\alpha w)_o P_{N_2O} n_e - k P_{N_2O} P_{N_2} n_e , \qquad \text{(IV-8)}$$

where n_e is the number density of electrons and ν_a is the electron attachment frequency. Now

$$\nu_a = \alpha w P_{N_2O} . \qquad \text{(IV-9)}$$

Thus, inserting (IV-9) into (IV-8), one obtains

$$\alpha w = (\alpha w)_o + k P_{N_2} . \qquad \text{(IV-10)}$$

The above relation is consistent with the data presented in Figure 8, page 67. Thus, one can determine the three-body rate coefficient, k, as a function of the mean electron energy for N_2. Figure IV-10 shows k plotted against $\langle \epsilon_e \rangle$. A thermal value of k was obtained by extrapolating, for each P_{N_2}, the data of αw versus E/P to E/P = 0 and determining the slope of the extrapolated attachment rates as a function of P_{N_2} (Figure IV-11). The thermal value of $3.0 \pm 0.5 \times 10^{-33}$ $cm^6 sec^{-1}$ thus obtained is shown near the origin of Figure IV-10. This value of the rate coefficient is comparable to those obtained by Phelps and Voshall (1968) ($6 \pm 1 \times 10^{-33}$ $cm^6 sec^{-1}$) and by Warman and Fessenden (1968) ($5.6 \pm 0.2 \times 10^{-33}$ $cm^6 sec^{-1}$) for process (IV-4) involving N_2O as the third body. The values of k for higher $\langle \epsilon_e \rangle$'s were determined from limited data and hence are considered less accurate than

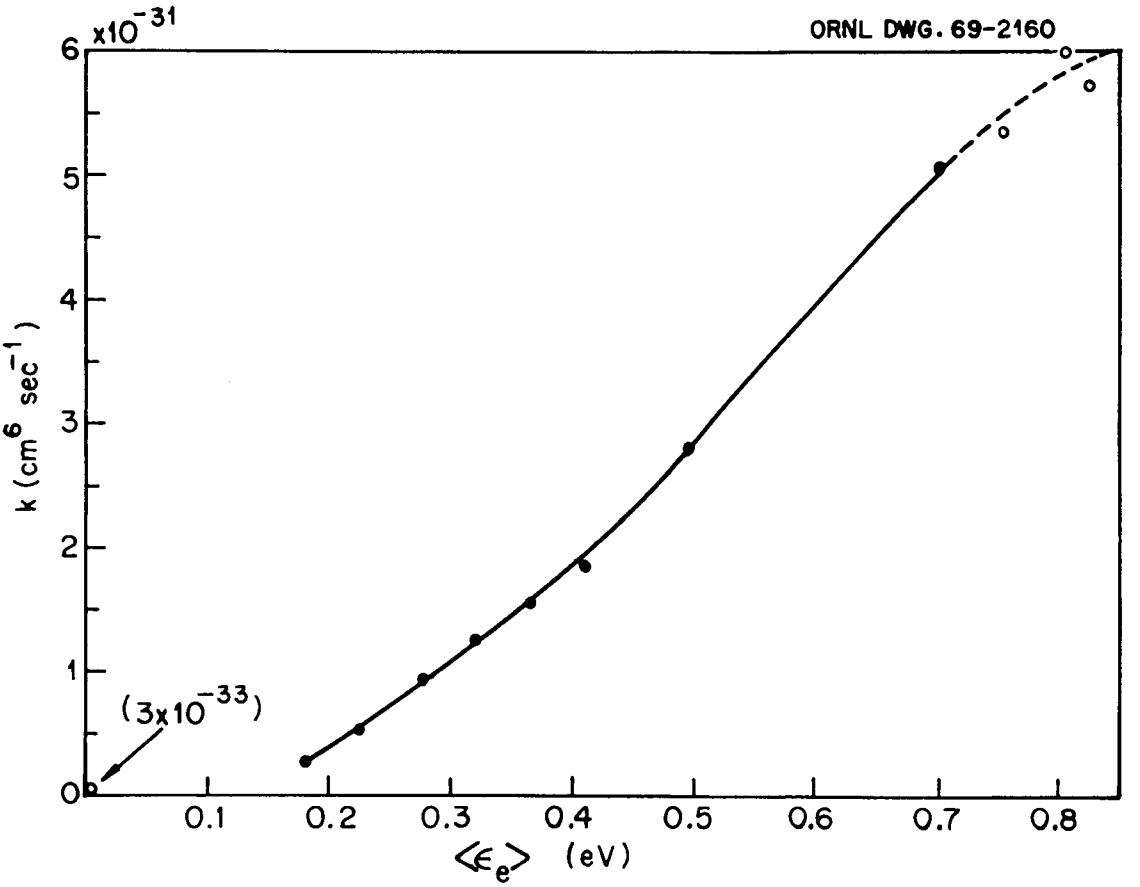

Figure IV-10. k versus $\langle \epsilon_e \rangle$ in N_2.

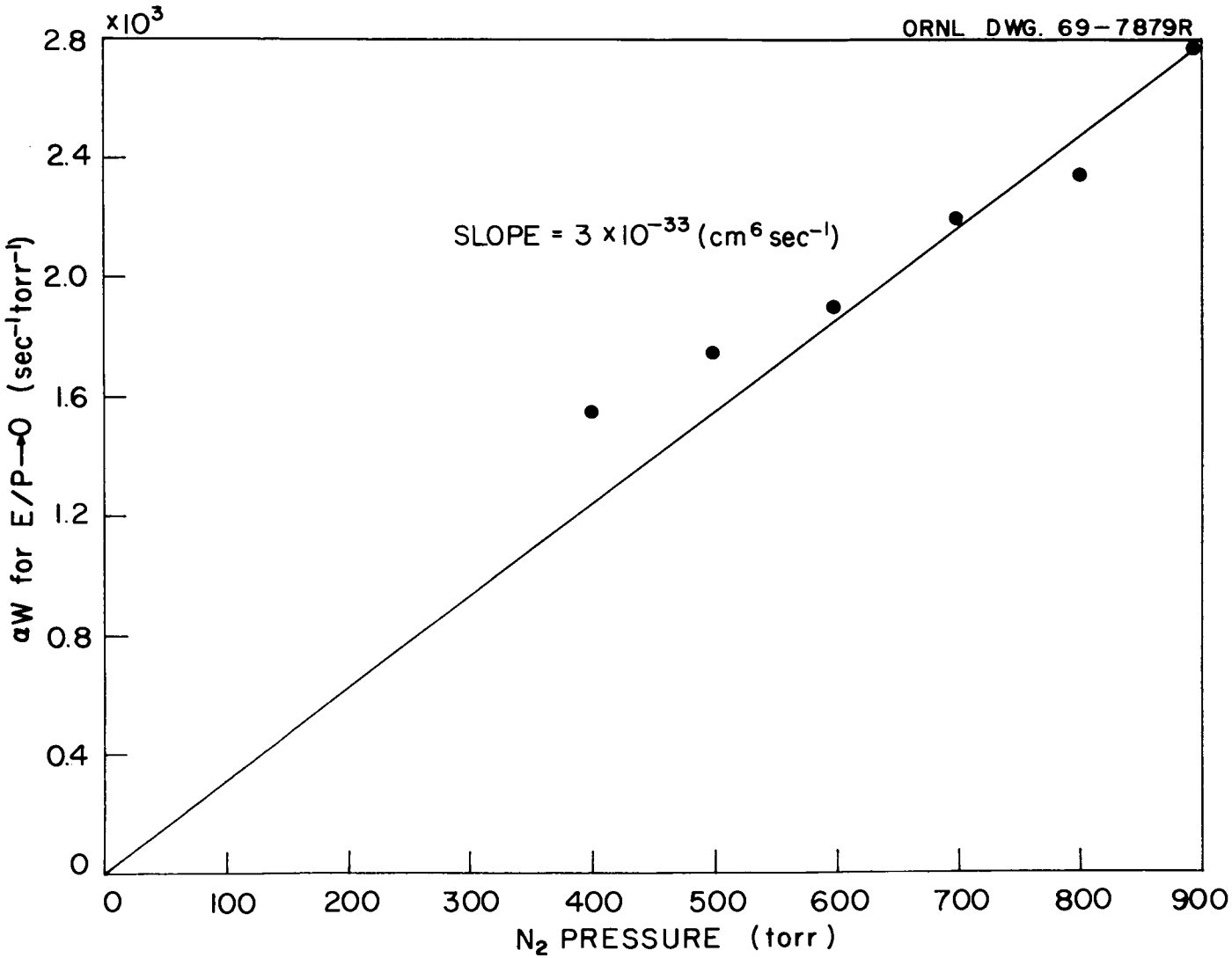

Figure IV-11. αw for $E/P \rightarrow 0$ in N_2 versus P_{N_2}.

those values at lower energies. However, the trend in the variation of k with $\langle \epsilon_e \rangle$ is clearly indicated. The fast increase of k with $\langle \epsilon_e \rangle$ and the tendency for k to level off at higher values of $\langle \epsilon_e \rangle$ is consistent with the hypothesis that the formation of N_2O^- requires activation energy, which, on the basis of Figure IV-10, page 72, is in the vicinity of 1 eV. Thus, N_2O^- is formed at lower electron energies with decreasing probability.

For N_2O-Ar mixtures the extrapolated attachment rates for $P_{N_2O} \rightarrow 0$ were independent of Ar pressure. Thus a process similar to (IV-7) does not seem to be occurring with Ar as the third body. This observation in a way is not surprising since the electron energies in Ar are such that process (IV-1) dominates. Further, the three-body attachment rate for Ar-N_2O mixtures may be quite small due to the atomic character of Ar.

The initial decrease of αw with N_2O pressure ($P_{N_2O} < 8$ microns) is not well understood. Examination of the absolute value of the slope $|d\alpha w/dP_{N_2O}|$ in this pressure region reveals that there is a good correlation between the shapes of the curves αw versus E/P and $|d\alpha w/dP_{N_2O}|$ versus E/P (Figure IV-12). Such a correlation suggests that the initial variation (low P_{N_2O}) of αw with N_2O pressure is closely related to the resonance dissociative capture process. Three possible effects are considered:

1. An effect of process (IV-1) on the number of electrons with energies in the resonance region.
2. An overall relaxation effect of N_2O on the electron energy distribution functions.

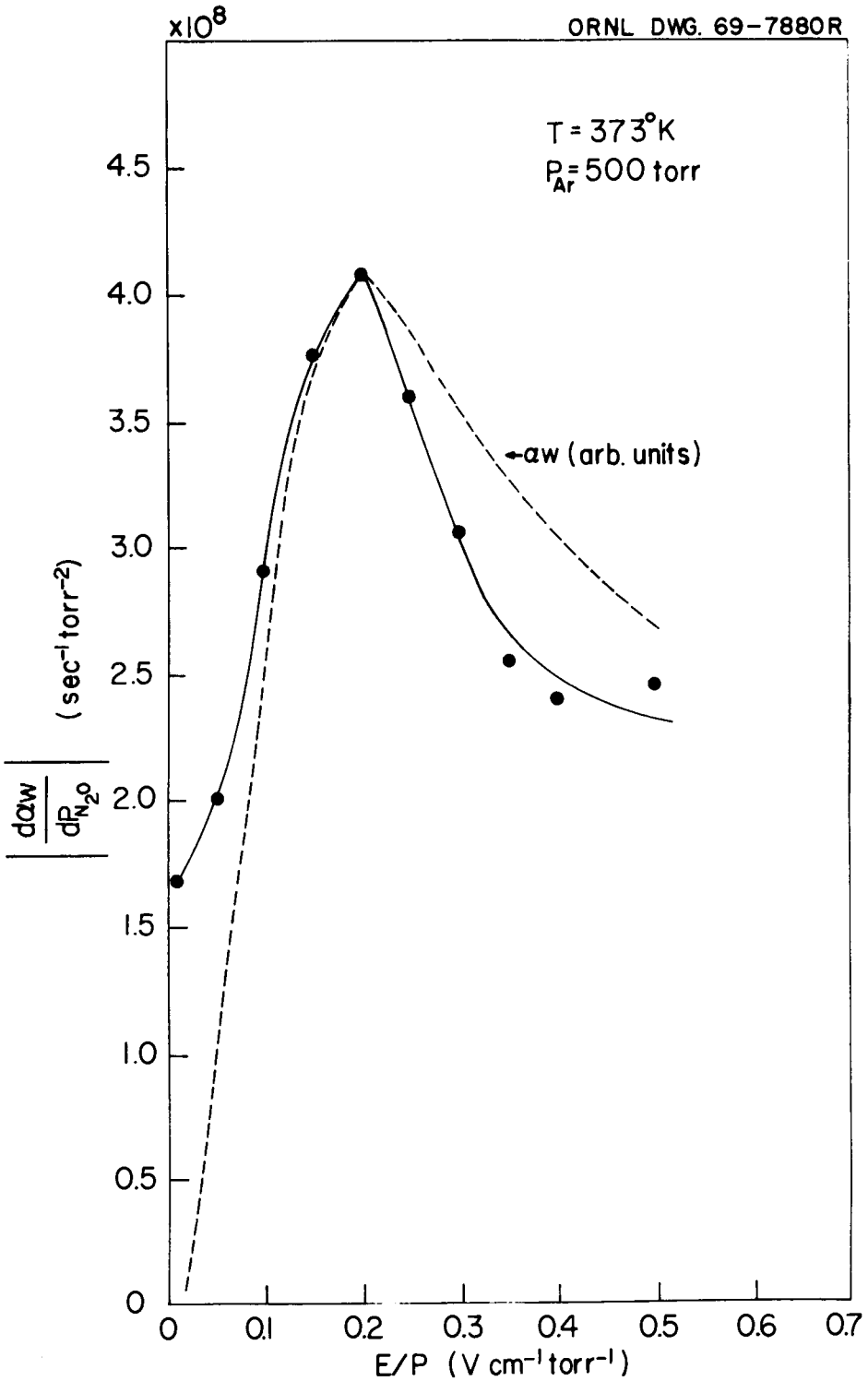

Figure IV-12. Comparison of the curves $|d\alpha w/dP_{N_2O}|$ versus E/P and αw versus E/P in Ar.

3. An electron detachment process involving O^- and N_2O.

The last process can be excluded due to the very low N_2O pressures. As far as effect 2 is concerned, if a gross shift of the electron energy distribution functions to lower energies did occur, then one would expect to find for E/P values > 0.2 (the E/P at which αw peaks) a pressure region where αw increases rather than decreases. This effect indeed is indicated in the transition region between the two sets of lines shown in Figure IV-1, page 55. Figure IV-13 shows this effect more graphically. For P_{N_2O} = 4 microns, the Ar pressure was decreased until the postulated increase in αw was observed for E/P values > 0.2 The increase apparently is due to the shift of the electron energy distribution to lower values, i.e., toward the resonance region. It is seen, then, that effect 2 probably does not occur in the initial region, although it cannot be completely excluded.

It is pointed out here that according to effect 1 an initial decrease in αw with increasing N_2O pressure for the N_2O-N_2 mixtures would be due to depletion of electrons with energies in the region of the dissociative attachment resonance. Such an effect would be important for Ar due to the long relaxation times involved for this atomic gas.

VI. SUMMARY

Electron attachment to N_2O has been studied with the swarm method in mixtures with Ar and N_2, and the measured absolute attachment rates

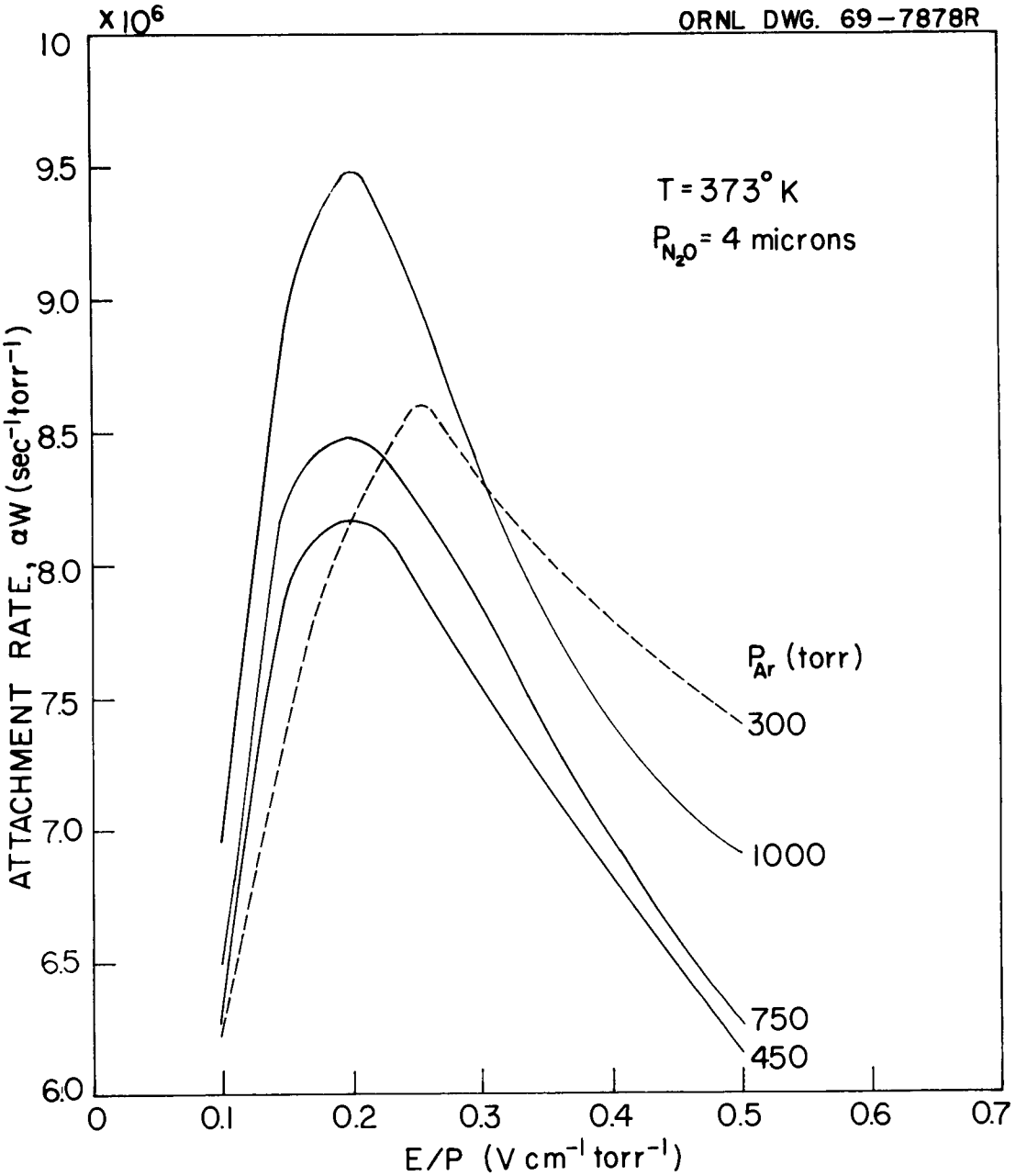

Figure IV-13. Experimental αw versus E/P in Ar for various P_{Ar}.

have been combined with beam data on the production of O^- from N_2O. The cross section for the production of O^- from N_2O at 373° K has a peak value of 8.3×10^{-18} cm^2 at 2.3 eV. In the energy region between ~ 0.2 and ~ 1.5 eV the cross section for the production of O^- from N_2O increases with increasing temperature ($323° \leq T \leq 473°$ K), suggesting dissociative attachment from higher vibrational levels of N_2O. The results on mixtures with N_2 provide evidence for the formation of N_2O^- via a three-body electron attachment process. The apparent three-body attachment rate coefficient increases with increasing electron energy, suggesting an activation energy for the formation of N_2O^-. The various swarm and beam data on electron attachment to N_2O have been compared and discussed.

CHAPTER V

ELECTRON ATTACHMENT TO AROMATIC HYDROCARBONS

I. INTRODUCTION

A limited number of low-energy, electron-impact studies have been made on organic molecules. The few studies that have been made have concentrated on more volatile substances. For solid materials the vapor pressures are usually such that room temperature experiments are difficult. However, electron-impact experiments are possible if a high-temperature apparatus is available.

Swarm experiments are particularly well suited for studies of electron attachment at thermal energies. The mean cross section as determined from swarm data alone using the relation

$$\langle \sigma_a \rangle_v = \frac{\alpha w}{N_o (2/m)^{\frac{1}{2}} \langle \epsilon_e \rangle^{\frac{1}{2}}} , \qquad \text{(V-1)}$$

where $\langle \sigma_a \rangle_v$ is the mean velocity-weighted attachment cross section and the other quantities are defined as for Equation (II-9), have been found by Blaunstein and Christophorou (1968a) to give a good approximation to the true cross section for energies $\lesssim 0.5$ eV. Beam experiments at thermal energies suffer from difficulties arising from a significant energy spread of the electron beam and from low beam currents.

The most important modes of electron attachment to organic molecules are discussed below.

Dissociative Attachment

Christophorou et al. (1966) studied electron attachment to a number of halogenated benzene derivatives using beam techniques and found that when the electron affinity of the halogen was greater than the corresponding bond-dissociation energy, halogen native ions were formed for electron energies above and close to thermal values. The peak energy of the cross section (0.0 to 1.1 eV) depended on the halogen substituent and decreased with increasing electron affinity of the halogen. Compton, Christophorou, and Huebner (1966) observed temporary-negative-ion resonances for the same compounds by examining inelastically scattered electrons. The temporary-ion resonances coincided with the dissociative attachment processes, indicating competition between the two modes of decay by the parent ion. No long-lived parent ions were observed.

Dorman (1966) observed that various fragments were formed on dissociation of the negative ion of acetaldehyde (CH_3CHO) for the same electron energy, indicating competing decomposition paths for the same state of the parent ion. This work has recently been confirmed by Collins and Christophorou (unpublished results).

Blaunstein and Christophorou (1968a) reported electron attachment rates and mean electron attachment cross sections for dissociative

attachment to a number of halogenated aliphatic hydrocarbons determined by electron swarm techniques. Additionally, mean electron attachment cross sections were calculated for 16 other aliphatic hydrocarbons from previously known attachment rates using Equation (V-1).

Dissociative attachment to hydrocarbons, as well as to other polyatomic molecules, is not energetically possible at thermal and epithermal electron energies if the electron affinities of the various fragment ions which may conceivably be formed on dissociation are not great enough to initiate dissociation.

Nuclear-Excited Feshbach Resonant Capture

Polyatomic molecules which capture electrons nondissociatively at very low electron energies usually have long negative-ion lifetimes [Compton *et al.* (1966)]. Thus stabilization of the ion is possible in high pressure experiments and the absolute rate for the forward reaction, electron attachment, can be measured without complications arising from the backward reaction, autoionization.

Christophorou and Blaunstein (1969) reported cross sections for nondissociative attachment of thermal and epithermal electrons to nine aromatic hydrocarbons determined in the high-temperature swarm apparatus used in the present study. The cross sections peaked sharply at thermal energies. By examining the temperature dependence of αw, it was found that the cross sections varied as the inverse of the electron velocity, a dependence which is to be expected for s-wave capture [Compton *et al.* (1966)].

Electron attachment at low energies has been studied for other hydrocarbons using the so-called pulse-sampling technique [see Wentworth and Steelhammer (1968) for a recent review]. However, attachment rates are not usually given in absolute units.

Compton et al. (1966) reported thermal attachment rates and parent negative-ion lifetimes at thermal energies for sulfurhexafluoride (SF_6) and nitrobenzene ($C_6H_5NO_2$) and also the parent negative-ion lifetime for biacetyl $(CH_3CO)_2$ at thermal energies. The lifetimes were 25, 40, and 12 μsec for SF_6^-, $C_6H_5NO_2^-$, and $(CH_3CO)_2^-$, respectively.

Naff, Cooper, and Compton (1968) measured the lifetimes at thermal energies of the parent negative ions formed by a number of alicyclic and aromatic fluorocarbons. The lifetimes increased with increasing complexity, ie., degrees of freedom, of the molecules. Transient negative-ion states for the fluorinated aromatics were detected at higher energies (0.1 to 2.0 eV) by examining inelastically scattered electrons.

Other studies similar to those described above are discussed in reviews by Christophorou and Compton (1967), Christophorou (1969), and Compton and Huebner (1969).

Electron-Excited Feshbach Resonant Capture

Christophorou, Carter, and Christodoulides (1969) found that p-benzoquinone attaches electrons nondissociatively via: (1) a thermal process with a cross section of 3.5×10^{-19} cm^2, and (2) a 2.1 eV process

with a cross section of 6.7×10^{-17} cm^2. Both swarm and beam studies were made. The thermal process was too weak to observe in the mass spectrometer. However, the parent negative ion at 2.1 eV was observed and the mean lifetime was found to decrease from ~ 50 μsec at 1.7 eV to ~ 8 μsec at 3.2 eV. Collins et al. (1969) ascribed the thermal-energy process to capture by the benzene ring and the 2.1 eV process to capture in the field of the lowest triplet state resulting from an $n \rightarrow \pi^*$ transition. This is the first reported case of nondissociative electron capture in the field of an excited electronic state with the parent negative ion so formed living as long as 1 μsec or more.

In the following sections the results of the present electron attachment studies on aromatic hydrocarbons of general physical, chemical, and biological interest are described.

II. ELECTRON ATTACHMENT TO BIPHENYL, ANILINE, AND ACENAPHTHENE

Biphenyl

Biphenyl $(C_6H_5)_2$ of 99.99% purity (James Hinton, Newport News, Virginia) was studied in mixtures with Ar, N_2, and C_2H_4 at temperatures of 423° K and 448° K and at total pressures of 500 torr (Ar, N_2, C_2H_4) and 1000 torr (N_2). No evidence for electron attachment was found for biphenyl pressures ranging from 25 to 500 μ in N_2 and for pressures of ~ 500 μ and

$\sim 850\ \mu$ in C_2H_4 and Ar, respectively. These results place an upper limit on αw at thermal energies of $\sim 10^4\ sec^{-1}\ torr^{-1}$.

Aniline

Stock grade aniline ($C_6H_5NH_2$) was repurified to better than 99.9% purity by the Chemical Technology Division of Oak Ridge National Laboratory using gas chromatography techniques. The repurified sample was used to study electron attachment to aniline in mixtures with C_2H_4 (500 and 1250 torr) and N_2 (500 torr) at 373° K (C_2H_4) and 473° K (N_2, C_2H_4). In C_2H_4 at 373° K and 473° K, respectively, thermal attachment rates of 7.2×10^4 and $7.7 \times 10^4\ sec^{-1}\ torr^{-1}$ were measured for sample pressures of $\sim 243\ \mu$ (373° K) and $\sim 1000\ \mu$ (473° K). The electron attachment rates measured in N_2 mixtures at 473° K for a sample pressure of $\sim 1000\ \mu$ are shown in Figure V-1 as a function of E/P. The rapid increase of αw with decreasing E/P at low E/P values is consistent with behavior observed for other aromatic hydrocarbons [Christophorou and Blaunstein (1969)]. The value of $\sim 5 \times 10^4\ sec^{-1}\ torr^{-1}$ for αw obtained by extrapolating the data shown in Figure V-1 to zero E/P (Figure V-2) is consistent with the measurements in C_2H_4.

Due to the low attachment rates the experimental results were reporducible only to within $\sim 30\%$; however, the qualitative behavior of the attachment rate with E/P was consistent, especially at the lower E/P values. The attachment rates at the higher E/P values tended to increase

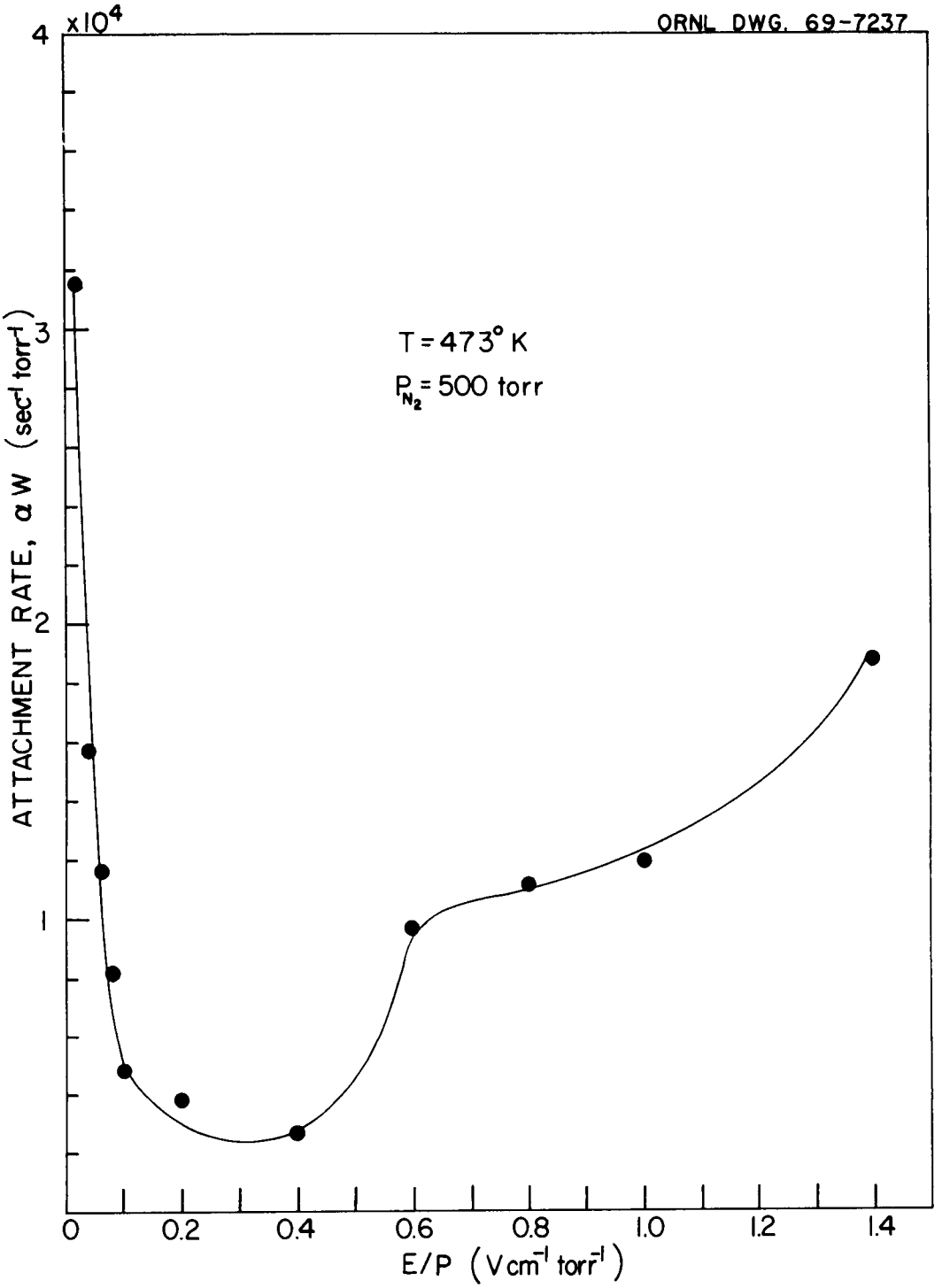

Figure V-1. Experimental αw for aniline in N_2 at 473° K versus E/P.

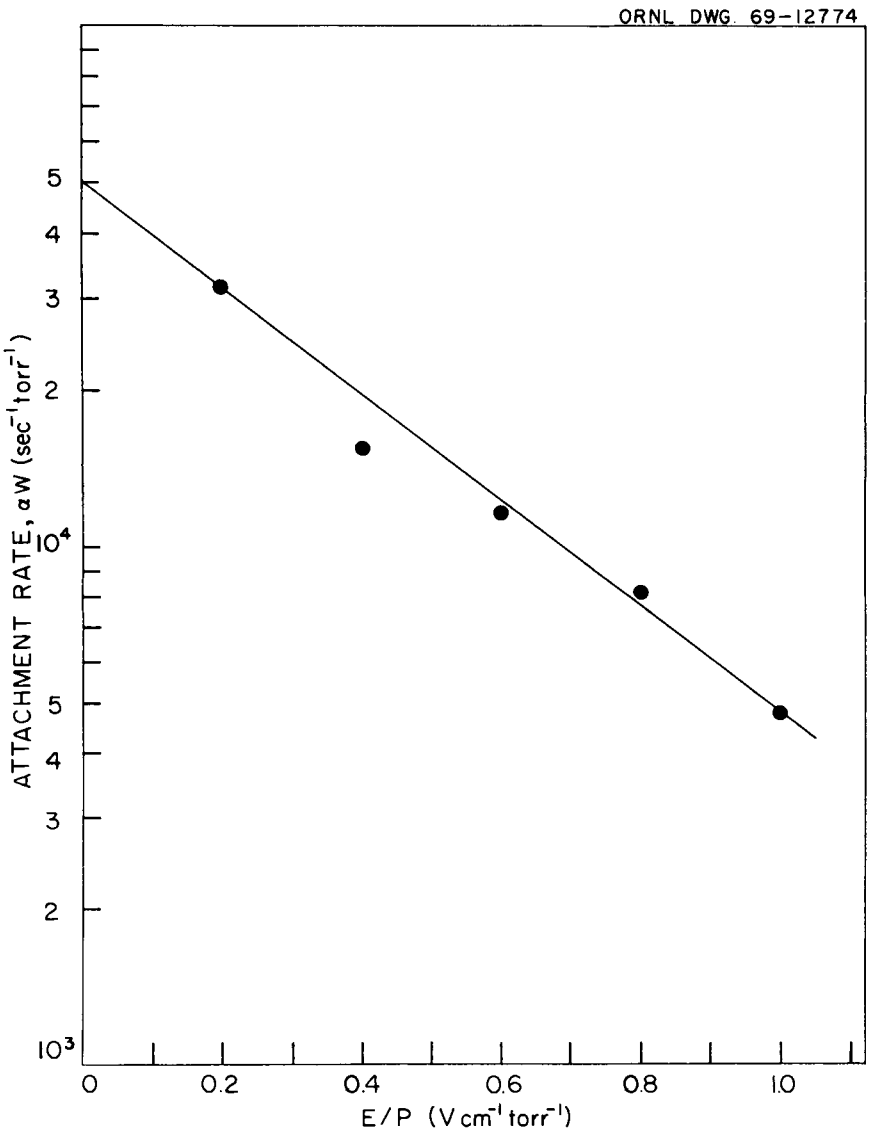

Figure V-2. αw for aniline in N_2 for $E/P \rightarrow 0$.

with increasing age of the sample. Since aniline undergoes spontaneous decomposition, the latter behavior may be associated with decomposition products of aniline.

Acenaphthene

Zone-refined acenaphthene ($C_{12}H_{10}$) of quoted purity > 99.99% (James Hinton, Newport News, Virginia) was studied in mixtures with C_2H_4 (500 torr) and N_2 (750 torr) at 423° K for acenaphthene pressures ranging up to 500μ. A thermal attachment rate of $\sim 5 \times 10^4 \text{ sec}^{-1} \text{ torr}^{-1}$ was measured in C_2H_4. No evidence of capture was observed in mixtures with N_2 for E/P values > 0.10 V cm^{-1} torr^{-1}. However, the value of $\sim 2 \times 10^4 \text{ sec}^{-1} \text{ torr}^{-1}$ for αw measured at E/P = 0.01 V cm^{-1} torr^{-1} in N_2 is consistent with the results in C_2H_4.

III. ELECTRON ATTACHMENT TO AZULENE

Introduction

Azulene ($C_{10}H_8$) is a chemical isomer of naphthalene consisting of one seven-member and one five-member carbon ring. Azulene exhibits peculiar optical properties, including fluorescence resulting from an electronic transition between the second excited singlet state (S_2) and the ground singlet state (S_o), and extremely weak phosphorescence. These anomalous emission characteristics, first observed for azulene but now known to occur for other molecules [see, for example, Poole and Dhingra (1969)],

have stirred quite an interest in the physical properties of the azulene molecule.

Azulene has been studied extensively with optical methods and to a much lesser extent by electron impact. Van Brunt and Wacks (1964) made a study of ionization-dissociation processes in azulene under impact of 70 eV electrons. Compton and Huebner (1968) measured an electron-impact excitation spectrum of azulene between ~ 1.5 eV and ~ 6.0 eV and related the results to optical levels. In addition, the authors measured the mean autoionization lifetime of $C_{10}H_8^-$ at low electron energies and found a value of 9 μsec. Results obtained on low-energy electron attachment using the pulse-sampling technique [Wentworth, Chen, and Lovelock (1966), Wentworth and Steelhammer (1968)] have been interpreted as indicative of an activation energy for electron attachment to azulene; see, however, a discussion later in this section. The latest electron-impact study has been reported by Chaney et al. (1969). The results of the latter study are presented and discussed below.

Experimental Results

Swarm data. Zone-refined azulene of quoted purity > 99.99% (James Hinton, Newport News, Virginia) was studied in mixtures with CO_2, C_2H_4, N_2, and Ar at 423° and 488° K for each carrier gas and at total pressures of 500 torr (CO_2, C_2H_4, and N_2), 750 torr (C_2H_4 and N_2), and 400 to 1275 torr (Ar). Azulene pressures ranged from ~ 0.5 μ for the CO_2, C_2H_4, and

N_2 mixtures to $\sim 3\mu$ for the Ar mixtures. No temperature dependence was observed over the range investigated. No reliable data below 423°K could be obtained due to condensation of the azulene vapor onto the walls of the chamber. A slight pressure dependence of αw (sec^{-1} $torr^{-1}$) on Ar pressure was observed and is shown in Figure V-3. Curve A of Figure V-4 shows αw for azulene plotted against the mean electron energy $\langle \epsilon_e \rangle$ for the carrier gases CO_2, C_2H_4, N_2, and Ar. The points shown for Ar and N_2 are averages of runs taken at 423° and 488° K. The points shown for Ar are for 1000 torr; curve D represents the approximate values of αw in Ar extrapolated to zero Ar pressure. The important features of curve A are:

1. There is no temperature dependence of αw over the range 423° to 488° K.
2. There is very good agreement between the values of αw measured in different carrier gases at different pressures, indicating that only primary processes are reflected in the attachment rates.
3. The attachment process peaks at thermal energies.
4. The variation of αw with $\langle \epsilon_e \rangle$ (or E/P) is distinctly different from that observed for other aromatic molecules known to capture via a nondissociative process at thermal energies [see, for example, Christophorou and Compton (1967) and Christophorou and Blaunstein (1969)]. The attachment rates

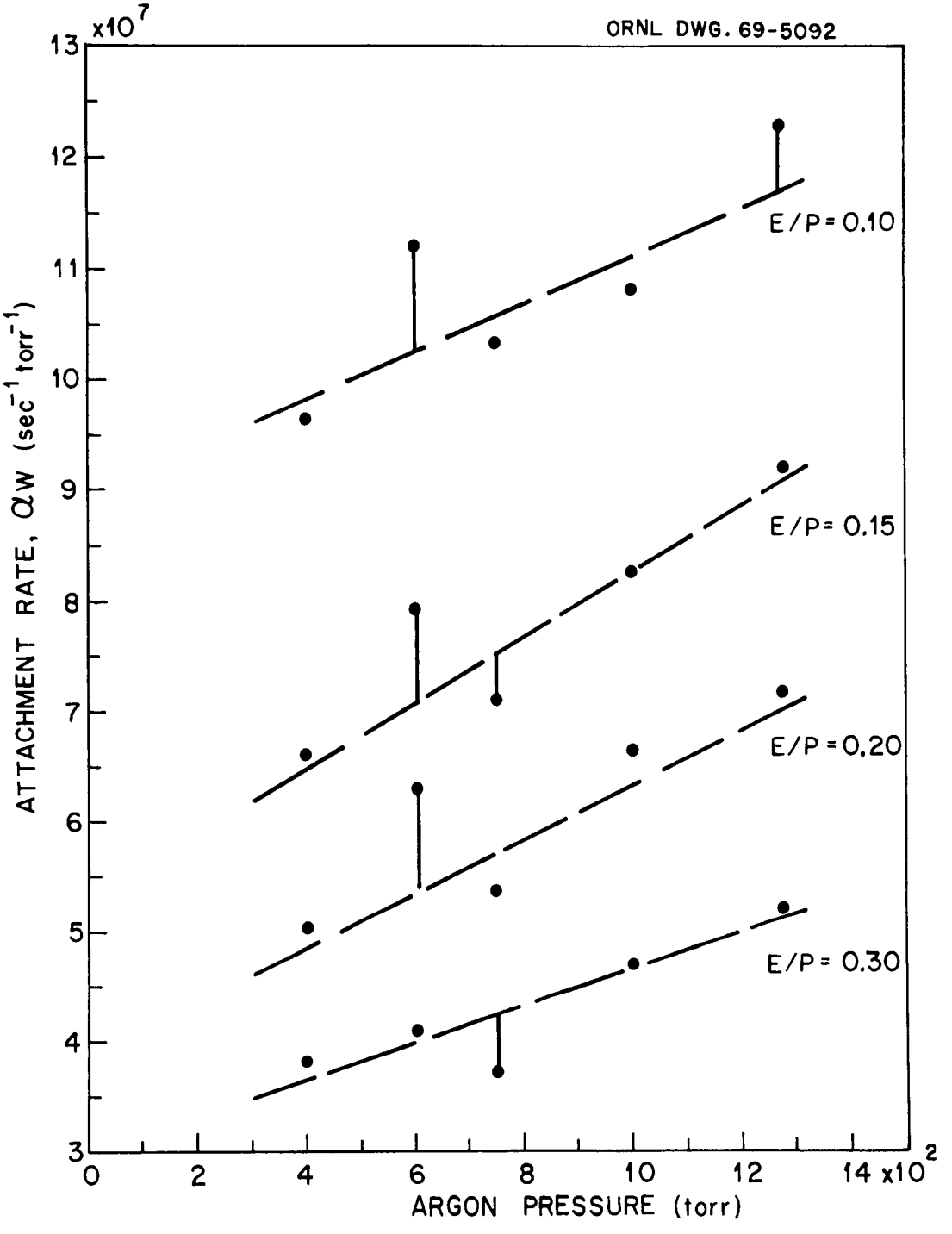

Figure V-3. Experimental αw for azulene in Ar versus P_{Ar} for various E/P values.

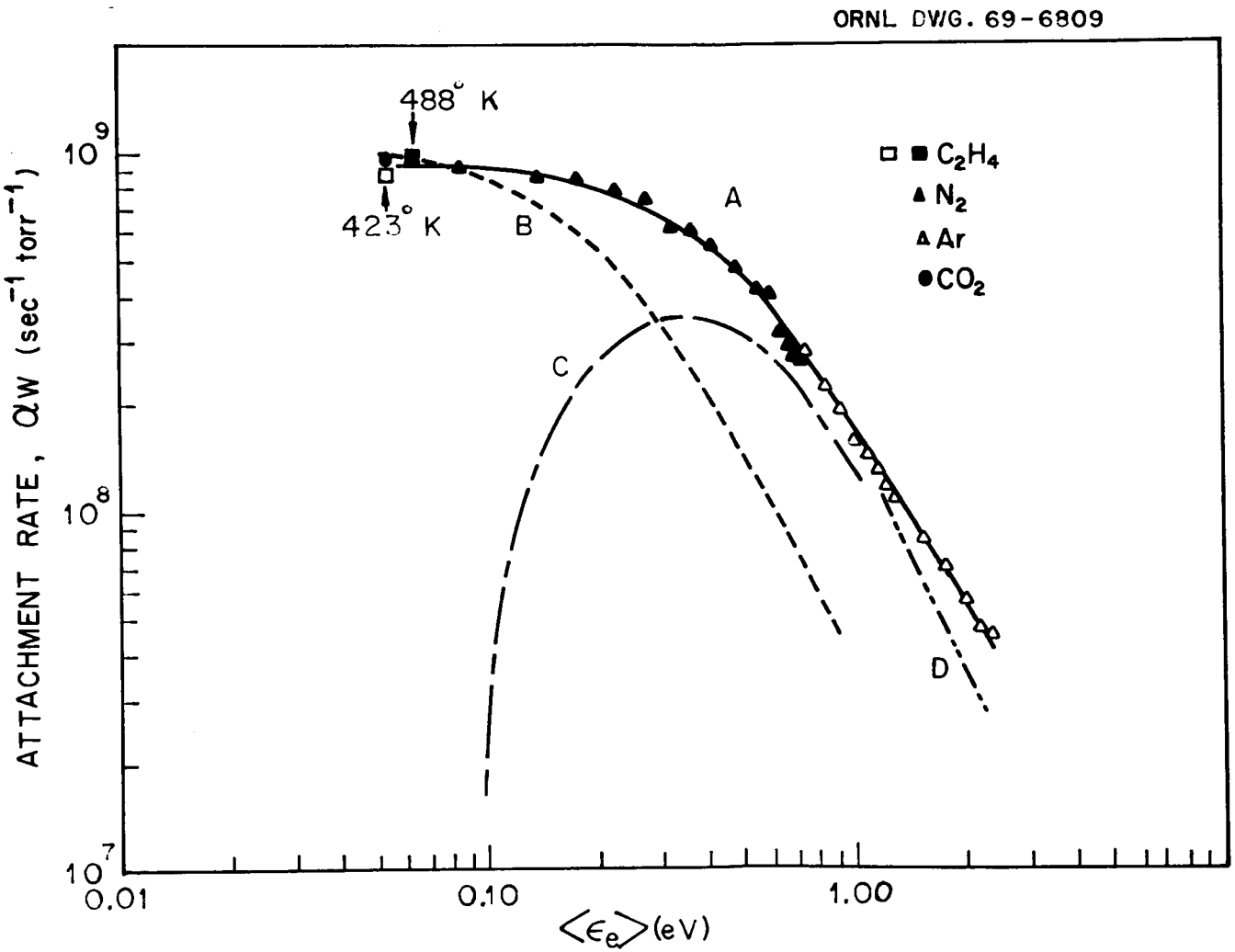

Figure V-4. Experimental αw for azulene versus $\langle \epsilon_e \rangle$ in C_2H_4, N_2, CO_2 and Ar.

for other aromatics decrease rapidly for $\langle \epsilon_e \rangle$ > thermal values; the same is not true for azulene.

Curves B and C of Figure V-4 are discussed later.

Beam data. Figure V-5 [Chaney et al. (1969)] compares the sharp electron attachment resonance observed for azulene in a TOFMS at near-thermal energies with the SF_6^- resonance which is known to peak at ~ 0.0 eV. The widths of both peaks are instrumental.

Although the SF_6^- resonance peaks at ~ 0.0 eV, the coincidence of the $C_{10}H_8^-$ and SF_6^- resonances does not necessarily imply that the $C_{10}H_8^-$ resonance peaks at zero energy. Due to surface potentials which may exist in the collision chamber of the spectrometer and which may vary for different substances being studied, the energy-scale calibration based on a zero-peaking resonance may be underestimated by as much as ~ 0.5 eV [Christophorou et al. (1965), Schulz (1960)]. However, the peak of the $C_{10}H_8^-$ resonance at zero energy was verified using the SF_5^- peak at 0.3 eV. This calibration is independently supported by the thermal-peaking absolute swarm data.

No ions were observed in the energy range 0 to 4 eV other than the thermal process. However, in the range 5.0 to 9.0 eV a broad, structured negative-ion peak less than one-hundredth the intensity of the $C_{10}H_8^-$ peak at low energies was observed. The ion observed had a mass equal to that of $C_{10}H_7^-$.

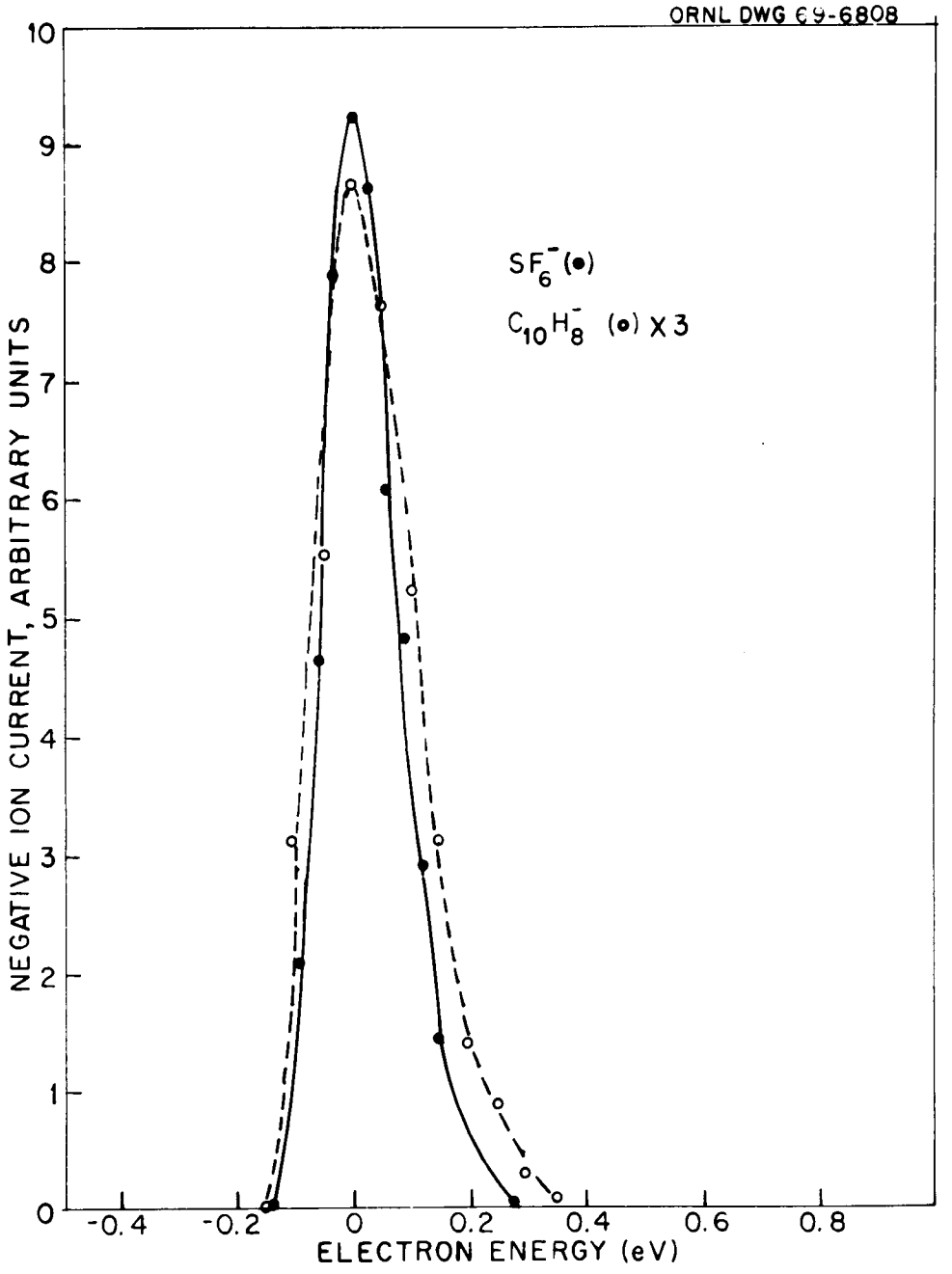

Figure V-5. Comparison of thermal electron attachment resonances for SF_6 and $C_{10}H_8$.

Swarm-Beam Combination. As mentioned previously, azulene captures electrons strongly at energies well above thermal values. In an effort to explain this phenomenon by one capture process we employed the swarm-beam combination using the data shown in curve A of Figure V-4, page 91, in conjunction with the negative-ion current due to $C_{10}H_8^-$ shown in Figure V-5, page 93, and the N_2 electron energy distribution functions of Engelhardt, Phelps, and Risk (1964). It was found that the experimental αw vs $\langle \epsilon_e \rangle$ could not be reproduced by assuming a single process identical in shape to that shown in Figure V-5 for $C_{10}H_8^-$ no matter what width was assumed for the process (0.1 to 0.8 eV) and no matter where the process peaked. For a width of 0.2 eV, for example, it was found that for a best fit to the experimental data, the cross section should peak at 0.12 eV with a peak value of 3.9×10^{-15} cm^2. The values of αw calculated from Equation (II-9) using the above cross section are given by curve B of Figure V-6 which is compared with the experimental data (curve A). It is seen that curve B is actually a very poor fit to the experimental data. It might be expected that better fits would be obtained by increasing the width of the trial cross section. However, this has been found not to be the case. The above behavior clearly demonstrates that the experimental data cannot be explained by assuming a single resonance process.

In connection with the above results it might be argued that the actual attachment cross section at low energies has a shape entirely

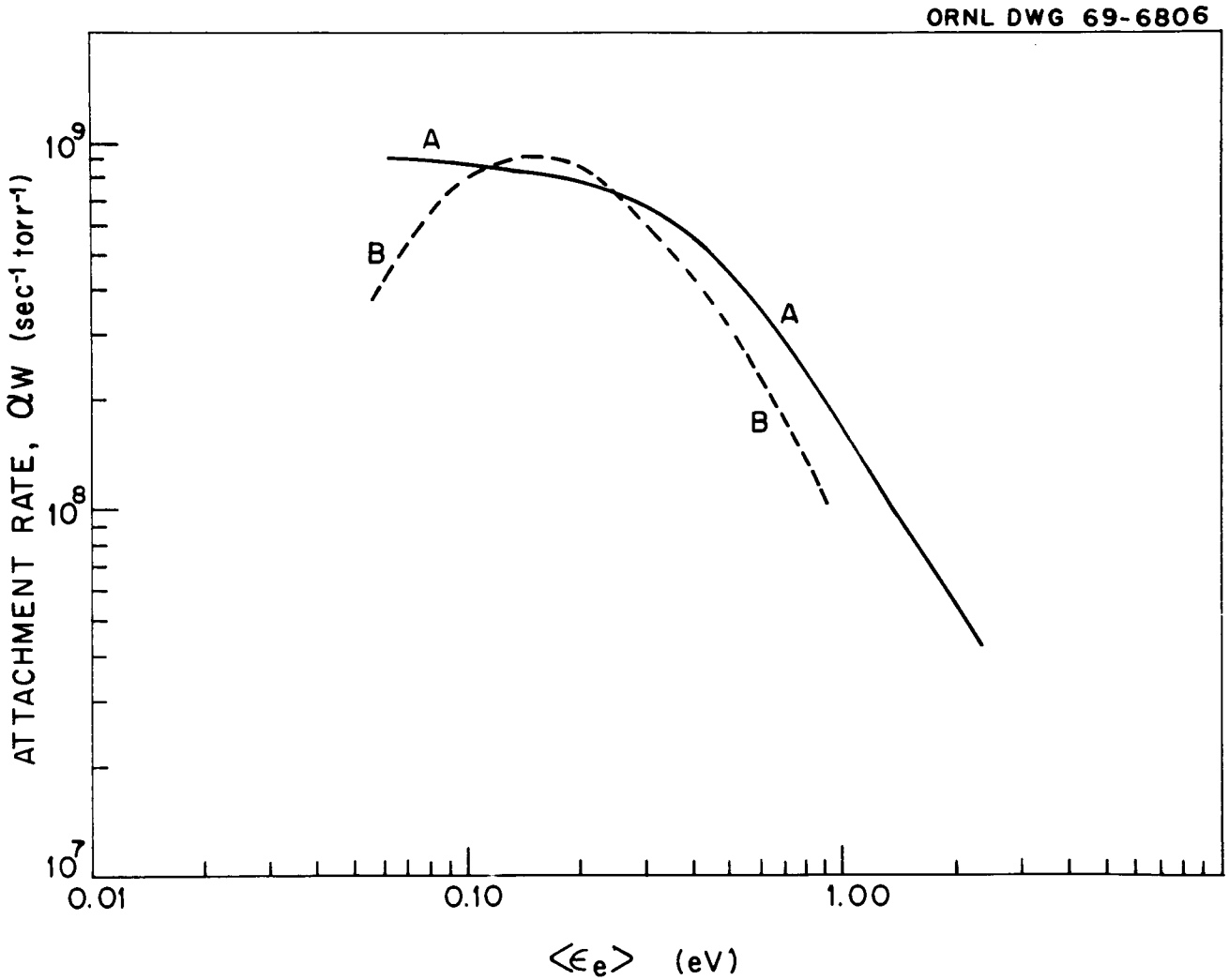

Figure V-6. Comparison of experimental and calculated αw for $C_{10}H_8$.

different from that shown in Figure V-5, page 93, and that the negative-ion current shown in Figure V-5 results only from those ions formed which live for a long time (7 μsec). However, such behavior is inconsistent with observations on other aromatic systems [Christophorou and Blaunstein (1969); Collins et al. (1969)]. In addition if this were the case, one would expect to find a variation in the negative-ion lifetime, at least on the high-energy side of the negative-ion peak. No such variation was detected. This observation is consistent with a sharp resonance at zero energy.

In view of the preceding analysis, it is reasonable to assume that the low-energy process observed for azulene in the mass spectrometer does in fact peak very sharply at ~0.0 eV and that the swarm data are explainable in terms of an additional process peaking at a higher energy. The assumption of a thermal-peaking cross section is strictly valid as pointed out earlier. In order to separate the two processes in the swarm data, the mean velocity-weighted attachment cross section $\langle\sigma_a\rangle_v$ ($\cong\sigma_a$) for azulene was calculated from Equation (V-1) using the present experimental value of the thermal attachment rate (= 9.4×10^8 sec^{-1} $torr^{-1}$). The resulting cross section value was used to normalize the negative-ion current at thermal energies shown in Figure V-5. The width chosen for the ion-current curve was 0.2 eV (the instrumental width) and may be considered an extreme case. The cross section resulting from the above normalization was then used to calculate αw from Equation (II-9) using the N_2 distribution functions of Engelhardt, Phelps, and Risk (1964).

Curve B of Figure V-4, page 91, shows the results of these calculations. Curve C of Figure V-4 was obtained by subtracting curve B from the experimental data given by curve A. There is good agreement between curve C and the extrapolated values of αw in Ar given by curve D. Curve C is a sharply peaking curve characteristic of a resonance process, and thus it is reasonable to assume a typical shape for a resonance-attachment process in order to explain curve C. Employing the swarm-beam combination using a sharp trial cross section and curve C in conjunction with the energy distribution functions for N_2 of Engelhardt, Phelps, and Risk (1964), it was found that the "true" cross section peaks at 0.37 eV. Changing the width of the trial cross section from 0.1 to 0.4 eV did not change the peak energy but did, of course, change the peak cross section value. For a width of 0.2 eV the peak cross section was found equal to 1×10^{-15} cm^2. Cross sections obtained from the above analysis were used with Equation (II-9) to calculate αw and it was found that curve C could be reproduced to within 5% over the center portion of the curve and to within 15% over the low- and high-energy "tails." When a delta function cross section was used to calculate curve B it was found that the cross section necessary to explain curve C should peak at 0.22 eV.

The preceding analysis clearly demonstrates that the absolute attachment rate for azulene at low energies ($\lesssim 5$ eV) can be explained by two resonance-capture processes, one peaking at thermal energies and one peaking between 0.22 and 0.37 eV.

Discussion and Conclusions

The experimental results presented above have shown that azulene negative ions are formed by resonance thermal-electron capture. This finding contradicts previously published reports [Wentworth, Chen, and Lovelock (1966); Wentworth and Steelhammer (1968)] as to the need of an activation energy (~0.15 eV) for the formation of $C_{10}H_8^-$. Barring experimental errors by the latter workers, a possible explanation of this discrepancy is discussed below.

The theoretical model of the pulse-sampling technique [Wentworth, Chen, and Lovelock (1966)] is based on the Arrhenius equation [see, for example, Menzinger and Wolfgang (1969)]. Theoretically the activation energy for a particular reaction is given by

$$\epsilon_{act} = \frac{\int_0^\infty \sigma(\epsilon)\epsilon^2 \exp(-\epsilon/kT)d\epsilon}{\int_0^\infty \sigma(\epsilon)\ \epsilon\exp(-\epsilon/kT)d\epsilon} - \frac{3}{2}\,kT \qquad \text{(V-2)}$$

where ϵ_{act} is the activation energy, $\sigma(\epsilon)$ is the cross section for the reaction at an electron energy ϵ, k is Boltzmann's constant, and T is the temperature. The exponential functions in the integrands of the above equation represent the energy distribution function of the electrons, which has been assumed to be Maxwell. If one assumes, for simplicity, that $\sigma(\epsilon)$ is composed of two delta-function processes at energies ϵ_1 and ϵ_2, then Equation (V-2) reduces to

$$\epsilon_{act} = \frac{\sigma(\epsilon_1)\epsilon_1^2 \exp(-\epsilon_1/kT) + \sigma(\epsilon_2)\epsilon_2^2 \exp(-\epsilon_2/kT)}{\sigma(\epsilon_1)\epsilon_1 \exp(-\epsilon_1/kT) + \sigma(\epsilon_2)\epsilon_2 \exp(-\epsilon_2/kT)} - \frac{3}{2} kT \quad . \qquad \text{(V-3)}$$

If ϵ_1 is 3/2 kT and ϵ_2 is between 0.22 and 0.37 eV, then the terms involving ϵ_2 in Equation (V-3) can be neglected and one finds

$$\epsilon_{act} \cong \frac{3}{2} kT - \frac{3}{2} kT = 0 \quad . \qquad \text{(V-4)}$$

If, however, the electron energy distribution is not Maxwell, as has been suggested by Stockdale, Hurst, and Christophorou (1964), considerable contributions can result from terms involving the higher energy process and ϵ_{act} would assume some value > 0. In this case, Equation (V-3), modified to account for the non-Maxwell form of the distribution function, would yield an "average" energy for the two capture processes. An analogous situation arises when one attempts to explain the present experimental attachment rates by a single process, which may be considered an "average" of two processes. One finds that the single process should peak at ~0.12 eV in order to best explain the data. The latter value is close to the value of 0.15 eV quoted as the activation energy for formation of $C_{10}H_8^-$ [Wentworth, Chen, and Lovelock (1966)]. A general conclusion from this analysis is that caution must be taken in interpreting the meaning of an activation energy based on the Arrhenius equation when there is a possibility that two or more processes exist that lie close together on the energy scale.

An analysis has been presented which strongly suggests that azulene attaches electrons via a resonance process peaking between 0.22 and 0.37 eV. The latter process, however, was not observed in the beam experiment. This may be due to the presence of surface potentials which cause the higher energy process to be masked by the more intense zero-energy process. Another possibility is that the $C_{10}H_8^-$ ion formed at higher energies decays in the flight tube ($\tau < 1$ μsec), although its observation in the swarm experiment and the absence of any pressure dependence of αw for $\langle \epsilon_e \rangle \lesssim 1$ eV suggests that the negative ion should be relatively long-lived. The pressure dependence of αw observed in Ar, which may be due to collisional stabilization of $C_{10}H_8^{-*}$ ions, supports the latter hypothesis.

Rentzepis (1969) has observed the emission spectrum of azulene in methyl cyclohexane at 77°K excited by an intense laser beam. The spectrum which is attributed to phosphorescence from the lowest triplet state (T_1) of azulene has a 0-0 transition at ~1.3 eV and a peak at 1.11 eV. The value of $T_1 \sim 1.3$ eV agrees reasonably with Lamola's (1965) estimate of $T_1 \geq 1.36$ eV from triplet energy transfer experiments and with Pariser's (1956) calculated value of $T_1 = 1.47$ eV. The heavy-atom-induced emission, originally attributed by Robinson and Frosch (1963) to a triplet-triplet transition in azulene, was subsequently found to be due to naphthalene impurity [G. W. Robinson (private communication)], thus invalidating their estimate of $T_1 \leq 0.74$ eV. If the capture process observed by us at ~0.37 eV is associated with electron attachment in the field of the first excited triplet state of azulene, then

the spectroscopic data of Rentzepis indicate an electron affinity in T_1 of ~0.8 eV, which is much higher than that of 0.46 eV calculated from the ground state (see Chapter VI).

IV. ELECTRON ATTACHMENT TO p-BENZOQUINONE AND 1,4-NAPHTHOQUINONE

Introduction

The quinones represent an extremely biologically important group of molecules. As an indication of their importance it will only be mentioned here that 1,4-naphthoquinone is the basic unit of the vitamin K series. Prior to the work of Christophorou, Carter, and Christodoulides (1969), no electron impact studies on the quinones have been reported in the literature. The present study summarizes the results of Christophorou, Carter, and Christodoulides and presents new swarm data on 1,4-naphthoquinone [Collins *et al.* (1969)].

p-Benzoquinone

Swarm Data. Figure V-7 [Christophorou, Carter, and Christodoulides (1969)] shows the absolute attachment rate for p-benzoquinone (BQ) as a function of the mean electron energy for C_2H_4, N_2, and Ar at room temperature. No pressure dependences were observed. The interesting feature of these data are the weak attachment at thermal energies and the strong peak at 2.1 eV.

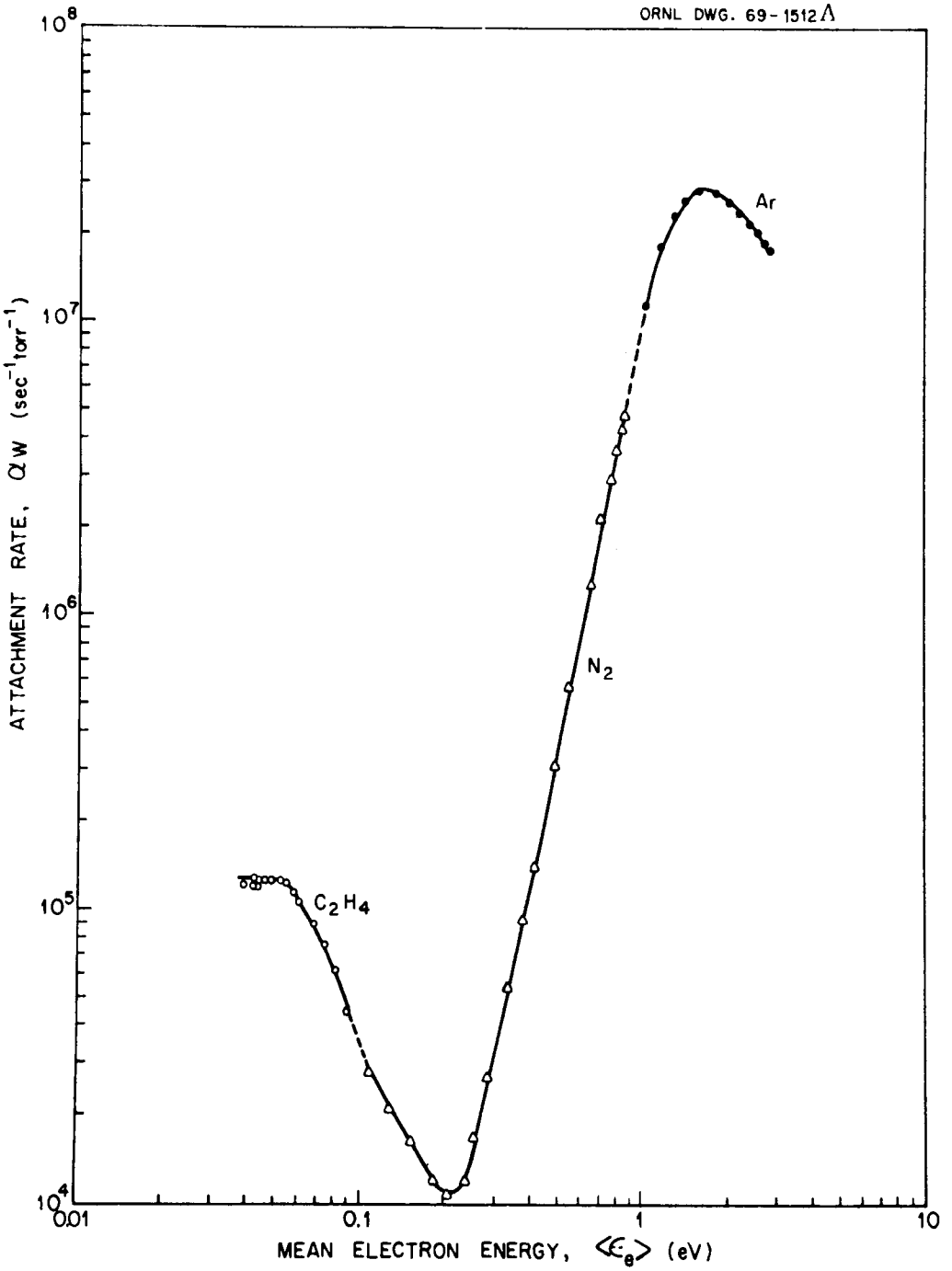

Figure V-7. αw versus $\langle \epsilon_e \rangle$ for BQ in C_2H_4, N_2, and Ar.

Beam Data. Figure V-8 [Christophorou, Carter, and Christodoulides (1969)] shows the attachment cross section for formation of long-lived parent negative ions of BQ at 2.1 eV. No ions were observed at lower energies. The negative-ion lifetime was observed to decrease from ~50 μsec at 1.7 eV to ~8 μsec at 3.2 eV.

1,4-Naphthoquinone

Swarm Data. Figure V-9 [Collins et al. (1969)] shows the absolute attachment rate for 1,4-naphthoquinone (NQ) as a function of mean electron energy for C_2H_4 (400 and 1000 torr), N_2 (400, 750, and 1000 torr), and Ar (400, 750, and 1000 torr) at 348°K. No carrier gas pressure dependence was observed and measurements at 363°K indicate no change in the attachment rate. Above 363°K reliable data could not be taken due to decomposition of NQ.

Beam Data. A sharp NQ^- resonance has been observed in the TOFMS at thermal energies [Collins et al. (1969)], in agreement with the thermal-peaking absolute swarm data. However, some structure was apparent on the high-energy tail of the resonance and has been interpreted as possibly due to excitation of higher-vibrational levels of NQ [Collins et al. (1969)]. The lifetime of the NQ^- ion was observed to decrease from ~350 μsec at 0.0 eV to ~10 μsec at ~1.5 eV.

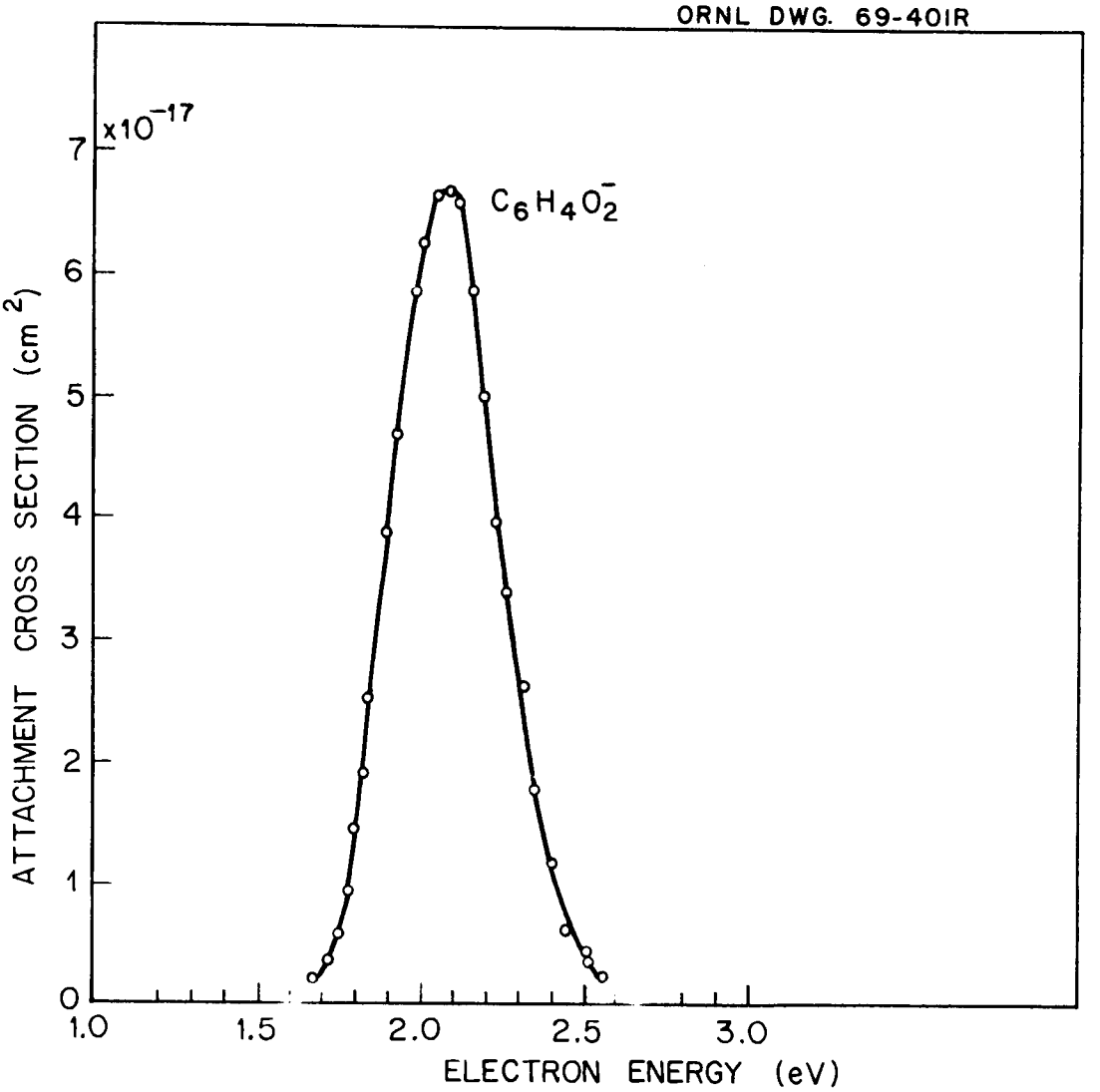

Figure V-8. $\sigma_a(\epsilon)$ for BQ^-/BQ peaking at 2.1 eV.

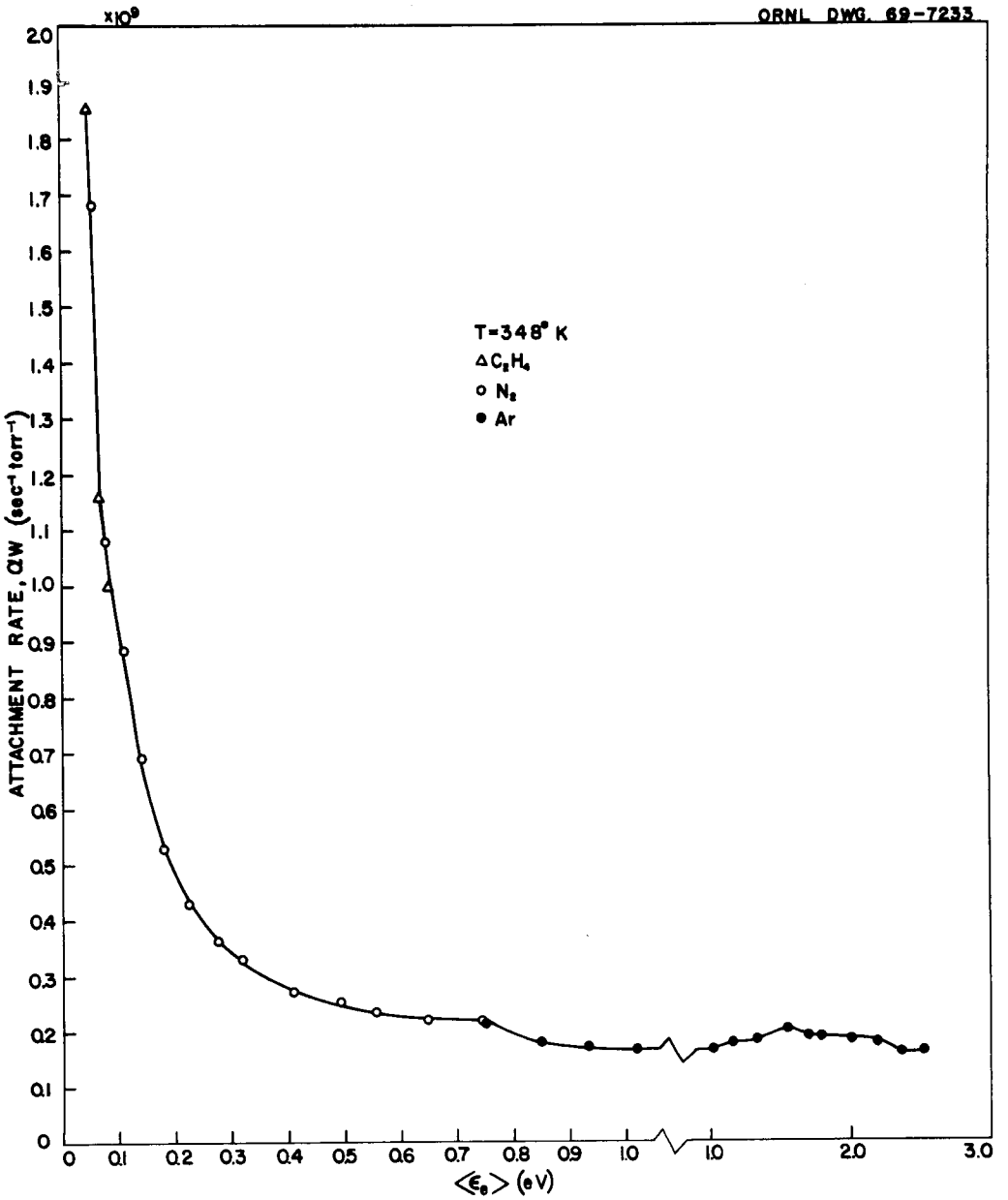

Figure V-9. αw versus $\langle \epsilon_e \rangle$ for NQ in C_2H_4, N_2, and Ar.

Discussion

The BQ^- ion at 2.1 eV has been attributed [Christophorou, Carter, and Christodoulides (1969)] to capture in the field of the lowest excited triplet state of BQ resulting from an n-π^* transition at 2.3 eV. This is the first reported case of a long-lived, polyatomic negative ion formed via an electron-excited Feshbach resonance. The decrease in τ with energy has been attributed [Collins et al. (1969)] to excess energy of the ionic system, which enhances autodetachment.

NQ^- is the first reported long-lived negative ion formed via a nuclear-excited Feshbach resonance whose lifetime has been observed to vary with electron energy. The decrease in τ with electron energy for NQ^- was also attributed [Collins et al. (1969)] to excess energy of the ionic system. In addition, the cross section for formation of NQ^- at thermal energies is the first reported case where vibrational structure is strongly indicated.

V. SUMMARY

Nondissociative electron attachment to aromatic hydrocarbons has been discussed and the absolute electron attachment rate as a function of mean electron energy has been presented for a number of molecules. For aniline and acenaphthene the attachment rates were found to be small and to peak at thermal energies. No evidence for attachment to biphenyl was observed. Azulene was found to attach electrons strongly at thermal and higher energies. Swarm data coupled with beam data provide evidence for

electron attachment in the field of a low-lying excited electronic state of azulene (possibly the lowest π-triplet state). The electron attachment rate for 1,4-naphthoquinone was found to peak at a high value at thermal energies, but significant attachment was observed at epithermal and higher energies. Electron attachment to p-benzoquinone has been briefly discussed.

CHAPTER VI

THEORETICAL CONSIDERATIONS OF ELECTRON ATTACHMENT TO POLYATOMIC MOLECULES AND THE MOLECULAR ELECTRON AFFINITY

I. A SIMPLE MODEL OF ELECTRON ATTACHMENT

Compton et al. (1966) considered the equilibrium reaction

$$M + e \underset{1/\tau}{\overset{\alpha w}{\rightleftarrows}} M^{-*} , \qquad \text{(VI-1)}$$

where M is some polyatomic molecular system that captures electrons nondissociatively, $\alpha w(\sec^{-1}\ \mathrm{torr}^{-1})$ is the forward rate for the reaction, and $1/\tau\ (\sec^{-1})$ is the rate for the backward reaction. Through the principle of detailed balance the authors obtained the formula

$$\tau = \frac{\rho^-}{\rho^o\ v\ \sigma_a(v)} \qquad \text{(VI-2)}$$

where $\sigma_a(v)$ is the attachment cross section for an electron of velocity v, ρ^- is the density of states for the ionic system, and ρ^o is the density of states for the molecule-free electron system. If the molecule is left in its ground state on detachment of the electron, then ρ^o is the density of states for a free electron, i. e.,

$$\rho^{o} = \frac{m^{2} v}{\pi^{2} \hbar^{3}} \tag{VI-3}$$

where m is the electron mass. The "v" in Equation (VI-3) is the same as that in Equation (VI-2), as implied by the principle of detailed balance.

If the molecule is regarded as a set of n (= number of atoms) weakly coupled harmonic oscillators and if it is assumed that the attaching electron shares its energy with the N (= 3n - 6 for nonlinear molecules) vibrational degrees of freedom of the molecule, then ρ^{-} can be written [Whitten and Rabinovitch (1963)]

$$\rho^{-} = \frac{[\epsilon_{T} + (1 - \beta\omega')\epsilon_{z}]^{N-1}}{(N-1)! \prod_{i=1}^{N} h\nu_{i}} \tag{VI-4}$$

where ϵ_{T} is the sum of the kinetic energy ϵ of the attaching electron, the electron affinity EA and any excess vibrational energy above the ground state (usually assumed zero), ϵ_{z} is the zero-point energy (= $1/2 \sum_{i=1}^{N} h\nu_{i}$), ν_{i} is the ith vibrational frequency, and $(1 - \beta\omega')$ is a correction factor described by Whitten and Rabinovitch (1963). β is given by

$$\beta = \frac{(N-1)\langle \nu^{2} \rangle}{N \langle \nu \rangle^{2}} \tag{VI-5}$$

where $\langle \nu^{2} \rangle$ is the mean square of the vibrational frequencies and $\langle \nu \rangle^{2}$ is the

square of the mean frequency. The quantity ω' is a function of $\epsilon' \equiv \epsilon_T/\epsilon_z$ and is given in Figure VI-1. The use of Equation (VI-4) is tantamount to assuming a nuclear-excited Feshbach resonance and the model is restricted to this type of resonance.

Introducing Equations (VI-3) and (VI-4) into Equation (VI-2) and assuming a spin degeneracy of 2 for the negative ion, one obtains

$$\sigma_a(\epsilon) = \frac{\pi^2 \hbar^2}{\tau m \epsilon \prod_{i=1}^{N} h\nu_i} \frac{[\epsilon + EA + (1-\beta\omega')\epsilon_z]^{N-1}}{(N-1)!} . \qquad \text{(VI-6)}$$

If there is a distribution of electron energies, then one can multiply Equation (VI-6) by the electron energy distribution and integrate, i. e., one can write

$$N_o\left(\frac{2}{m}\right)^{\frac{1}{2}} \int_0^\infty \sigma_a(\epsilon) f(\epsilon) \epsilon^{\frac{1}{2}} d\epsilon$$

$$= \frac{2\pi^2 \hbar^3 N_o (m/2)^{\frac{1}{2}}}{m^2 (N-1)! \prod_{i=1}^{N} h\nu_i} \int_0^\infty \frac{[\epsilon + EA + (1-\beta\omega')\epsilon_z]^{N-1}}{\tau \epsilon^{\frac{1}{2}}} f(\epsilon) d\epsilon \qquad \text{(VI-7)}$$

where N_o is the number of attaching molecules per cm^3 per torr at room temperature and $f(\epsilon)$ is the electron energy distribution function. The left side of Equation (VI-7) is the usual form of expressing the electron attachment rate αw [see Equation (II-9)]. If it is assumed that $f(\epsilon)$ is Maxwell

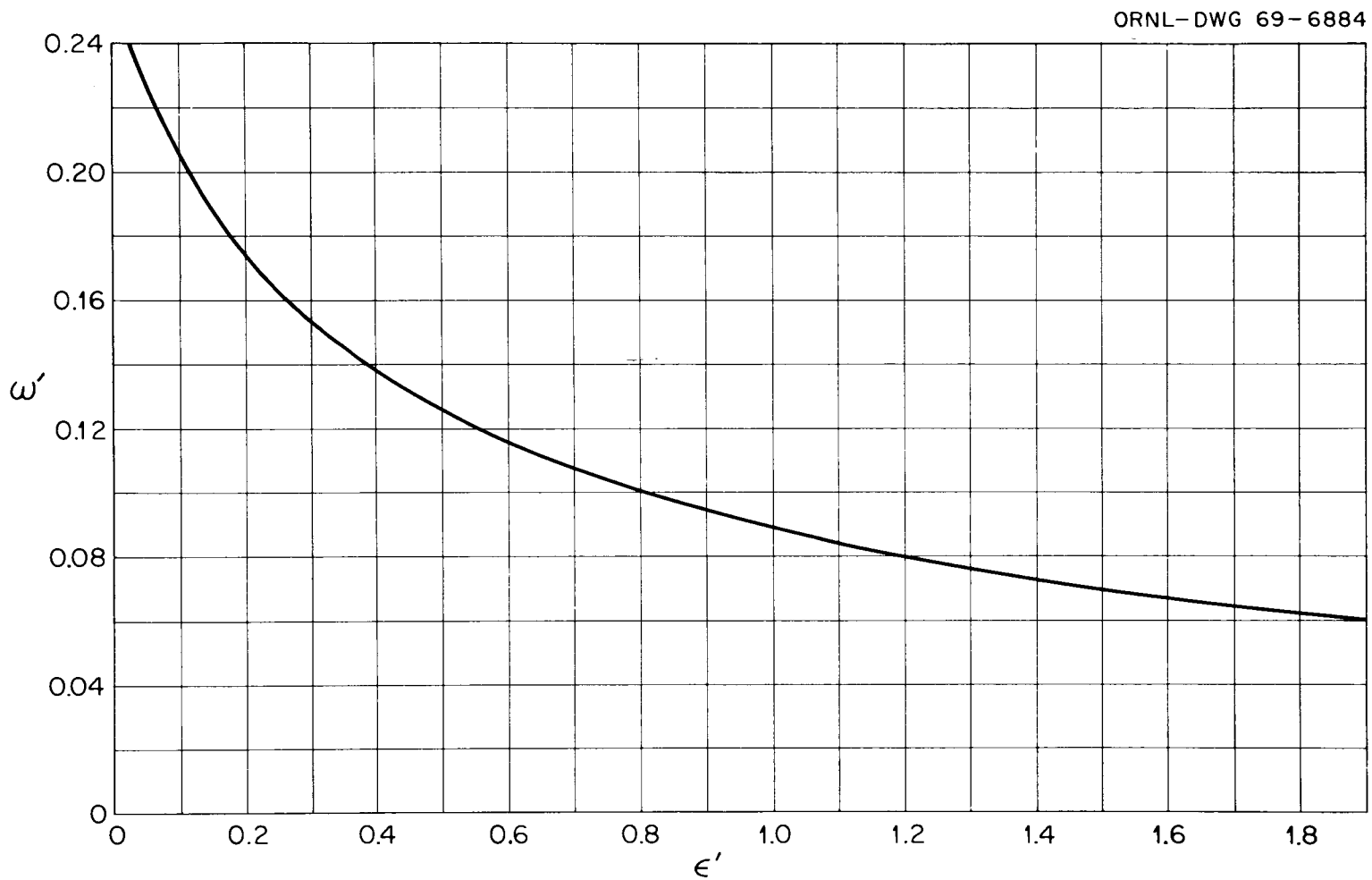

Figure VI-1. Correction factor ω' versus ϵ'.

and that τ does not vary much over the distribution, one can integrate the right side of Equation (VI-7) by parts and obtain

$$\alpha w = \frac{2\pi^2 \hbar^3 N_o (m/2)^{\frac{1}{2}}}{\tau m^2 \prod_{i=1}^{N} h\nu_i \langle \epsilon^{\frac{1}{2}} \rangle} \sum_{\ell=0}^{N-1} \left[EA + (1 - \beta\omega_o') \epsilon_z \right]^{N-\ell-1} \frac{(kT)^{\ell}}{(N-\ell-1)!} \qquad \text{(VI-8)}$$

where $\langle \epsilon^{\frac{1}{2}} \rangle = (4/\pi kT)^{\frac{1}{2}}$, k is Boltzmann's constant, T is the absolute temperature, and ω_o' is the correction factor ω' for $\epsilon = 0$. Equation (VI-7) was integrated under the assumption that ω' does not vary significantly with ϵ, which is certainly true for $EA \gg \epsilon$. This is the case at thermal energies for the molecules of interest in the present study.

There are a few comments that should be made concerning the model described above and the applications of Equations (VI-7) and (VI-8):

1. Each degree of freedom has been assumed to participate equally in trapping the molecule. This is a questionable assumption and one that bears investigation.
2. In applying the above formulae, one normally uses the mean autoionization lifetime as determined from beam experiments. Since this type determination is not performed under equilibrium conditions, it has been pointed out by Klots (1967) that the equations yield only a lower limit when used for calculating the electron affinity.

3. The vibrational frequencies of the negative ion are assumed to be the same as those for the neutral molecule when applying the above formulae since little or no data are available on the vibrational frequencies for negative ions. For large molecules this is probably a good approximation.
4. There is very little error involved in the use of the correction factor $1 - \beta\omega'$ [Whitten and Rabinovitch (1963)].
5. Physical reasoning based on the model described above leads one to conclude that for similar molecular systems the lifetime τ should increase with increasing N. Thus the model has been qualitatively verified by Naff, Cooper, and Compton (1968) who found that τ increased with increasing N for a series of fluorinated hydrocarbons.
6. The model is further supported by the fact that reasonable values for EA can be obtained from Equations (VI-7) and (VI-8). Unfortunately, only a limited amount of the necessary data are available for these calculations.
7. Since autoionization is a unimolecular process one would expect Equation (VI-6) to be consistent with unimolecular rate theory. Klots (1967) has shown this to be the case.
8. In the light of a recent study by Collins _et al_. (1969), it is questionable whether or not Equation (VI-4) is a good approximation for ρ^- at epithermal and higher electron energies.

Collins et al. (1969) found τ to vary with ϵ for the parent ion of 1,4-naphthoquinone at thermal and epithermal energies. It can be shown that unreasonably large values of $\sigma_a(\epsilon)$ result when one uses the data of Collins et al. (1969) in Equation (VI-6). This is due to the presence of the electron energy, ϵ, in the expression for ρ^- [Equation (VI-4)].

II. ELECTRON AFFINITY CALCULATIONS

The electron affinity, EA, of a molecule is defined as the energy difference between the neutral molecule in its electronic, vibrational, and rotational ground states and the singly-charged negative molecular ion in its ground states. This definition can be generalized to define an electron affinity with respect to an excited electronic state. The electron affinity is positive when the energy of the ionic system is less than that of the neutral system. In this case the electron affinity can be thought of as the upper limit for the binding energy of the extra electron.

The electron affinity is essential in considering the energetics of the various electron scattering, electron capture, and charge transfer processes and thus is an important quantity to know. However, for molecular systems EA is difficult to measure. What is usually measured is the vertical detachment energy, i.e., the minimum energy required to detach an electron from the negative ion in its ground states without a change in

nuclear configuration, leaving the neutral system in its electronic ground state. Only in the special case where the neutral molecule is formed in its ground vibrational and rotational states is the vertical detachment energy equal to the electron affinity.

The limited amount of work that has been done on determining values of the electron affinity for molecules has been reviewed by Pritchard (1953), Moiseiwitsch (1965), Briegleb (1964), and Page and Goode (1969). Tables of values of the electron affinity, with references, can be found in Christophorou and Compton (1967), Christophorou (1969), Compton and Heubner (1969), Kunii and Kuroda (1968), and Vedeneyev et al. (1966). At best, only fair agreement exists between different experimental values for the same molecule and thus various theoretical predictions, when they do exist, cannot be checked with certainty.

Table VI-1 gives the results of EA calculations using Equations (VI-6) and (VI-8) for molecules for which sufficient data are available. These calculations are compared with other values in the literature.

III. SUMMARY

A simple model of electron attachment has been discussed and results of electron affinity calculations based on this model have been presented for several molecules.

TABLE VI-I

SOME CALCULATED ELECTRON AFFINITIES

Molecule	Electron Affinity (eV)	
	Others	Present Calculation[a]
Azulene ($C_{10}H_8$)	(0.59, 0.66)[b] 0.052[c], 0.92[d]	(0.46, 0.45)[e]
Sulfurhexafluoride (SF_6)	1.49[f], 1.4[g]	(1.06, 0.96)[h, i] (1.34, 1.23)[h, j]
Nitrobenzene ($C_6H_5NO_2$)	0.4[g]	(0.53, 0.49)[i, k]
Biacetyl $(CH_3CO)_2$	1.1[g]	(0.41, 0.37)[i, ℓ]
1,4-Naphthoquinone ($C_{10}H_6O_2$)	0.7[m], 1.60[n]	(0.60, 0.60)[o, p]
p-Benzoquinone ($C_6H_4O_2$)	1.37[q], 0.77[m]	~ 0[r]

[a]The two numbers in parentheses represent calculations using Equations (VI-6) and (VI-8), respectively.

[b]W. E. Wentworth, E. Chen, and J. E. Lovelock, J. Phys. Chem. 70, 445 (1966).

[c]S. Ehrenson, J. Phys. Chem. 66, 706 (1962).

[d]J. R. Hoyland and L. Goodman, J. Chem. Phys. 36, 21 (1962).

[e]Using the vibrational spectrum of A. van Tets and H. H. Günthard, Spectrochim. Acta 19, 1495 (1963), and the lifetime and attachment rate reported by E. L. Chaney, L. G. Christophorou, P. M. Collins, and J. G. Carter, J. Chem. Phys. (submitted) (see also text).

[f]J. Kay and F. M. Page, Trans. Faraday Soc. 60, 1042 (1964).

TABLE VI-I (continued)

[g]R. N. Compton, L. G. Christophorou, G. S. Hurst, and P. W. Reinhardt, J. Chem. Phys. 45, 4634 (1966).

[h]Using the vibrational spectrum of T. Y. Wu, Vibrational Spectra and Structure of Polyatomic Molecules (Edwards Brothers, Inc., Ann Arbor, Michigan, 1946).

[i]Using the lifetime and attachment rate given in Table I by L. G. Christophorou and R. P. Blaunstein, Rad. Res. 37, 229 (1969); the swarm value of the attachment rate for SF_6 was used.

[j]Using the microwave value of the attachment rate given in Reference i.

[k]Using the vibrational spectrum of J. H. S. Green, W. Kynaston, and A. S. Lindsay, Spectrochim. Acta 17, 486 (1961).

[ℓ]Using the vibrational spectrum of J. W. Sidman and D. S. McClure, J. Am. Chem. Soc. 77, 6471 (1955).

[m]G. Briegleb, Angew. Chem. 76, 326 (1964).

[n]T. L. Kunii and H. Kuroda, Theoret. Chim. Acta 11, 97 (1968).

[o]Using the vibrational spectrum of S. N. Singh and R. S. Singh, Spectrochim. Acta 24A, 1591 (1968).

[p]Using the lifetime and attachment rate reported by P. M. Collins, L. G. Christophorou, E. L. Chaney, and J. G. Carter, Chem. Phys. Letters (submitted) (see also text).

[q]A. L. Farrager and F. M. Page, Trans. Faraday Soc. 62, 3027 (1966).

[r]Using the vibrational spectrum of T. Anno and A. Sado, J. Chem. Phys. 32, 1602 (1960), and the attachment rate reported by L. G. Christophorou, J. G. Carter, and A. A. Christodoulides, Chem. Phys. Letters 3, 237 (1969). No parent ion was observed at thermal energies by the latter workers and thus an upper limit to the lifetime of ~ 1 μsec was assumed.

CHAPTER VII

SUMMARY

Experimental data have been considered which strongly support certain forms for the energy distribution functions for electron swarms in Ar, N_2, and C_2H_4. For Ar and N_2, the distributions of Ritchie and Whitesides (1961) and of Engelhardt, Phelps, and Risk (1964), respectively, were found to be consistent with experimental data. For C_2H_4, a Maxwell distribution was found to be the representation of the energy distribution function which is consistent with those mentioned above for Ar and N_2.

Electron attachment to N_2O has been studied in mixtures with N_2 and Ar and the measured absolute attachment rates have been combined with beam data on the production of O^- from N_2O (O^-/N_2O). Using a technique for combining electron swarm and electron beam data, the absolute cross section for O^-/N_2O at 373° K was found to peak at 2.3 eV with a peak value of 8.3×10^{-18} cm^2. Over the energy range 0.2 to 1.5 eV, the attachment rate was found to increase with increasing temperature ($323° \leq T \leq 473°$ K), suggesting dissociative attachment from higher vibrational levels of N_2O. The results on N_2O-N_2 mixtures provide evidence that N_2O^- is formed as a primary product of electron attachment at energies $\lesssim 1$ eV via a three-body process involving N_2 as the stabilizing agent. The apparent three-body attachment rate coefficient increases with

increasing electron energy, suggesting an activation energy for the formation of N_2O^-. The various swarm and beam data on electron attachment to N_2O have been compared and discussed.

Results of electron attachment studies on biphenyl, acenaphthene, aniline, azulene, and 1,4-naphthoquinone have been reported. No evidence for electron attachment to biphenyl was observed. Acenaphthene and aniline were found to attach electrons weakly, with the attachment rate peaking at thermal energies. Azulene was found to capture electrons strongly. The attachment rate peaked at thermal energies and decreased slowly with electron energy. Swarm data coupled with beam data suggest that azulene attaches electrons at low energies via two resonance-capture processes, one peaking at thermal energies and another peaking between 0.22 and 0.37 eV. 1,4-naphthoquinone was found to attach electrons strongly at thermal and epithermal energies.

A simple model of nondissociative electron attachment to polyatomic molecules has been discussed and electron affinity calculations based on this model have been made for a number of molecules.

BIBLIOGRAPHY

Allis, W. P., "Motions of Ions and Electrons," in Handbuch der Physik, Vol. XXI (Springer-Verlag, Berlin, 1956), p. 383.

Anno, T., and A. Sado, Bull. Chem. Soc. Japan 31, 728 (1958).

Anno, T., and A. Sado, J. Chem. Phys. 32, 1602 (1960).

Bailey, V. A., and J. B. Rudd, Phil. Mag. 14, 1033 (1932).

Bannon, J., and H. L. Brose, Phil. Mag. 6, 817 (1928).

Barbiere, D., Phys. Rev. 84, 653 (1951).

Bardsley, J. N., and F. Mandl, "Resonant Scattering of Electrons by Molecules," in Reports on Progress in Physics, Vol. XXXI, part 2, edited by C. I. Pedersen (The Institute of Physics and the Physical Society, London, 1968), p. 471.

Beer, M., and H. C. Longuet-Higgins, J. Chem. Phys. 23, 1390 (1955).

Blaunstein, R. P., and L. G. Christophorou, J. Chem. Phys. 49, 1526 (1968a)

Blaunstein, R. P., and L. G. Christophorou, Oak Ridge National Laboratory Report ORNL-TM-2216 (1968b).

Bloch, F., and N. E. Bradbury, Phys. Rev. 48, 689 (1935).

Bortner, T. E., and G. S. Hurst, Health Phys. 1, 39 (1958).

Boyd, R. L. F., "The Direct Study of Ionization in Space," in Advances in Atomic and Molecular Physics, Vol. 4, edited by D. R. Bates and I. Estermann (Academic Press, New York, 1968), p. 411.

Bradbury, N. E., and H. E. Tatel, J. Chem. Phys. 2, 835 (1934).

Branscomb, L. M., "Negative Ions," in Advances in Electronics and Electron Physics, Vol. IX (Academic Press, New York, 1957), p. 43.

Branscomb, L. M., D. S. Burch, S. J. Smith, and S. Geltman, Phys. Rev. 111, 504 (1958).

Briegleb, G., Angewandte Chemie 76, 326 (1964).

Burke, P. G., "Resonances in Electron Scattering by Atoms and Molecules," in Advances in Atomic and Molecular Physics, Vol. 4, edited by D. R. Bates and I. Estermann (Academic Press, New York, 1968), p. 173.

Carleton, N. P., and L. R. Megill, Phys. Rev. 126, 2089 (1962).

Chaney, E. L., and L. G. Christophorou, J. Chem. Phys. 51, 883 (1969).

Chaney, E. L., L. G. Christophorou, P. M. Collins, and J. G. Carter, submitted to J. Chem. Phys. (1969).

Chantry, P. J., Bull. Am. Phys. Soc. 14, 258 (1969a).

Chantry, P. J., Westeringhouse Research Laboratories Scientific Paper 69-9E4-CO-Gas-P3 (1969b).

Chantry, P. J., Westinghouse Research Laboratories Scientific Paper 69-9E4-CO-Gas-P2 (1969c).

Chapman, S., and T. G. Cowling, The Mathematical Theory of Non-uniform Gases, Second Edition (Cambridge University Press, London, 1952).

Chen, J. C. Y., "Theory of Transient Negative Ions in Simple Molecules," in Advances in Radiation Chemistry, edited by M. Burton and J. L. Magee (John Wiley and Sons, Inc., New York, 1969) (in press).

Christophorou, L. G., Atomic and Molecular Radiation Physics (John Wiley and Sons, Inc., New York, 1969) (in press).

Christophorou, L. G., and R. P. Blaunstein, Rad. Res. 37, 229 (1969).

Christophorou, L. G., and J. G. Carter, Chem. Phys. Letters 2, 607 (1968).

Christophorou, L. G., J. G. Carter, and A. A. Christodoulides, Chem. Phys. Letters 3, 237 (1969).

Christophorou, L. G., E. L. Chaney, and A. A. Christodoulides, Chem. Phys. Letters 3, 363 (1969).

Christophorou, L. G., and A. A. Christodoulides, unpublished results (1969).

Christophorou, L. G., and R. N. Compton, Health Phys. 13, 1277 (1967).

Christophorou, L. G., R. N. Compton, and H. W. Dickson, J. Chem. Phys. 48, 1949 (1968).

Christophorou, L. G., R. N. Compton, G. S. Hurst, and P. W. Reinhardt, J. Chem. Phys. 43, 4273 (1965).

Christophorou, L. G., R. N. Compton, G. S. Hurst, and P. W. Reinhardt, J. Chem. Phys. 45, 536 (1966).

Christophorou, L. G., and J. A. D. Stockdale, J. Chem. Phys. 48, 1956 (1968).

Clark, L. B., J. Chem. Phys. 43, 2566 (1965).

Cochran, L. W., and D. W. Forester, Phys. Rev. 126, 1785 (1962).

Collins, P. M., and L. G. Christophorou, unpublished results (1969).

Collins, P. M., L. G. Christophorou, E. L. Chaney, and J. G. Carter, submitted to Chem. Phys. Letters

Compton, R. N., L. G. Christophorou, and R. H. Huebner, Phys. Letters 23, 656 (1966).

Compton, R. N., L. G. Christophorou, G. S. Hurst, and P. W. Reinhardt, J. Chem. Phys. 45, 4634 (1966).

Compton, R. N., and R. H. Huebner, Bull. Am. Phys. Soc. 13, 1696 (1968).

Compton, R. N., and R. H. Huebner, "Collisions of Low Energy Electrons with Molecules: Threshold Excitation and Negative Ion Formation," in Advances in Radiation Chemistry, edited by M. Burton and J. L. Magee (John Wiley and Sons, Inc., New York, 1969) (in press).

Curran, R. K., and R. E. Fox, J. Chem. Phys. 34, 1590 (1961).

Dalgarno, A., "Collisions in the Ionosphere," in Advances in Atomic and Molecular Physics, Vol. 4, edited by D. R. Bates and I. Estermann (Academic Press, New York, 1968), p. 381.

Davis, F. J., and D. R. Nelson, Chem. Phys. Letters 3, 461 (1969).

Davis, F. J., and D. R. Nelson, unpublished results (1969).

Dorman, F. H., J. Chem. Phys. 44, 3856 (1966).

Druyvesteyn, M. J., Physica 10, 61 (1930).

Ehrenson, S., J. Phys. Chem. 66, 706 (1962).

Eldridge, H. B., Oak Ridge National Laboratory Report ORNL-3090 (1962).

Engelhardt, A. G., A. V. Phelps, and C. G. Risk, Phys. Rev. 135, A1566 (1964).

Farrager, A. L., and F. M. Page, Trans. Faraday Soc. 62, 3072 (1966).

Fehsenfeld, F. C., E. E. Ferguson, and A. L. Schmeltekopf, J. Chem. Phys. 47, 3085 (1967).

Fox, R. E., W. M. Hickam, D. J. Grove, and T. Kjeldas, Jr., Rev. Sci. Instr. 26, 1101 (1955).

Frost, L. S., and A. V. Phelps, Phys. Rev. 136, A1538 (1964).

Golden, D. E., and H. W. Bandel, Phys. Rev. 149, 58 (1966).

Green, J. H. S., W. Kynaston, and A. S. Lindsay, Spectrochim. Acta 17, 486 (1961).

Hendrick, W. G., L. G. Christophorou, and G. S. Hurst, Oak Ridge National Laboratory Report ORNL-TM-1444 (1968).

Hoyland, J. R., and L. Goodman, J. Chem. Phys. 36, 21 (1962).

Huxley, L. G. H., and R. W. Crompton, "Motions of Slow Electrons in Gases," in Atomic and Molecular Processes, edited by D. R. Bates (Academic Press, New York, 1962), p. 336.

Kaufman, F., J. Chem. Phys. 46, 2449 (1967).

Kay, J., and F. M. Page, Trans. Faraday Soc. 60, 1042 (1964).

Kitagawa, T., Y. Harada, H. Inokuchi, and K. Kodera, J. Mol. Spectry. 19, 1 (1966).

Klots, C. E., J. Chem. Phys. 46, 1197 (1967).

Knox, B. E., and B. P. Burtt, J. Chem. Phys. 28, 1256 (1958).

Kunii, T. L., and H. Kuroda, Theoret. Chim. Acta 11, 97 (1968).

Lamola, A. A., W. G. Herkstrocter, J. C. Dalton, and G. S. Hammond, J. Chem. Phys. 42, 1715 (1965).

Loeb, L. B., "Formation of Negative Ions," in Handbuch der Physik, Vol. XXI (Springer-Verlag, Berlin, 1956), p. 445.

Loeb, L. B., Basic Processes of Gaseous Electronics, Second Edition (University of California Press, Berkeley, 1960).

Mann, D. E., J. R. Platt, and H. B. Klevens, J. Chem. Phys. 17, 481 (1949).

Massey, H. S. W., Negative Ions, Second Edition (Cambridge University Press, Cambridge, 1950).

Massey, H. S. W., and E. H. S. Burhop, Electronic and Ionic Impact Phenomena (Clarendon Press, Oxford, 1952).

McClure, D. S., "The Triplet States of p-Benzoquinone," in Excitons, Magnons, and Phonons in Molecular Crystals, edited by A. B. Zahlan (Cambridge University Press, Cambridge, 1968), p. 165.

McDaniel, E. W., Collision Phenomena in Ionized Gases (John Wiley and Sons, Inc., New York, 1964).

Menzinger, M., and R. Wolfgang, Angew. Chem. Internat. Edit. 8, 438 (1969).

Moisewitsch, B. L., "Electron Affinities of Atoms and Molecules," in Advances in Atomic and Molecular Physics, Vol. I, edited by D. R. Bates and I. Estermann (Academic Press, New York, 1965), p. 61.

Moruzzi, J. L., and J. T. Dakin, Westinghouse Research Laboratories Scientific Paper 68-1EO-Gases-P3 (1968).

Naff, W. T., C. D. Cooper, and R. N. Compton, J. Chem. Phys. 49, 2784 (1968).

Nelson, D. R., and F. J. Davis, Oak Ridge National Laboratory Report ORNL-TM-2222 (1968).

O'Malley, T. F., Phys. Rev. 150, 14 (1966).

Pack, J. L., R. E. Voshall, and A. V. Phelps, Phys. Rev. 127, 2084 (1962).

Page, F. W., and G. C. Goode, Negative Ions and the Magnetron (John Wiley and Sons, Inc., New York, 1969).

Pariser, R., J. Chem. Phys. 25, 1112 (1956).

Paulson, J. F., Advan. Chem. Ser. 58, 28 (1966).

Phelps, A. V., and R. E. Voshall, Westinghouse Research Laboratories Scientific Paper 68-1EO-Gases-P2 (1968).

Poole, J. A., and C. Dhingra, "Experimental Investigations of Compounds Exhibiting Anomalous Emission," in Molecular Luminescence, edited by E. C. Lim (W. A. Benjamin, Inc., New York, 1969), p. 813.

Prasad, A. N., and J. D. Craggs, "Attachment and Ionization Coefficients," in Atomic and Molecular Processes, edited by D. R. Bates (Academic Press, New York, 1962), p. 206.

Pritchard, H. O., Chem. Rev. 52, 529 (1953).

Rapp, D., and Briglia, D. D., J. Chem. Phys. 43, 1480 (1965).

Rempt, R. D., Phys. Rev. Letters 20, 1337 (1968).

Rentzepis, P. M., Chem. Phys. Letters 3, 717 (1969).

Ritchie, R. H., and G. E. Whitesides, Oak Ridge National Laboratory Report ORNL-3081 (1961).

Robinson, G. W., private communication (1969).

Robinson, G. W., and R. P. Frosch, J. Chem. Phys. 38, 1187 (1963).

Schulz, G. J., Phys. Rev. 116, 1141 (1959).

Schulz, G. J., J. Appl. Phys. 31, 1134 (1960).

Schulz, G. J., J. Chem. Phys. 34, 1778 (1961).

Schulz, G. J., unpublished paper presented at the Atomic and Molecular Physics Congress, University of Manchester, England (1969).

Seaton, M. J., "Atomic Collision Processes in Gaseous Nebulae," in Advances in Atomic and Molecular Physics, Vol. 4, edited by D. R. Bates and I. Estermann (Academic Press, New York, 1968), p. 331.

Sidman, J. W., and D. S. McClure, J. Am. Chem. Soc. 77, 6471 (1955).

Singh, S. N., and R. S. Singh, Spectrochim. Acta 24A, 1591 (1968).

Stockdale, J. A. D., G. S. Hurst, and L. G. Christophorou, Nature 203, 1270 (1964).

Utterback, N. G., and T. Griffith, Jr., Rev. Sci. Instr. 37, 866 (1966).

van Brunt, R. J., and M. E. Wacks, J. Chem. Phys. 41, 3195 (1964).

van Tets, A., and H. H. Günthard, Spectrochim. Acta 19, 1495 (1963).

Vedeneyev, V. I., L. V. Gurvich, V. N. Kondrat'yev, V. A. Medvedev, and Ye. L. Frankevich, Bond Energies, Ionization Potentials and Electron Affinities (St. Martin's Press, New York, 1966).

Wagner, E. B., F. J. Davis, and G. S. Hurst, J. Chem. Phys. 47, 3138 (1967).

Warman, J. M., and R. W. Fessenden, J. Chem. Phys. 49, 4718 (1968).

Wentworth, W. E., E. Chen, and J. E. Lovelock, J. Phys. Chem. 70, 445 (1966).

Wentworth, W. E., and J. C. Steelhammer, "Thermal Electron Attachment Studies by the Pulse-Sampling Technique," in Radiation Chemistry (American Chemical Society, Washington, D. C., 1968), p. 75.

Whitten, G. Z., and B. S. Rabinovitch, J. Chem. Phys. 38, 2466 (1963).

Wu, T. Y., Vibrational Spectra and Structure of Polyatomic Molecules (Edwards Brothers, Inc., Ann Arbor, Michigan, 1946).

INTERNAL DISTRIBUTION

1. Biology Library
2-4. Central Research Library
5. Reactor Division Library
6-7. ORNL Y-12 Technical Library Document Reference Section
8-32. Laboratory Records Dept.
33. Laboratory Records, ORNL RC
34. E. T. Arakawa
35-44. R. D. Birkhoff
45. A. E. Carter
46. J. G. Carter
47-81. L. G. Christophorou
82. P. M. Collins
83. R. N. Compton
84. F. J. Davis
85. J. A. Harter
86. C. E. Klots
87. J. L. Liverman
88. H. G. MacPherson
89. D. L. McCorkle
90-91. K. Z. Morgan
92. W. T. Naff
93. D. R. Nelson
94. M. Pisanias
95. D. Pittman
96. P. W. Reinhardt
97. R. H. Ritchie
98. H. C. Schweinler
99. M. J. Skinner
100. W. S. Snyder
101. J. A. Stockdale
102. A. M. Weinberg
103. R. P. Blaunstein (consultant)
104. J. E. Cantlon (consultant)
105. A. A. Christodoulides (consultant)
106. C. D. Cooper (consultant)
107. J. C. Frye (consultant)
108. Edward Gerjuoy (consultant)
109. J. B. Hursh (consultant)
110. G. S. Hurst (consultant)
111. J. L. Magee (consultant)
112. H. O. Wyckoff (consultant)

EXTERNAL DISTRIBUTION

113. P. Ausloos, Radiation Chemistry Branch, National Bureau of Standards, Gaithersburg, Md. 20760
114. N. Bardsley, Dept. of Physics, University of Pittsburgh, Pittsburgh, Pennsylvania
115. N. F. Barr, Division of Biology and Medicine, U.S. Atomic Energy Commission, Washington, D.C. 20545
116. R. S. Becker, Dept. of Chemistry, University of Houston, Houston, Texas 77004
117. J. B. Birks, Dept. of Physics, Schuster Laboratory, The University, Manchester 13, England
118. J. C. Bowe, Radiological Physics Division, Argonne National Laboratory, 9700 S. Cass Ave., Argonne, Ill. 60440
119. L. Bouby, Lavoratoire de Collisions Electroniques, Faculte des Sciences, Orsay (Essonne), France
120. H. H. Brongersma, Arthur A. Noyes Laboratory, California Institute of Technology, Pasadena, California 91109
121. W. M. Bugg, Dept. of Physics, University of Tennessee, Knoxville 37916
122-131. E. L. Chaney, Dept. of Physics, University of Western Ontario, London, Ontario, Canada.

132. R. W. Crompton, Research School of Physical Sciences, The Australian National University, Ion Diffusion Unit, Box 4, G.P.O., Canberra, A.C.T., Australia
133. M. Durop, Physico-Chimie des Rayonnements, Orsay, France.
134. Florence Fayard, Laboratoire de Collisions Electroniques, Facultes des Sciences, Orsay (Essonne), France.
135. W. H. Fletcher, Dept. of Chemistry, University of Tennessee, Knoxville 37916
136. G. R. Freeman, Dept. of Chemistry, The University of Alberta, Edmonton, Canada.
137. D. C. Frost, University of British Columbia, Vancouver 8, Canada.
138. R. E. Glick, Institute of Molecular Biophysics, Florida State University, Tallahassee, Florida 32306
139. W. H. Hamill, Radiation Laboratory, University of Notre Dame, Indiana 46556
140. J. B. Hasted, University College London, London, England
141. A. Henglein, Hahn-Meitner-Institut fur Kernforschung, Berlin-Wamsee, W. Germany
142. H. Hering, D.D.C - Cph, B.P. 2, 21 Gif-s-Yvette, France.
143. A. Herzenberg, Dept. of Physics, Yale University, New Haven, Connecticut.
144. R. H. Huebner, Radiological Physics and Instrumentation Branch, Division of Biology and Medicine, U.S. Atomic Energy Commission, Washington, D.C. 20545
145. M. Inokuti, Radiological Physics Dept., Argonne National Laboratory, 9700 S. Cass Avenue, Argonne, Illinois 60440
146. W. P. Jesse, St. Procopius College, Physical Sciences Laboratory, Lisle, Illinois 60532
147. G. R. A. Johnson, Dept. of Chemistry, University of Newcastle upon Tyne, England
148. J. J. Kaufman, Dept. of Chemistry, The Johns Hopkins University, Baltimore, Md. 21218
149. L. J. Kieffer, Information Center, Joint Institute for Laboratory Astro-Physics, University of Colorado, Boulder 80302
150. T. King, The Physical Labs, The University, Manchester 13, England
151. E. N. Lassettre, Mellon Institute, 4400 Fifth Avenue, Pittsburgh, Pa. 15213
152. C. Lifshitz, Aerospace Research Laboratories (ARC), Bldg. 450, Wright Patterson AFB, Ohio 45433
153. S. A. Lough, Division of Biology and Medicine, USAEC, Washington, D.C. 20545
154. R. J. Lovell, Dept. of Physics, University of Tennessee, Knoxville 37916
155. H. S. W. Massey, University College London, London, England
156. E. W. McDaniel, Georgia Institute of Technology, School of Physics, Atlanta, Georgia 30332

157. J. W. McGowan, Dept. of Physics, University of Western Ontario, London 72, Ontario, Canada
158. G. G. Meisels, Dept. of Chemistry, University of Houston, Houston, Texas 77004
159. C. E. Melton, Dept. of Chemistry, University of Georgia, Athens, Georgia 30601
160. T. F. Moran, Georgia Institute of Technology, School of Chemistry, Atlanta, Georgia 30332
161. E. E. Muschlitz, Dept. of Chemistry, University of Florida, Gainesville, Florida 32601
162. A. H. Nielsen, Dept. of Physics, University of Tennessee, Knoxville 37916
163. T. F. O'Malley, Defense Research Corporation, P. O. Box 3587, Santa Barbara, California 93105
164. F. M. Page, Dept. of Chemistry, University of Aston in Birmingham, Birmingham 4, Great Britain
165. R. G. Parr, Dept. of Chemistry, Johns Hopkins University, Baltimore, Md. 21218
166. W. J. Person, Argonne National Laboratory, 9700 S. Cass Avenue, Argonne, Illinois 60440
167. A. V. Phelps, Westinghouse Research Labs, Beulah Road, Pittsburg, Pa. 15235
168. J. R. Platt, Dept. of Physics, University of Chicago, Illinois 60637
169. R. D. Present, Dept. of Physics, University of Tennessee, Knoxville 37916
170. F. F. Rieke, 203-C-149, Argonne National Laboratory, Argonne, Illinois 60440
171. G. J. Schulz, Dept. of Physics, Yale University, New Haven, Conn. 06520
172. T. E. Sharp, Lockheed Missiles and Space Co., 3251 Hanover Street, Palo Alto, California 94304
173. H. S. Taylor, Dept. of Chemistry, University of Southern California, Los Angeles, California 90007
174. W. E. Wentworth, Dept. of Chemistry, University of Houston, Texas 77004
175. R. W. Wood, Division of Biology and Medicine, USAEC, Washington, D. C. 20545
176. Oak Ridge Associated Universities, Fellowship Office
177. Laboratory and University Division

178-192. Division of Technical Information Extension (DTIE)